ECONOMIC GEOLOGY
OF THE BIG HORN MOUNTAINS
OF WEST-CENTRAL ARIZONA

BUREAU OF GEOLOGY
AND MINERAL TECHNOLOGY

by

George B. Allen

December 15, 1985

Arizona Bureau of Geology and Mineral Technology
Open-File Report 85-17

This report is preliminary and has not been edited or reviewed for conformity with Arizona Bureau of Geology and Mineral Technology standards.

PREFACE

This study of the economic geology of the Big Horn Mountains was completed by George Allen in partial fullfillment of the requirements for an M.S. degree at the Department of Geosciences, University of Arizona. The study is intended to complement recent geologic mapping of the Big Horn and Belmont Mountains as part of the Cooperative Geologic Mapping Program (COGEOMAP), funded jointly by the Arizona Bureau of Geology and Mineral Technology and the U.S. Geological Survey. Preliminary geologic maps of the Belmont and eastern Big Horn Mountains have been released as AZBGMT Open-File Report 85-14 (Capps and others, 1985) and will be included in a Bureau Bulletin on the geology and mineral resources of the area (Reynolds and others, in prep.). This contribution by George Allen will be included as a chapter in the forthcoming bulletin, following review and editing by Bureau staff. The availability of this bulletin will be announced in a future issue of Fieldnotes, the Bureau's quarterly publication.

Dr. Stephen J. Reynolds
COGEOMAP Coordinator
Arizona Bureau of Geology
and Mineral Technology

LIST OF TABLES

Table.		Page
1.	Big Horn Gold District	12
2.	Precious- and Base-Metal Assays	29
3.	Trace Elements	41
4.	Tiger Wash District	48
5.	Eastern Harquahala District	50
6.	Aguila Manganese District	74
7.	Osborne District	96
8.	Potassium-Metasomatized Rocks	129

ACKNOWLEDGMENTS

Financial support for this project was provided by the Arizona Bureau of Geology and Mineral Technology. Dr. Stephen J. Reynolds of the Bureau provided encouragement and guidance throughout the course of this study. Conversations with Chris Capps and Dr. Joaquin Ruiz greatly aided progress. Reviews by Dr. Joaquin Ruiz, Dr. Paul E. Damon, and especially, Dr. Stephen J. Reynolds greatly improved the manuscript. TRICON Mining Ltd. and Nicor Inc. provided geochemical assays. Parry Willard of TRICON provided a geologic map of the Pump Mine. Joy Mehulka of the Bureau drafted all of the figures.

LIST OF ILLUSTRATIONS

Figure		Page
1.	Big Horn Mountains District Location Map.....	3
2.	Selective Outcrop Map of the Big Horn District...	9
3.	Geologic Cross Section of the Northwest-Facing Open Cut of the El Tigre Mine.....	17
4.	Geologic Map of the El Tigre Mine.....	19
5.	Au vs. As plot.....	23
6.	Au vs. Ag plot.....	25
7.	Au vs. Pb plot.....	27
8.	Geologic Map of The Knabe Mine.....	33
9.	Geologic Map of the Pump Mine.....	37
10.	REE Plot of Big Horn Mountains Igneous Rocks.....	39
11.	Location Map of the Tiger wash Barite-Fluorite District and the eastern Harquahala District.....	53
12.	Geologic map of the Northern Portion of the Tiger Wash barite-Fluorite District.....	55
13.	Histograms of Homogenization temperatures From Fluid Inclusions.....	63
14.	Histograms of Weigth percent NaCl Equivalent of Fluid Inclusions.....	65
15.	Map of the Aguila District.....	73
16.	Geologic Cross Section of the South-Facing Wall of the Black Rock Mine.....	87
17.	Osborne District Location Map.....	95
18.	Geologic map and Cross Section of the U.S. Mine..	103
19.	Geologic Map and Cross Section of the Tonopah-Belmont Mine.....	113
20.	Volcanic Enrichment Factors.....	119
21.	Schematic Cross Section of the Big Horn Mountains	127

OSBORNE DISTRICT..... 92

Introduction..... 92
Geologic Setting..... 92
Characterization of Mineralization..... 101

The U.S. Mine..... 102
The Tonopah-Belmont Mine..... 110
The Scott Mine..... 116
Volcanic Enrichment Factors..... 117
Osborne District Summary..... 120
Osborne District Discussion..... 121

INTERRELATIONSHIP OF MIDDLE TERTIARY DISTRICT..... 124

A MODEL FOR MIDDLE TERTIARY MINERALIZATION..... 130

APPENDIX: INDUSTRIAL MINERAL RESOURCES..... 135

LIST OF REFERENCES..... 136

TABLE OF CONTENTS

	Page
LIST OF ILLUSTRATIONS	iv
LIST OF TABLES	v
ABSTRACT	vi
INTRODUCTION	1
BIG HORN DISTRICT	6
Introduction	6
Geologic Setting	7
The El Tigre Mine	11
The Knabe Mine	31
The Pump Mine	34
The Dead Horse Prospect	35
REE Data	42
Summary	42
Discussion	44
TIGER WASH DISTRICT	46
Introduction	46
Geologic Setting	47
Structural Setting	47
Structural Control Over Mineralization	56
Paragenesis	57
Fluid Inclusion Studies	58
Hypothetical Mechanisms for Barite-Fluorite Mineralization	66
A Model for Barite-Fluorite Mineralization	69
AGUILA DISTRICT	71
Introduction	71
Previous Investigations	71
Geology of the Manganese Deposits	84
Host Rocks	84
Structural Relations to Mineralization	84
Timing of Mineralization	85
Paragenesis	88
Fluid Inclusion Studies	88
Genesis of the Aguila District	89

ABSTRACT

The Big Horn Mountains are a geologically complex range that extends over 500 square km in west-central Arizona. Three major lithologic terranes outcrop: (1) Proterozoic amphibolite, phyllite, schists, gneiss, and granite; (2) Mesozoic monzonite to diorite intrusives; and (3) Cenozoic mafic to silicic volcanic rocks and clastic rocks. The entire area is in the upper plate of a detachment fault and, consequently, contains many low- to high-angle normal faults.

Each lithologic terrane has its associated mineral occurrences. The Big Horn district is exclusively hosted in the pre-Tertiary terrane. Most of its mineral occurrences are spatially related to the Late Cretaceous intrusive rocks. One occurrence, the Pump Mine, may be a metamorphic secretion deposit, and therfore, would be middle Proterozoic.

The vast majority of the mineral occurrences in the Big Horn Mountains are middle Tertiary in age and occur in three districts: the Tiger Wash barite-fluorite district; the Aguila manganese district; and the Osborne base and precious metal district. Fluid inclusions from Tiger Wash fluorite (T_h 120 to 210° C, NaCl wt. equivalent 17 to 18 percent not corrected for CO_2) and nearby detachment-fault- hosted Harquahala district fluorite (T_h 150 to 230° C., NaCl wt. equivalent 15.5 to 20 percent not corrected for CO_2) suggest cooling and dilution of fluids as they are presumed to evolve from the detachment fault into the upper plate. Mass-balance calculations suggest that the proposed evolution of fluids is sufficient to account for the observed tonnage of barite and fluorite. The Tiger Wash occurrences grade directly into calcite-gangue-dominated manganese oxides of the Aguila district. A wide

range of homogenization temperatures (T_h 200 to 370° C.), an absence of CO_2 and low salinities (NaCl wt. equivalent 1 to 2 percent) in the Aguila district calcite-hosted fluid inclusions argue for distillation of fluids during boiling or boiling of non saline-meteoric waters. Mass-balance calculations modeling the evolution of Ca and Mn during potassium metasomatism of plagioclase in basalt suggest that little if any influx of these cations is necessary to form the calcite-dominated manganese oxide tonnage observed. The Aguila district grades directly to the east into the base-metal and precious-metal occurrences of the Osborne district. Preliminary data describing geological settings, fluid inclusions, and geochemistry suggest that the Osborne district has a continuum between gold-rich to silver-rich epithermal occurrences. The gold-rich systems have dominantly quartz gangue, with or without fluorite, and are hosted in a variety of rocks, but are proximal to Precambrian phyllite or mid-Tertiary rhyolite. Fluid inclusions from two occurrences representative of the gold-rich systems spread across a minor range (T_h 190 to 230° C., NaCl wt. equivalent 17 to 23 percent not corrected for CO_2). Dilution of highly saline fluids is the inferred mechanism for precipitation of gold in the gold-quartz systems.

The silver-rich systems have dominantly calcite gangue with or without quartz, and are hosted in mid-Tertiary basalt. Calcite fluid inclusions from a representative high-silver occurrence display a wide range of homogenization temperatures and salinities (T_h 120 to 370° C., NaCl wt. equivalent 7 to 23 percent). Boiling and consequent neutralization of acidic solutions is the inferred mechanism for the silver-rich, calcite gangue systems.

A model inferring a regional fluid-flow regime and local sources of

metals is proposed. Four possible regional and local causes of fluid flow in upper-plate detachment regimes are proposed: (1) regional elevation of geothermal gradients as a result of middle-crustal, lower-plate rocks rising to upper crustal levels; (2) meteoric water recharge along the southeast flank of the Harquahala antiform and consequent displacement of connate waters in the upper-plate of the Big Horn Mountains; (3) local emplacement of feeder stocks to rhyolitic flows; (4) and tilting of major upper-plate structural blocks.

INTRODUCTION

The Big Horn Mountains, and its contiguous range, the Belmont Mountains, extend over 500 square km in west-central Arizona (Figure 1). The most recent geologic map of Arizona (Wilson et al., 1969) delineates six crystalline units in the range; Proterozoic gneiss, Proterozoic schist, Proterozoic Granite, Cretaceous andesite, Cretaceous rhyolite, and Tertiary-Cretaceous rhyolitic intrusives. The range was also briefly described by Rehrig et al.(1980). They established the volcanics as middle Tertiary as opposed to the Cretaceous age inferred by Wilson. Furthermore, they noted that the volcanics in the eastern two thirds of the range are steeply to moderately tilted to the northeast and that the volcanics in the western third of the range are tilted to the west and southwest. From these relationships they inferred the range is dissected by listric normal faults.

The ensuing economic geology study is part of a joint U.S.G.S.-Arizona Bureau of Geology COGEOMAP project to gain a refined understanding of the geology and mineral occurrences of the Big Horn and Belmont Mountains. The resulting investigations (this volume) extensively details the stratigraphy and structure of the Big Horn and Belmont Mountains. Major amendments to the stratigraphy involve: the presence of Proterozoic granite in the western third of the range; the presence of an extensive Late Cretaceous monzonitic to granodioritic intrusive that has affinity to the Wickenburg Batholith of Rehrig et al. (1980); the presence of fluvial clastic rocks and laharic sedimentary rocks at the base of the Miocene section; the presence of mafic volcanics interspersed throughout the Miocene section; and the likelihood that the Belmont granite is mid-Tertiary (Reynolds et al.,

Figure 1. Location map for Big Horn Mountains mineral districts.

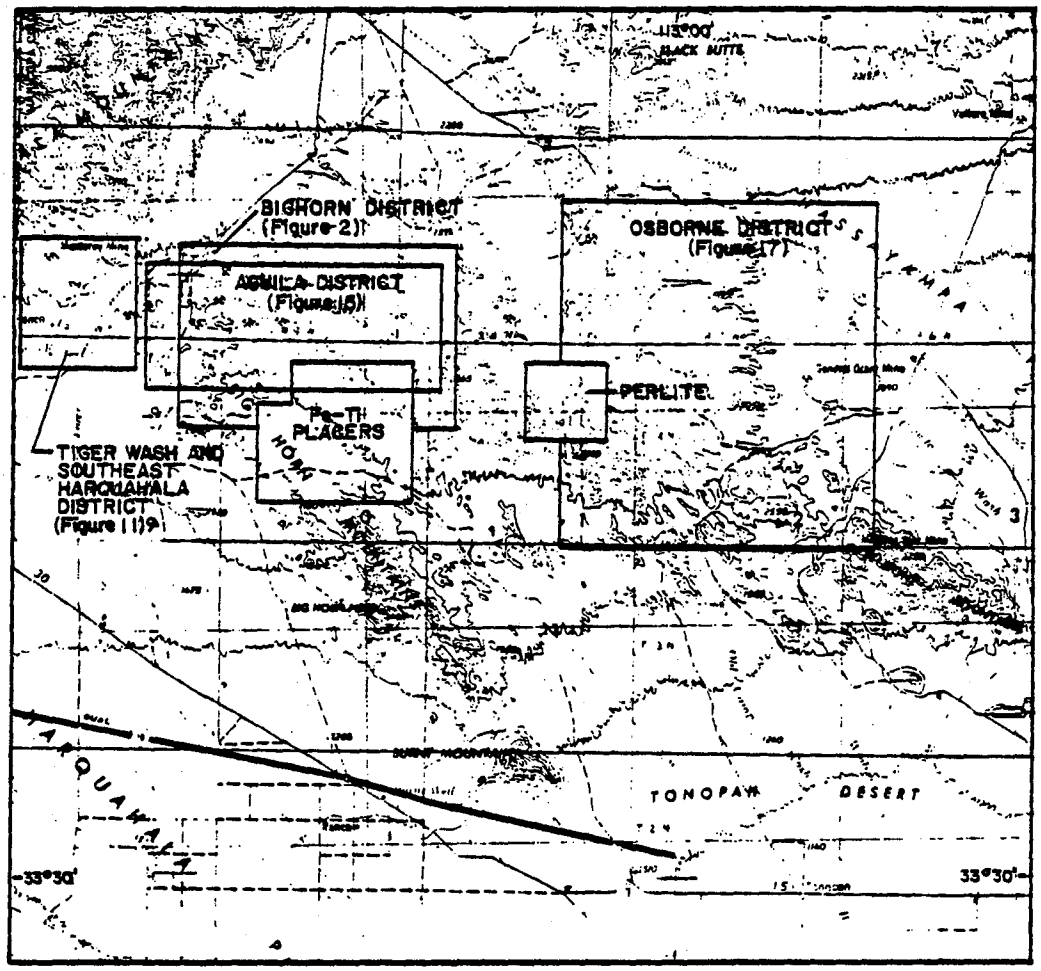

Km 0 5

BIG HORN MOUNTAINS DISTRICT
LOCATION MAP

1985) in age as opposed to a Precambrian age (Wilson et al., 1957). Structural revelations are: the presence of major northeast-trending faults in the eastern half of the range that may have considerable strike-slip offset; and the existence of high-to moderate-angle faults cutting low-angle structures in the western extreme and in the south-central portion of the range. These latter relationships suggest multiple generations of normal faulting.

The great aerial extent of the range and the variety of terranes offers innumerable opportunities for economic geology studies. As a regional study, the emphasis here is to illuminate district-to-district disparaties and affinities, thereby establishing a metallogeny for the range. The geologic framework for establishing metallogeny is a product of the renaissance of regional and detailed geologic studies of the past five years in west-central Arizona (Coney and Reynolds, 1980; Reynolds, 1980; Reynolds et al., 1980; Rehrig and Reynolds, 1980; Rehrig, 1980; Reynolds, 1982; Richard, 1982; Reynolds and Spencer, 1985; Hardy, 1984; Capps et al., 1985). These works established the lower-plate detachment setting of the Harquahala Mountains on the western perimeter of the Big Horn Mountins. The southeast dip of the Bullard detachment fault on the western flank of the Big Horn Mountains suggests that the Big Horn Mountains are underlain by one or more detachment faults. The relationship between this major structural discontinuity, hydrothermal fluids, and mineral occurrences high in the upper plate has not been addressed. However, numerous investigations have been undertaken near immediately exposed detachment surfaces (Coney and Reynolds, 1980; Wilkins and Heidrick, 1982; Berg et al., 1982; Spencer and Welty, 1985; Van Nordt and Harris, 1985,; and Beane and Wilkins, 1985). These investigations mostly describe mineral occurrences in the Colorado

Trough area at deep levels of exposure in detachment terranes. One avenue of this study was to obtain homogenization temperatures and freezing point depressions on fluid inclusions from precious-metal occurrences on the Harquahala detachment fault and compare them to fluid inclusions from Middle Tertiary occurrences high in the upper plate and at extensive distances away from the exposed detachment fault. Similarly, establishment of the diverse character of middle Tertiary occurrences that run in a west-east transect from the Harquahala Mountains to the Belmont Mountains would place preliminary constraints on the character of detachment contemporaneous middle Tertiary fluid flow. Hewett (1964) discusses the phenomena of lateral and assumed vertical zonation of barite-fluorite-manganese-precious metal-base metal occurrences. In this paper evidence is presented to refine and delimit Hewett's model of epithermal zonation.

The virtual spatial coincidence of the Big Horn gold district with the Aguila manganese district, merits clarification. By analogy with other gold-quartz vein districts in Central Arizona, and, presumably, on the basis of its spatial coincidence with the middle Tertiary manganese mineralization, Keith et al. (1983) argued that the Big Horn district is of middle Tertiary age. Welty et al. (1985) further this inference by noting that the proximity of the Harquahala detachment fault suggests that the gold veins could be a detachment-related occurrence. Welty et al. (1985) suggest some of the Big Horn occurrences may be Laramide because they have associated northeast-trending silicic dikes.

BIG HORN DISTRICT

Introduction

The Big Horn district is located in the northwest quarter of the Big Horn Mountains (Figure 1), but includes one outlier in the north-central part of the range. The district is a northeast-trending swath of prospect pits, shafts, and inclines. The historic production of the Big Horn district is reported as; 2,800 oz. gold, 1000 oz. silver, 26,300 lbs. copper, and 6000 lbs. lead (Keith et al., 1983).

The Big Horn district is one of five basement-hosted, gold-quartz-vein districts in Maricopa County, and one of thirty-three in the state. Until recently, the age and mode of origin of these deposits had received little attention. An absence of demonstrably associated Phanerozoic rocks and a dearth of radiometric data from gangue minerals inhibits age designations. Rehrig and Heidrick's (1972) study of late Phanerozoic vein and fracture trends provided a first comprehensive tool for metallogeny. Davis (1981) established the evolution of strain through time for southeast Arizona and adjacent areas, thereby establishing a valuable framework for relating fracture and intrusive trends to episodes of mineralization. Dreier (1985) specifically studied the orientation of mineralized veins from the Late Cretaceous through the Tertiary, thereby allowing age constraints to be placed on late Phanerozoic veins without radiometric age determinations. Keith et al. (1983) used these criteria, radiometric age determinations of mineralization-related rocks, and geologic settings to produce a metallogenic map of Arizona, where they infer a mid-Tertiary age for the Big Horn district and for all of the basement-hosted gold deposits.

Welty et al. (1985) detailed criteria from literature reviews that are the basis for age designations, and, in some cases, further inferences that conflict with Keith et al. Welty et al. (1985) refined the category of basement-hosted, probable mid-Tertiary gold deposits by lithotectonic distinctions. They note that fifteen of the thirty-three deposits are related to mid-Tertiary detachment terranes. Further, they distinguish a category of microdiorite-dike-related deposits. Eleven of the the thirty-three basement-hosted deposits are spatially related to microdiorite dikes. By analogy to detailed geochronologic work on microdiorite-related deposits in the South Mountains (Reynolds, 1984), these deposits are mid-Tertiary as well. Welty et al. (1985) classification leaves seven basement hosted districts of equivocal lithotectonic setting and age. These are the Big Horn, Vulture, Cave Creek, Winifred, Gila Bend, Pikes Peak, San Domingo, and Sunrise. In view of the current interest in gold exploration, an understanding of these central Arizona gold districts would be an important aid to exploration. This study was undertaken to characterize the Big Horn district geologic setting to constrain its age.

Geologic Setting

Reynolds et al. (this volume) describe the geology of the northwest and west-central Big Horn Mountains. Proterozoic rocks constitute about two thirds of the encompassing Big Horn district. The oldest Proterozoic rocks are schist and gneiss which outcrop in the geographic center of the district and account for about half of the total outcrop. These schists are typically fine-grained amphibolites with 35 to 60 percent amphibole, 35 to 60 percent feldspar and up to 5 percent quartz. The gneissic-textured amphibolites have ptygmatic veinlets and

Figure 2. Selective outcrop map for the Big Horn gold district. Individual prospects are described in Table 1.

SELECTIVE OUTCROP MAP OF THE BIG HORN DISTRICT

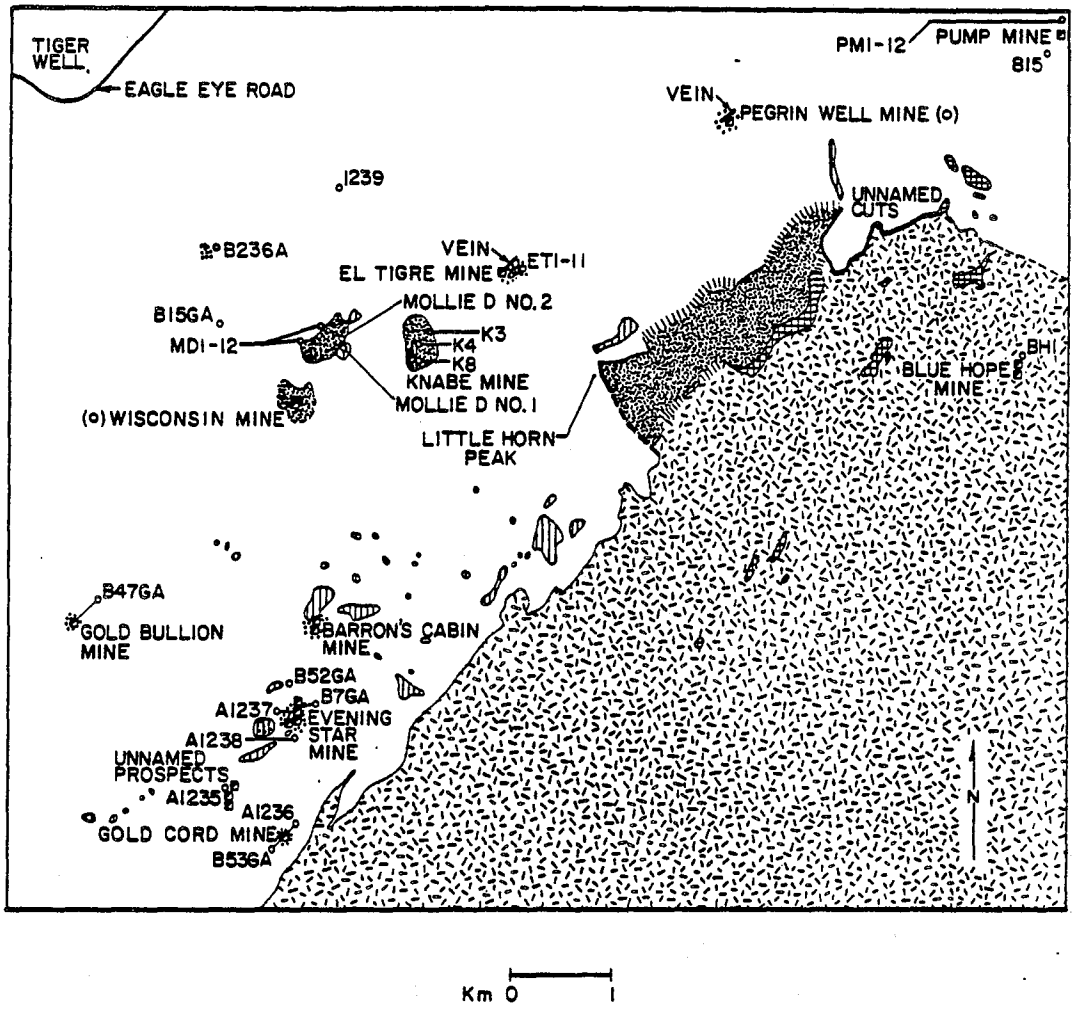

Late Cretaceous quartz diorite to diorite intrusives

Late Cretaceous aplitic monzonite intrusives

Late Cretaceous granodiorite to monzonitic intrusion

Late Cretaceous intrusives and commingled Precambrian crystalline rocks

contact, dashed where approximately located

fault, dashed where approximately located

gradational contact

iron oxide stain

shaft or incline

•AI234 sample location

veins of medium-grained to pegmatitic granite. Intruding these is a Proterozoic medium-grained biotite granite which accounts for one third of the total outcrop. The granite has 60 to 80 percent feldspar, 15 to 25 percent quartz, and 12 to 20 percent biotite. The biotite is commonly weathered to chlorite. Ridge-tops of the district expose coarse-grained to pegmatitic granite pods with up to 10 percent muscovite. The granite has sporadically developed, widely occurring mylonitic fabrics. The contacts between the granite and the older Proterozoic rocks are typically gradational.

Fine-grained monzodioritic to dioritic intrusions make up about one percent of the total outcrop (Figure 2). These intrusions are frequently northeast-aligned exposures or have related northeast-trending dikes. These intermediate composition intrusives are highly varied : 45 to 75 percent plagioclase; 15 to 30 percent biotite or amphibole, but not both; and 0 to 10 percent quartz. Rarely, some dikes have potassium feldspar. These rocks are not mylonitized, and, as discussed in the REE section, are assumed to be Late Cretaceous relatives of the batholithic granodiorites.

The remaining twenty percent or so of the outcrop is composed of the undifferentiated dark gray, brown, and red, vesicular to massive multi-flows of the mid-Miocene Dead Horse basalt. The basalt rests unconformably on the basement and is porphyritic to aphyric. The porphyritic basalts contain 5 to 20 percent phenocrysts ranging form 2 to 10 percent olivine, 2 to 15 percent clinopyroxene, 2 to 5 percent plagioclase, and trace to 3 percent orthopyroxene (Capps et al., 1985). In many places the basalt is brecciated and veined with calcite.

The Proterozoic schists and gneisses are intensely folded. Crystalloblastic foliation attitudes vary greatly, but northwest to

east-west strikes with consistent moderate to steep northeast to north dips are typical. In the east-central part of the district the major gradational contact between the Proterozoic metamorphic rocks and the fine- to medium- grained granite trends N35°W. The linearity of this contact suggests it is a Proterozoic tectonic structure. The Proterozoic granite has rare, local mylonitic fabrics, which, in the Big Horn district, have no consistent trend.

The middle Tertiary structures are locally complex. Minor structures are typically north- to north-northwest-striking, high-angle normal faults. The major structures of the district are N40°W-striking, low- to moderate-angle normal faults. In places, strike-slip movement in tear faults is suggested by horizontal slickensides and apparent displacement. Apparent shingling of low-angle faults in the Lion's Den Mine area suggest at least two generations of normal faulting.

Character of Mineralization

Mineral occurrences of the Big Horn district are gold-rich, basement-hosted, narrow-quartz-pods and veins that are commonly associated with northeast-trending, Late Cretaceous, intermediate-composition intrusives, and commonly have sericitic alteration. Table 1 summarizes the geology of individual prospects. The ensuing sections describe the geology of occurrences that display the variety in the character of the Big Horn district.

The El Tigre Mine

The El Tigre mine is in the northwest part of the range, 1.6 Km northwest of Little Horn Peak (Figure 2). The El Tigre mine is the premier gold producer of the district, accounting for over 80 percent of

Table 1. Big Horn Gold District.

PROSPECT	LOCATION	PRODUCTION/ DEVELOPMENT	HOST	STRUCTURE/ GEOMETRY	MINERALOGY/ GEOCHEMISTRY
Barron's Cabin	NW 1/4 Sec 8 T4N R9W, Big Horn 15'.	Unknown.	Precambrian granite and Late K diorite (?).	Unknown. Assumed to be pods and veins.	Unknown. Mineralization is spatially related to a qtz. diorite intrusion.
Blue Hope	NE 1/4 Sec 31 T5N R8W, Big Horn 15'.	No production. Small pits.	Late K monzodiorite.	Pods of indistinct orientation.	Abundant chrysocolla and lesser malachite. Biotite in Late K host monzodiorite is chloritized.
Dead Horse	NE 1/4 Sec 15 T5N R8W Aguila 15'.	No production. One 13 m deep shaft to level. Three trenches ave. 9m long.	Late K granodiorite.	Pods and indistinctive veins. Overall mineralization appears to be east-west aligned. Minor mineralization is localized along a N52E, 80SE structure.	Chrysocolla is abundant. Some chalcocite cores to chrysocolla. Extensive iron oxide staining. Some greasey green mica. Sericite is common. Mineralization is commonly associated with qtz flooding.

El Tigre	SW 1/4 Sec 27 T5N R9W, Big Horn 15'.	Approx. 2300 oz. Au, 150 oz. Ag, and 700 lbs. Cu from 9500 tons. 3 shafts: one 15m, the others approx. 60m deep. Total of 250m of workings.	Gabbro and granite pegmatite.	Two qtz lenses, 1.5 to 2m wide and app. 25 m long. Attitude is app. N35E 30NW. A N45W-striking SW- dipping low-to mod. angle flt. cuts the vns. at the west end. A similar normal flt. is inferred to cut the veins on the NE.	Milky quartz gangue dominates. Area is iron oxide stained. Some jarosite, some Mn oxide staining at depth. Native gold is rare. Qtz. diorite intrusive spatially associated with vein has limonite after pyrite.
Evening Star	SW 1/4 Sec 7 T4N R9W, Big Horn 15'.	A small amount of Au, Ag, Cu, and Pb were produced. A 21m shaft an a 60m incline. Principle vein opened by cuts over 0.8 km strike length.	Precambrian granite gneiss.	Veins and pods. Northernmost vein oriented N10E 60SW to to N10W 55NW.	Iron-oxide-stained quartz vein. Pod at the west end of main shaft has propable alunite, wulfenite, trace mimetite, and probable cuprite.
Gold Bullion	NW 1/4 Sec 12 T4N R9W, Big Horn 15'.	No production. 9m deep shaft	Precambrian granite.	Pod that appears to have an east-west alignment. Up to 1 km east of shaft, limonite after py. is along east-trending slickensides in slightly mylonitized Precambrian granite.	Quartz vein breccia with some possible felsite dike material host specular hematite, minor calcite, and chrysocolla. Some limonite after pyrite boxworks.

Gold Cord	NE 1/4 Sec 18 T4N R9W, Big Horn 15'.	No production. Single 25m deep shaft and scattered pits.	Precambrian granite.	Pod of indistinct orientation.	Hematite-stained grey to white qtz. Trace chrysocolla. Some limonite after pyrite boxwork.
Knabe	NE 1/4 Sec 33 T5N R9W, Big Horn 15'.	No production. Four pits.	Precambrian (?) granite and Late K diorites.	Pods of indistinct orientation. Spatially associated diorite dikes have a vaguely arcuate outcrop pattern.	Quartz pods host iron-oxide staining and some limonite after pyrite. Pods are associated with large, coarse sericite making up to 20% of surrounding rocks. Argillic alteration of encompassing granite is common.
Mollie Davenport	NW 1/4 Sec 33 T5N R9W, Big Horn 15'.	No production. Shaft approx 40m deep. Haulage adit approx 80m long.	Precambrian granite and schist and Late K monzodiorite.	Indistinct pods that appear to have NE trends.	Iron-oxide staining proximal to qtz. pods which outcrop 0.2 to 0.3 km SW of the main shaft. Some sericitic alteration. Mineralization is associated with felsite and monzonitic to dioritic intrusives.

Pegrin Well	SE 1/4 Sec 23 T5N R9W, Aguila 15'.	No production. 9m long incline in collapsed workings. 10m long open cut.	Precambrian granite and gneiss.	9 to 12m X 1.5 to 2.5m vein oriented N62E, 60SE.	Iron-oxide staining in qtz. vein is proximal to felsite dike. Some limonite after py. Sericite is common.
Pump or Purple Pansey	NE 1/4 Sec 19 T5N R8W, Aguila 15'.	Approx. 200 oz. Au, 50oz. Ag, 150 lbs Cu, from 2277 tons suspected production. 3 shafts cut main vein: 90m, 50m, and 25m. Pits extend over 1200m.	Precambrian amphibolite, phyllite, mylonitic granite.	1200m long vein or and shear zone that ranges from 0.1 to 2.5m wide. SE half trends east-west, dips 40 to 55N. NW portion trends N40 to 60W, and dips 30 to 45 NE. Vein is cut off by NNW-trending, west-WSW-dipping low- to moderate-angle normal flt.	Intensley iron-oxide stained, yellow greasey qtz. vein and hosting metamorphic rocks. Chlorite is common.
Wisconsin	SE 1/4 Sec 32 T5N R9W, Big Horn 15'.	No production. Shaft approx. 20m and adit approx 11m. No production. Shaft approx. 20m and adit approx 11m.	Precambrian granite and Late K granitoids.	Pod with indistinc trend. Possibly of NE trend.	Iron-oxide staining of quartz vein. Specularite is in small cavities. Sericite is app. 1% of enclosing host rock.

Figure 3. Geologic cross section of the northwest-facing open cut of the El Tigre mine.

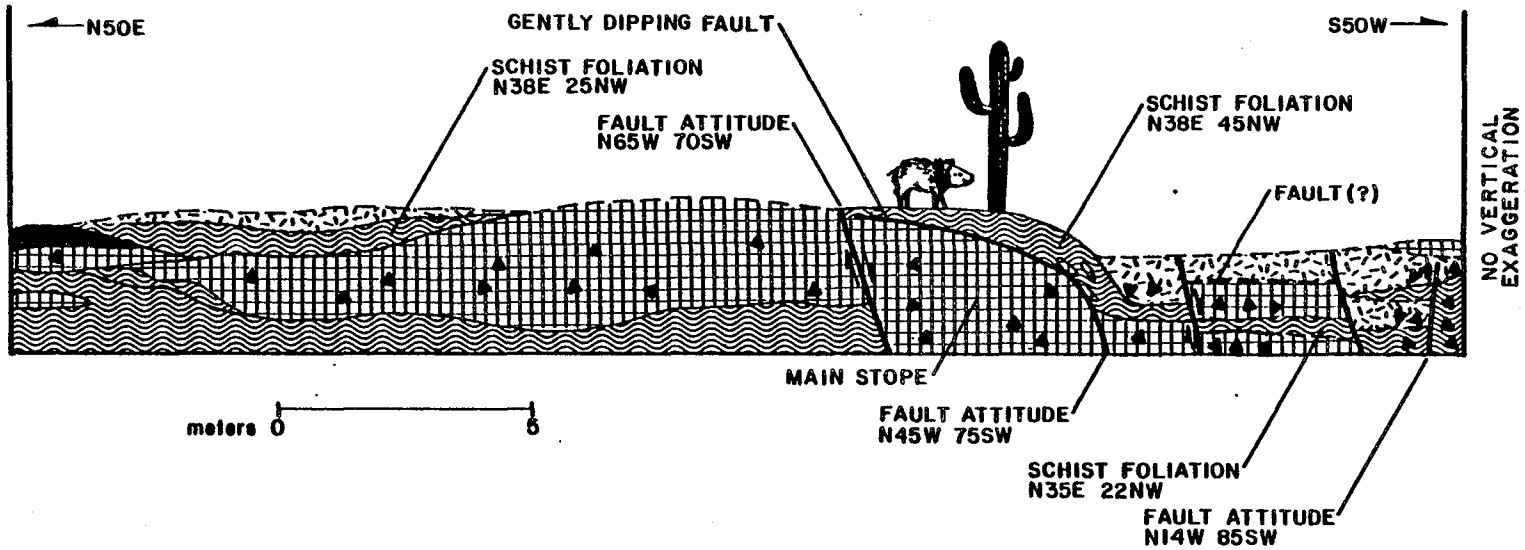

GEOLOGIC CROSS SECTION OF THE NORTHWEST-FACING OPEN CUT OF THE EL TIGRE MINE

TKmd	Cretaceous-Early Tertiary(?) mafic dike	◄ ▲ ◄	breccia
TKq	Cretaceous-Early Tertiary(?) bull quartz vein	— — —	contact, dashed where approximately located
p€g	Precambrian foliated granite	⇌	fault, with arrows showing offset
p€gs	Precambrian gneiss and schist	- - - - -	surface dashed where approximate

Figure 4. Geologic map of the El Tigre mine.

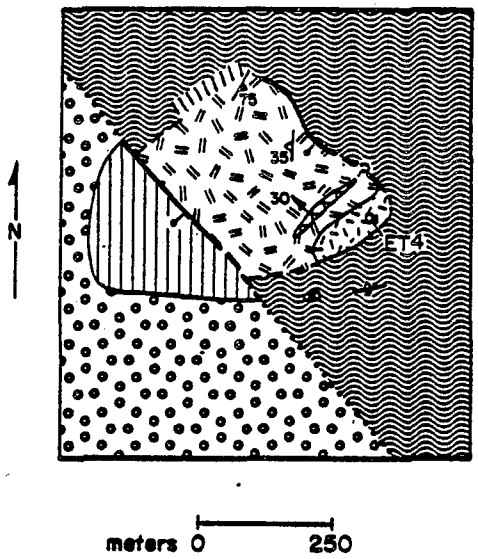

GEOLOGIC MAP THE EL TIGRE MINE

- QTg — Late Tertiary - Quaternary gravels
- Tb — Miocene basalt
- TKa — Cretaceous - Early Tertiary milky quartz vein
- TKd — Cretaceous - Early Tertiary quartz diorite
- p€-TKgp — Precambrian or Cretaceous - Early Tertiary gabbro and pegmatite
- p€sgg — Precambrian schist, gneiss and granite
- contact, dashed where approximately located
- gradational contact
- fault, dashed where approximately located, dotted where concealed, barb on down thrown side
- vertical foliation
- 50 — strike and dip of foliation

the district's production. The workings consist of a single, open incline that is approximately 74 meters deep, two levels of development, a large, northwest-facing open-cut (Figure 3), and numerous prospect pits.

The El Tigre vein is hosted in a moderately complex assemblage of crystalline rocks (Figure 4). The oldest rocks are intensely deformed Proterozoic schists with gneiss bands and granitic pods. These rocks are intruded by an assemblage of coarse-grained to pegmatitic granite and gabbroic pegmatites. The gabbro contains pyroxenes up to 5 cm in diameter and is locally foliated. The granitic pegmatite is not foliated.

The youngest intrusive unit at the mine is a medium- grained, equigranular quartz diorite whose contact to the gabbro-pegmatite assemblages trends northeast. The quartz diorite is gossan stained and the feldspars are slightly argillically altered. The quartz diorite is considered to be younger than the schist complex and the gabbro-pegmatite assemblage because the quartz diorite lacks foliation and has a relatively "fresh" appearance. A second criterion, whose systematics are discussed separately, the coincidence of the REE pattern of a sample from the quartz diorite (ET 1) with the pattern of the 70.1 Ma regional granodiorite (Reynolds et al., this volume), argues for a Late Cretaceous age for the quartz diorite intrusive at the El Tigre. The crystalline rocks are overlain by Miocene Dead Horse basalt and poorly to moderately sorted Late Tertiary-Quaternary gravels.

The structural geology of the El Tigre mine is relatively simple. The El Tigre vein itself trends N40°E 30° NW and is along a fault or shear zone (Figure 3). Slickensides striae and mullions plunge down the dip. A regional structure, the Little Horn Peak fault, trends N50 °W

and has a low to moderate southwest dip. The fault drops moderately dipping mid-Tertiary basalt down against the Proterozoic rocks and cuts off the El Tigre vein on its southwest end. The El Tigre vein is similarly cut off to the northeast by an inferred structure that is presumably sympathetic to the Little Horn Peak fault.

The El Tigre vein outcrops along strike for 30 m and is 2 m thick over a 3 to 5 m length. To either side of this bulge, the vein thins down significantly (Figure 3). The major lens is paralleled by several smaller ones and is discordant to Proterozoic foliation. The vein material is brecciated, iron-oxide-stained bull quartz that locally contains native gold. At depth, specularite, limonite, and manganese oxides are abundant. The wall rocks have spotty, moderately intense alteration.

A single doubly polished slide of milky quartz was made from vein material. Fluid inclusions of greater than 5 microns are rare and difficult to find. Most of the inclusions are less than 3 microns. The inclusions are simple two phase, vapor-liquid inclusions and range from 8 to 20 percent vapor (avereage of 12 percent vapor). None of the inclusions homogenized when heated to 400° C. Presumably the inclusions would either homogenize at higher temperatures or would never homogenize because the small size metastably inhibits homogenization. The small size of the inclusions precluded reasonable expectations of achieving freezing point depressions, and so no attempts were made.

Assays (Table 2) from a number of different sources were plotted to characterize metals from the Big Horn district (Nicor files, 1985; Tri-con files, 1984; this study). Plots display fairly tight clustering of the El Tigre assays (Figures 5, 6, and 7). The relative homogeneity of

Figure 5. As vs. Au assay plot for selective prospects of the Big Horn district. Each assay is from high grade dump or vein material from the repective mine. Pump mine and Molly Davenport assays courtesy of TRICON Mining.

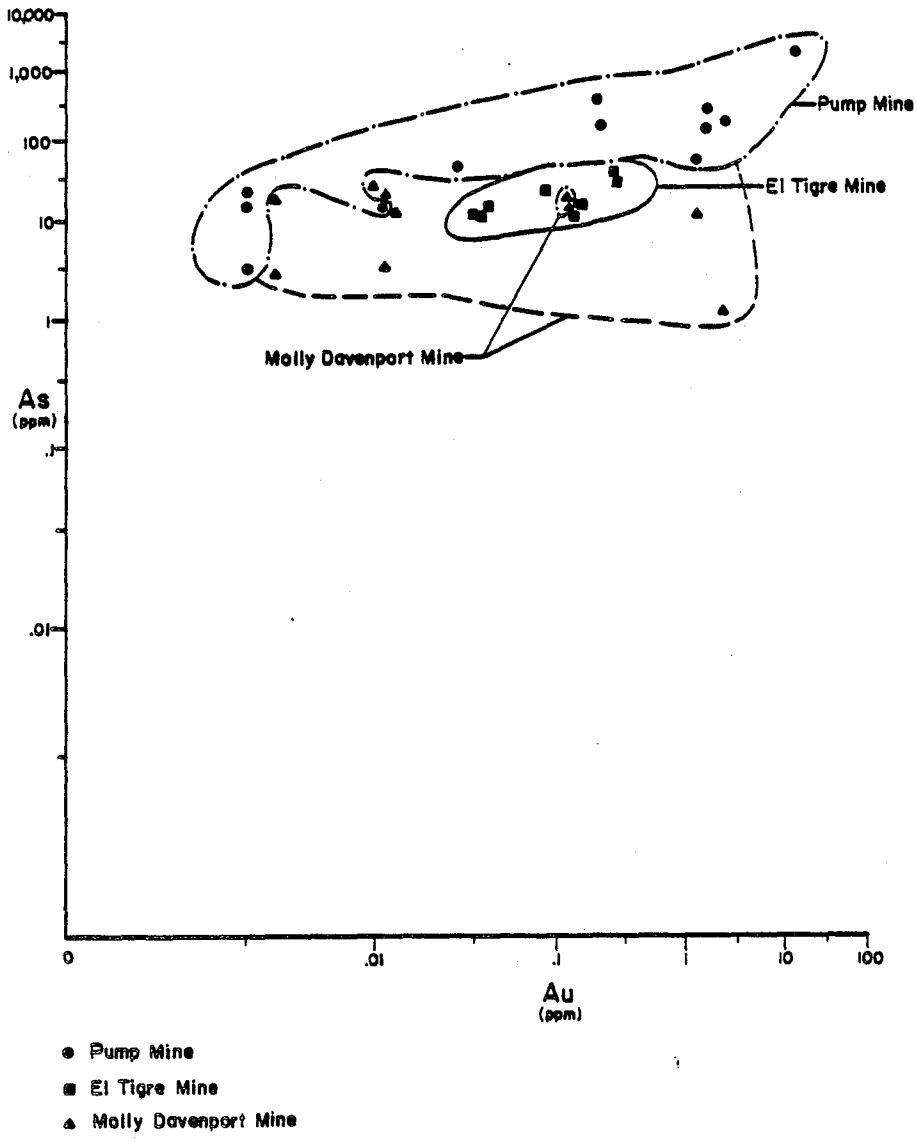
10,000
1,000
100
10
1
.1
.01
As
(ppm)
Pump Mine
El Tigre Mine
Molly Davenport Mine
0
.01
.1
1
10
100
Au
(ppm)
Pump Mine
El Tigre Mine
Molly Davenport Mine

Figure 7-6 Ag vs. Au plot for selective prospects from the Big Horn district. Each assay is from high grade dump or vein material from the repective mine. Pump mine and Molly Davenport assays courtesy of TRICON Mining.

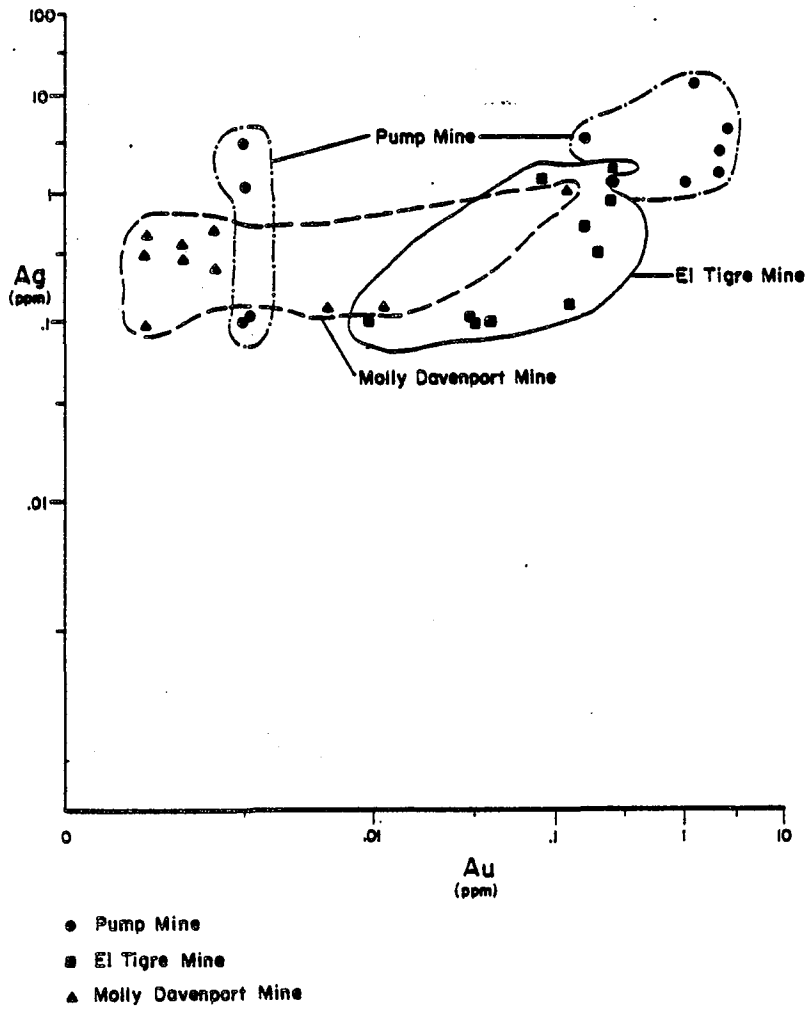
100
10
1
.1
.01
Ag
(ppm)
Pump Mine
El Tigre Mine
Molly Davenport Mine
0
.01
.1
1
10
Au
(ppm)
Pump Mine
El Tigre Mine
Molly Davenport Mine

Figure 7. Pb vs. Au plot for selective prospects from the Big Horn district. Each assay is from high grade dump or vein material from the repective mine. Pump mine and Molly Davenport assays courtesy of TRICON Mining.

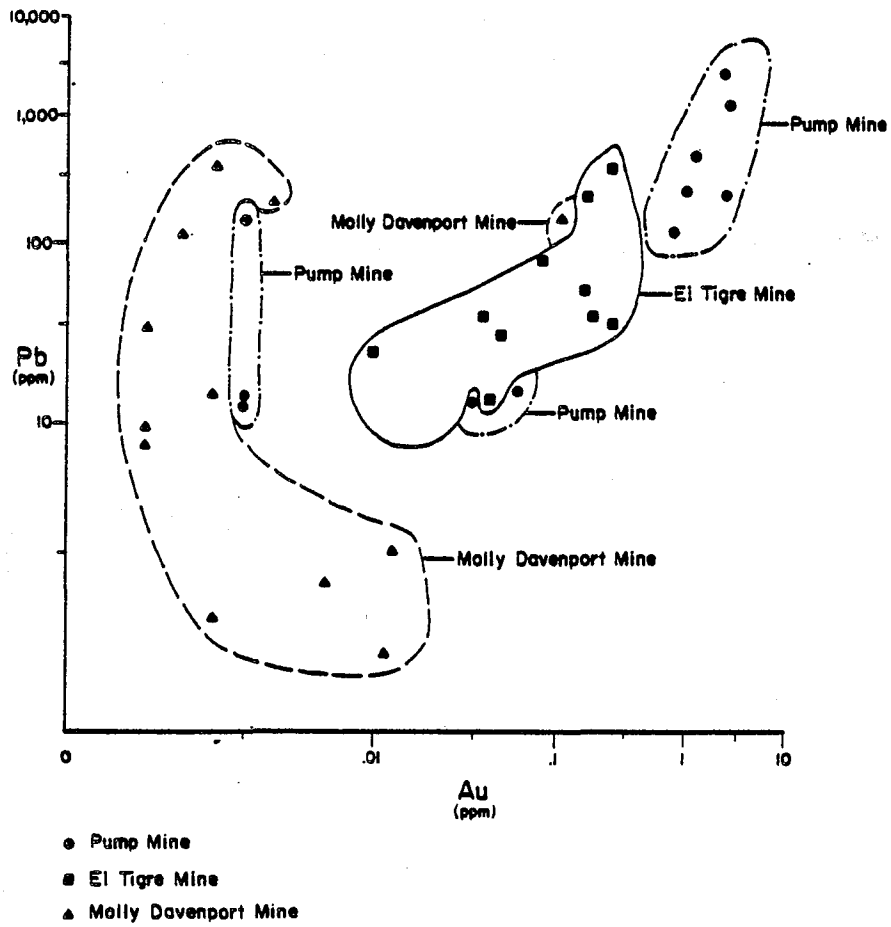
10,000
1,000
100
10
Pb
(ppm)
0
.01
.1
1
10
Au
(ppm)
Pump Mine
Molly Davenport Mine
El Tigre Mine
Pump Mine
Pump Mine
Molly Davenport Mine
Pump Mine
El Tigre Mine
Molly Davenport Mine

Table 2. Metal assays are from high grade dump grab samples. High grade samples were taken to illuminate anamalous metals and are not intended to represent ore grades. Samples locations are on district location maps.

UNITS?

Table 2. Precious and Base Metal Assays

Sample	Au	Ag	Pb	Zn	Cu	As	Sb
B53GA	23.99	19.88					
B15GA	0.09	2.4					
B52GA	0.01	1.4					
B47GA	0.46	3.0					
B7GA	0.26	30.0					
B23GA	< 50	<0.5	96	200	26	68	22
BH1	<50	5.5	38	130	96	<5	0.8
K3	<50	<0.5	32	270	130	5	1.0
ET4	<50	<0.5	34	69	290	12	0.5
Dead Horse	0.03	3.2					
Pegrin Well	0.16	0.8					
K4	<0.2	0.2					
Wisconsin	3.5	0.2					
Mollie D.	<0.02	0.2					
Mollie D.	<0.02	0.4					
ET1	0.09	2.0	87	123	30	37	2
ET2	0.435	2.4	543	653	60	44	2
ET3	0.21	0.7	32	106	20	13	2
ET4	0.425	0.9	50	170	38	61	2
ET5	0.250	0.5	55	277	53	24	2
ET6	0.18	0.2	70	400	65	17	2
ET7	0.055	0.1	26	154	82	13	2
ET8	0.065	0.1	45	128	61	23	2
ET9	0.055	0.1	57	228	77	15	2
ET10	0.010	0.1	33	124	65	27	2
A1235	3.3	23	10,000	4700	15,000		
A1236	6.8	20	90	250	75		
A1237	0.17	2.6	1400	100	930		
A1238	<0.02	1.4	110	55	290		
PM1	0.005	5.1	273	256	317	12	
PM2	0.005	1.3	17	86	20	28	
PM3	1.61	10.2	691	615	4797	277	
PM4	1.040	1.4	375	60	473	136	
PM5	3.350	2.9	4326	1376	406	113	
PM6	4.400	2.5	1363	188	2099	576	
PM7	0.970	0.2	139	596	390	87	
PM8	0.05	0.1	26	163	42	10	
PM9	3.9	4.0	334	140	523	218	
PM10	0.075	0.1	27	148	38	14	
PM11	0.005	0.4	21	99	32	12	
PM12	56.00	10.0	23,442	1249	4129	4925	
MD1	0.115	1.1	282	99	64	24	2
MD2	0.002	0.7	32	236	32	12	2
MD3	0.003	0.5	51	451	51	9	2
MD4	0.003	0.6	43	272	43	2	2
MD5	0.002	0.1	19	20	19	20	2
MD6	0.004	0.4	24	23	24	10	2
MD7	0.016	0.2	10	6	10	10	2
MD8	0.008	0.2	29	28	29	15	2
MD9	0.002	0.5	26	16	26	179	2

MD10	0.004	0.7	83	67	83	9	2
MD11	0.004	0.1	40	48	40	37	2
MD12	0.006	0.2	115	371	115	41	2
BH110	<1						
Rainbow	<0.02	<.2					
Rainbow X.	<0.02	0.2					
Weldon	0.04	47					
Snowball	0.05	0.4					
Alaska	1.3	1.4					
Paleoz.	<0.02	0.02					
Paleoz.	0.41	1.2	25	140	4400		
Black Q.	<0.02	1.0					
Black Nug.	0.05	<0.2					
Apache	0.04	<0.2					
Valley V #1	<0.02	3.4					
Valley V #2	0.03	0.4					
Fugatt	<0.02	3.2					
B23GA	5.5	>4000	270				
Scott	<0.02	3.4					
XR3	0.32	13	330	270	270	7	2.2
Well	0.05	0.6					
Black Dia.	0.83	2.8	55	40	205	90	<2
Black Dia.	0.06	6.2	200	305	950	20	<2
A-1811	1.6	62	13,500	16,000	10,500	20	4
A-1812	3.1	>350	17,000	24,000	89,000	220	16
XR12	<0.05	0.5	160	360	22	22	2.3
XR13	2.1	1000	24,000	8600	120,000	980	58
A-1816	1.9	3.4	245	155	1300	40	2
A-1817	1.1	1.4	170	70	800	<10	<2
A-1818	0.86	1.4	60	65	740	30	2
A-1819	8.5	2.4	15	100	1450	30	<2
XR1	1.9	7.0	2600	99	9500	53	3.4
XR9	170	0.5	130	32	330	15	1.0
A-1823	0.96	1.2	20	110	5500		
A-1242	0.34	0.6	51,000	1500	75		
A-1243	0.05	5.8	64,000	1400	120		
A-1244	<0.02	3.6	26,000	105	25		
XR11	0.03						

the ratios suggests a single mineralizing event.

The Knabe Mine

The Knabe Mine is located in northwest part of the range. The mine is approximately 2 km west of Little Horn Peak. No mineral production has been documented from the property and development is limited to three prospect pits, three-meter deep drill holes, and some bulldozer scrapings adjoining the pits.

The oldest rocks in the Knabe area are the same schists and gneisses that are found 1.6 km to the north at the El Tigre mine (Figure 8). The metamorphic rocks are intruded by a granite which hosts mineralization and is locally highly fractured. The granite is typically medium-grained, but locally pegmatitic. Biotite constitutes up to 4 percent of the granite, and is commonly altered to chlorite. Limonite after pyrite is common in fractures. Muscovite is common in the limonitic zones where it occurs as clots and composes up to 10 percent of the rock volume. Quartz-eye porphyry texture also commonly occur in alteration zones. The granite is argillically altered in mineralized zones. It is unclear from field relations whether the granite is Proterozoic, Late Cretaceous, or an assemblage of both. At the boundaries of the granite, in areas immediately surrounding the Knabe pit, are porphyritic, limonitic diorite dikes of varied orientations. Their outcrop pattern suggests they are border phases. This interpretation would make the main granite more likely to be late Cretaceous than Proterozoic because the REE pattern of dioritic dikes is exactly coincident with the REE pattern of the 70.1 Ma granodiorite (Figure 10). Alternatively, dikes that are spatially associated with mineralization could postdate the biotite granite. The total area of

Figure 8. Geologic map of the Knabe mine.

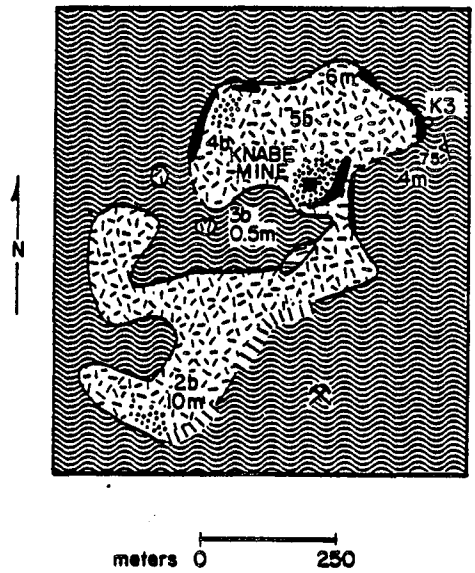

GEOLOGIC MAP OF THE KNABE MINE AREA

TKf	Cretaceous–Early Tertiary felsite dike
TKd	Cretaceous–Early Tertiary fine-grained diorite dike
p€g	Precambrian iron-oxide-stained medium-grained granite
p€sgg	Precambrian schist, gneiss and granite
	iron-oxide alteration
xb	percent biotite present
ym	percent muscovite present
	contact, dashed where approximately located
	gradational contact
50	strike and dip of crystalloblastic foliation
	manganese prospect
	shaft

alteration does not exceed 200 square meters and occurs in numerous patches. Mineralization is mostly expressed as iron-oxide staining in granite adjacent to dioritic dikes. Outcrops in the northwesternmost prospect pit have up to 20 percent limonite after pyritohedral pyrite. The feldspars of the host granite are 50 percent argillically altered. Coarse sericite is abundant in the mineralized zones, but was not observed outside of the immediate Knabe area's granite.

The Pump Mine

The Purple Pansey or Pump Mine is located in the northern end of the range. The mine has produced a small amount of gold and consists of three major shafts and numerous pits. In 1984, TRICON Minerals of Vancouver tried a heap leaching operation which left a small ore pile near the main road. The following discussion is based on mapping by P. Willard, TRICON Minerals (1984).

The country and host rocks are medium-grade metavolcanic and meta-intrusive rocks. The meta-intrusive rocks are intensely mylonitized near the vein. The Pump is coincident with the westernmost occurrence of sericite schist in the Big Horn Mountains (Reynolds et al, this volume). Mineralization occurs in a 1440-m-long quartz vein of highly varied thickness (Figure 9) The quartz vein is in a shear or fault zone that ranges from 15 cm to 2 m in thickness. The southern half of the vein trends N80^{o}E to N80^{o}W, dips 40°, and cuts crystalline rocks that have a N65^{o}E, 45°NW attitude. At its west end, the vein bends to the north, probably in response to drag on a mid-Tertiary low- to moderate-angle fault. Metzger (1938) reports iron, copper, lead, and zinc oxide at the surface with their respective sulfides at depth. Epidote is a pervasive gangue. Wulfenite and an unidentified yellow mineral

(massicot ?) were found on a dump west of the main road. Metal-ratio plots display a bimodal distribution for Pump Mine gold values (Figures 6,7 and 8). The larger population is distinctly higher than representative Big Horn district gold occurrences at the El Tigre and Molly Davenport Mines. The second, smaller population is typical of the district. In comparison with the El Tigre and Moly Davenport mines, the metal plots also point to higher arsenic values for the larger of the two Pump populations.

The Pump mine is distinctive from the other mines within the Big Horn district for the following reasons; (1) the absence of Late Cretaceous rocks, (2) the presence of silicic metavolcanic hosts, (3) the east-west and northwest strikes, (4) the rough coincidence of mineralization with crystalloblastic foliation, (5) the apparently elevated arsenic values, (6) the presence of abundant epidote, and (7) and the great linear extent of the Pump Mine. The general attributes of the Pump are permissive of a metamorphic origin as proposed by Boyle (1979) for the Archean occurrences of Canada.

The Dead Horse Prospect

Dead Horse prospect is located at the northernmost headwaters of Dead Horse Wash. No production is known from the prospect. Development consists of short trenches and a vertical shaft, which is 15 m deep that serves a level of unknown extent. The country rocks and host are pegmatitic and aplitic varieties of the regional Late Cretaceous monzonitic to granodioritic intrusives. The biotites of the monzonite are conspicuously fresh. Mineralization is localized in quartz pods of indistinct orientation, but iron-oxide staining is roughly aligned east-west and covers an area 100 m by 7 m. There is also a mineralized

Figure 9. Geologic outcrop map of the Pump mine (modified after mapping by P. Willard of TRICON Minerals, 1984).

Tba	Miocene basaltic andesite	=====	road
KpЄp	Precambrian or Late Cretaceous pegmatites	50	shaft with vein dip
pЄms	Precambrian muscovite schist	30	vein, bars on down dip side
pЄsg	Precambrian schist and gneiss	- — - -	contact, dashed where approximately located
pЄgg	Precambrian granite gneiss	50	strike and dip of crystalloblastic foliation
pЄad	Precambrian amphibolite or diorite	— ? —	approximately located fault, barb on down thrown side, question marks where inferred

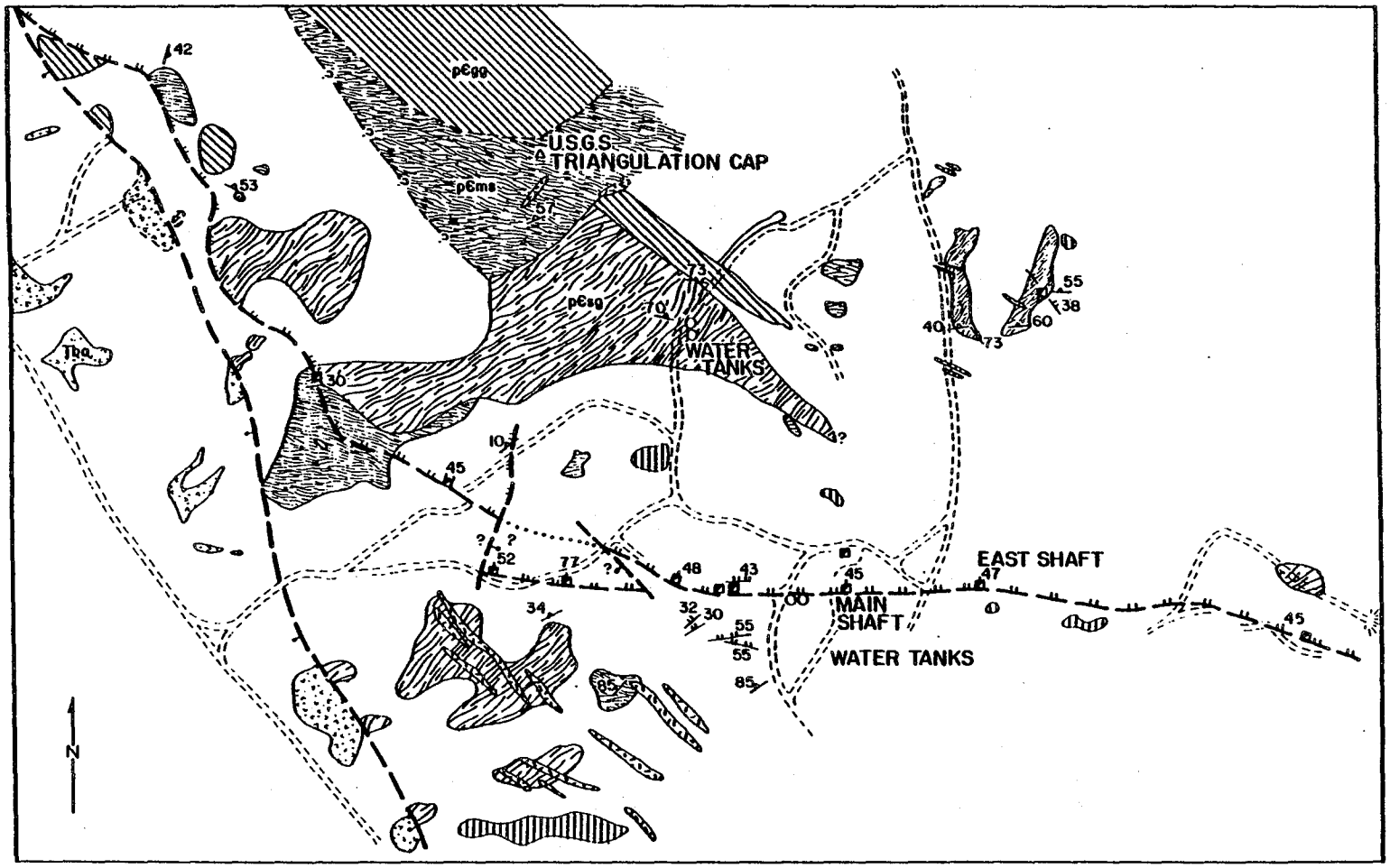

meters 0 50

GEOLOGIC OUTCROP MAP OF THE PUMP MINE

Figure 10. Chondrite normalized REE plot of mid-Tertiary volcanics, ore related intrusives (K3, ET 4, B23GA), and the Late Cretaceous granodiorite. Leedey chondrite used for normalization (Masuda et al., 1973). The Belmont Granite and the Beer Bottle rhyolite Eu assays are below detection limits of 0.2 ppm and 0.4 ppm respectively. Those limits were arbitrarely choosen to depict the unknown concentration for the REE plots. Capps et al. and Reynolds et al. (this volume) provide descriptions and age determinations respectively for the Belmont Granite and Big Horn suite rocks.

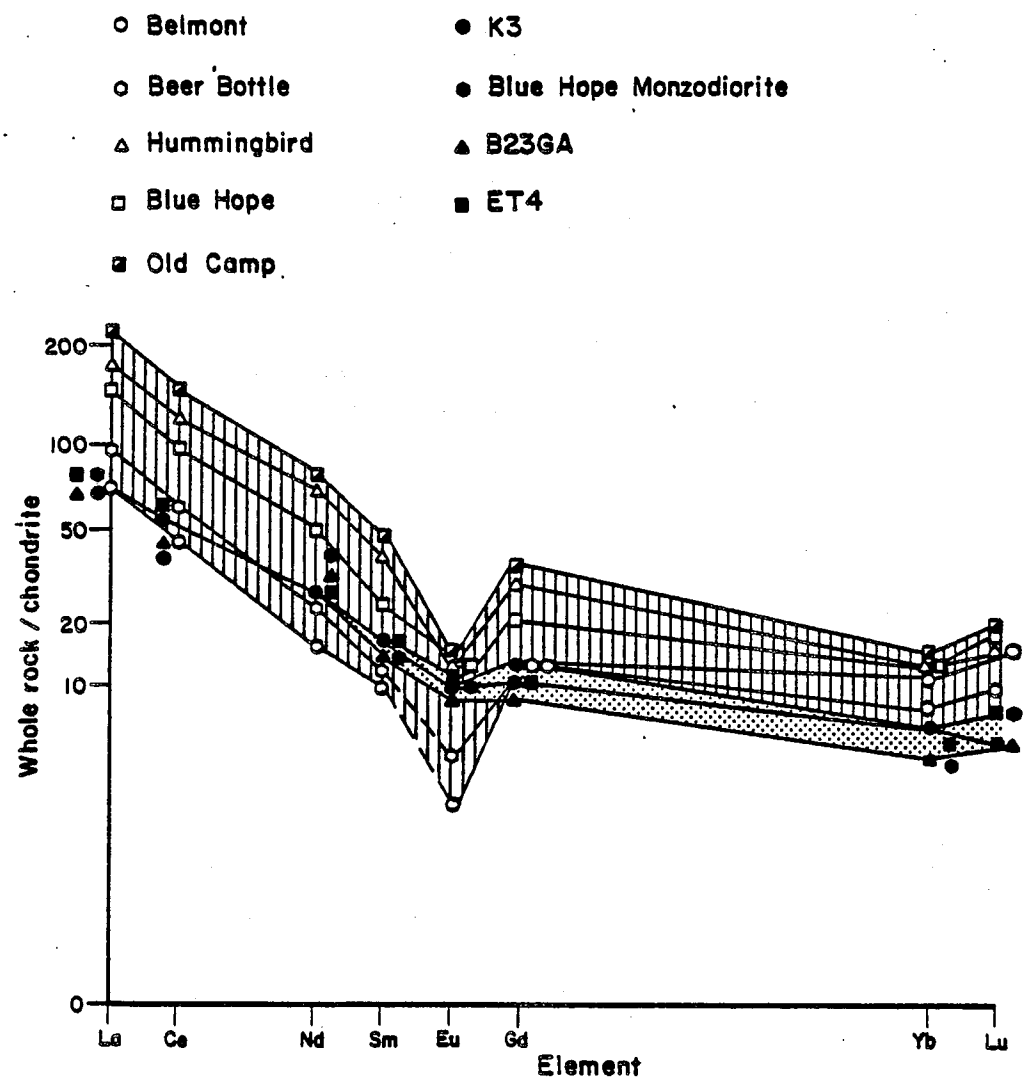

REE PLOT OF BIG HORN MOUNTAIN IGNEOUS ROCKS

Table 3. Trace element assays are mostly from altered but not replaced host rock material from various prospects. Sample locations are keyed to district maps. XR13 is a sample of vein replacement material from the Tonopah-Belmont mine.

Table 3. Trace Elements.

Sample	SC	CR	MN	FE	CO	NI	SE	BR	RB	SR	MO
XR1	3.5	240	92	9.1%	<5	14	<10	<5	<100	<1000	10
K3	15.0	10	840	7.3%	19	18	<10	<5	260	290	<1
XR3	12.0	70	870	2.4%	5	15	<10	<5	<100	<1000	<1
Blue Hope	8.4	300	960	4.2%	11	21	<10	<5	200	830	<1
B23GA	15.0	200	4300	5.0%	12	34	<10	<5	180	300	<1
ET4	8.1	300	560	4.5%	6	20	<10	<5	160	790	<1
XR9	3.0	190	350	36%	<5	<5	<10	<5	<100	<1000	10
XR12	4.3	200	92	1.2%	<5	6	<10	<5	250	70	<1
XR13	<0.5	80	40	3.8%	100	11	<10	<5	<100	<1000	20

	CD	CS	Y	ZR	NB	BA	LA	CE	ND	SM	EU
XR1	<2	<2				<0.1%	15	35	10	1.7	0.5
K3	<2	24	<10	140	30		23	55	20	4.1	0.9
XR3	<2	<2				8000	2	8	<10	1.3	0.9
Blue Hope	<2	3	10	160	10		28	61	20	3.8	0.9
B23GA	<2	9	10	120	20		24	44	20	3.7	0.8
ET4	<2	4	<10	160	20		31	58	20	4.1	1.1
XR9	<2	<2				<1000	3	8	<10	<0.5	<0.5
XR12	2	3	50	210	20		76	142	60	9.9	1.1
XR13	2	<2				<1000	1	8	<10	1.2	<0.5

	YB	LU	HF	TA	W	TH	U
XR1	1.7	0.2	2	<2	470	4	<5
K3	1.5	0.2	4	<2	<10	3	<5
XR3	1.5	0.2	<1	<2	40	1	<5
Blue Hop	1.5	0.3	6	<2	<10	8	<5
B23GA	1.0	0.2	3	<2	20	2	<5
ET4	1.5	0.3	5	<2	<10	7	<5
XR9	<0.2	<1	<2		1900	3	<5
XR12	4.0	0.7	8	<2	<10	12	14
XR13	<0.5	<0.5	<1	<2	20	<1	19

structure that trends N52°E 80°SE. Sericite and green mica are both common. Chrysocolla is abundant in vein material. Chrysocolla rims on remnant chalcocite cores also occur in dump material. An assay of highly altered, chrysocolla- bearing monzonite yielded 0.03 ppm Au and 3.2 ppm Ag. The Dead Horse prospect is noteworthy because it is exclusively hosted in the Late Cretaceous plutonic rocks, thereby suggesting that the Big Horn district mineralization cannot exclusively be the result of Proterozoic events.

REE Data

To constrain the age of Big Horn mineralization REE assays were obtained from three mineralized intrusives that are spatially related to Big Horn district prospects, the regional Late Cretaceous intrusives, the Belmont Granite, and four of the major mid-Tertiary silicic flow units. These data show a distinctive bimodal pattern (Figure 10). The Big Horn district assays all cluster tightly together with chondrite-normalized La/Tb averaging 6.41 and ranging from 5.07 to 6.83. The silicic flows and their inferred relation, the Belmont Granite (Reynolds et al., this volume), have a lower average chondrite-normalized La/Tb of 6.34 and a greater range of 4.14 to 7.98. These data make it highly unlikely that Big Horn district mineralization is related to mid-Tertiary volcanism. The strong similarity of the REE pattern of altered Big Horn district intrusives with that of the regional granodiorite suggest they are comagmatic, and therefore, the Big Horn district is a product of Late Cretaceous plutonic events.

Summary

Four styles of mineralization occur in the Big Horn district: (1)

northeast-trending quartz-veins with associated intermediate intrusive rocks; (2) indistinct quartz-pods without associated intermediate intrusive rocks; (3) Late Cretaceous intrusive-hosted chrysocolla bearing quartz-pods, (4) and a metavolcanic and meta-intrusive hosted linearly extensive quartz vein. The vast majority of the occurrences are the northeast-trending quartz-vein and pods with associated intermediate rocks. The intrusives range in composition from monzonite to diorite and typically contain limonite after pyrite. These deposits have low Ag/Au ratios (average of historic production 5). Their alteration consists of limited argillic and sericitic halos with abundant iron-oxide staining.

The second category of occurrences is represented by minor prospects bounding the western perimeter of the district. The Gold Bullion mine, the Gold Cord mine, and location B15GA are quartz pods of indistinct orientation and without spatially related intrusives. These prospects have quartz with limonite after pyrite, jarosite, and rare copper carbonates. Prospect B15GA has sphalerite, malachite, wulfenite, and probably barite.

Three occurrences differ from the majority of the prospects. Numerous characteristics distinguish the Pump mine. It is longer than any other vein in the Big Horn district, and it trends east-west and northwest in contrast to the typical northeast trends. In addition, it is not proximal to intermediate-composition intrusives, and it is hosted and roughly conformable to an amphibolite-sericite schist sequence. Furthermore, assays suggest the Pump may have two populations of gold, arsenic and lead values; one of which is consistent with values considered typical for the district, whereas the other has higher gold and arsenic values. The Dead Horse prospect and the Blue Hope mine

constitute a fourth, somewhat, distinctive style of Big Horn district mineralization. Both are hosted in Late Cretaceous granitoids in indistinct quartz pods and veins. Chrysocolla is the dominant metal phase, and sericite is the characteristic alteration.

Discussion

Lithologic and structural relationships combined with a matching of REE patterns of associated igneous rocks to that of the 70.1 Ma regional granitoid suggest that most of the Big Horn district is related to the evolution of the regional intrusives. The structural evidence is manifold, if somewhat oblique. The consistent discordance of the veins with Proterozoic foliation argues that the mineralization postdates the main pulse of metamorphism. The documented occurrence of gold-quartz veins that are discordant to metamorphic fabric but are still roughly contemporaneous with metamorphism (Colvinel et al., 1984) renders discordance only permissive evidence for a post-metamorphism chronology. The prevalence of northeast attitudes, in the light of the regional deformation history (Rehrig and Heidrick, 1976; Davis, 1981; Dreier, 1985), lends further structural support to a Late Cretaceous origin for most of the Big Horn district. The fact that mineralization associated igneous rocks are unlikely to be mid-Tertiary and the fact that the mid-Tertiary Little Horn Peak fault cuts off the El Tigre vein both argue that the district is pre-Miocene. Eliminating Proterozoic metamorphism metallogeny and Miocene volcanic metallogeny makes a Laramide age preferred, if for no other reason, for lack of another gold-quartz vein metallogeny. A fourth, alternative, metallogenic setting is that the district is related to the Proterozoic biotite granite. P. Anderson (personal communication, 1985) suggests that quartz veins similar to

those in the Big Horn district are found surrounding the Proterozoic Crazy Basin batholith in southern Yavapai County. The completely barren nature of the Proterozoic granite in the Big Horn Mountain and the absence of mineralized apophyses argues against this intrusive as the progenitor of the Big Horn occurrences.

The Dead Horse prospect and the Blue Hope mine are chrysocolla-dominated, quartz pods and veins that are hosted in the Late Cretaceous granitoid. Their close association with the Late Cretaceous granitoid suggests they are associated with the evolution of the granitoid.

The Pump mine alone eludes Late Cretaceous affinity. The fact that the vein does not have the characteristic northeast trend, but instead has a east-west general trend argues against a Late Cretaceous affinity. A Proterozoic age is permitted by the fact that the vein is nearly coincident with crystalloblastic Proterozoic foliation, the apparent arsenic anomaly, and the interpretation that the occurrence is hosted in a metavolcanic sequence. These characteristics roughly correspond to Boyle's (1979) model for metamorphic secretion deposits. It is unclear whether the extensive length of the vein supports or detracts from the secretion model.

TIGER WASH DISTRICT

Introduction

The barite-fluorite prospects of the extreme western end of the Big Horn Mountains are here named the Tiger Wash district. The Tiger Wash District is one of 60 distinct mid-Tertiary barite occurrences that lie in a northwest-trending belt running from Cochise through Mohave County (Hewett, 1964). The greatest producer of these districts was the Granite Reef Mine near Phoenix which produced 300,000 tons (Stewart and Pfister, 1960). Vein systems surrounding the Plomosa Mountains, 150 kilometers west of the Big horns, constitute the greatest single concentration of barite veins in Arizona (Stewart and Pfister, 1960). This study of field relations and fluid inclusion characteristics of the Tiger Wash and the adjacent east Harquahala district has been undertaken to place preliminary constraints over fluid-flow dynamics from the Bullard detachment fault into the upper plate. To achieve this the project was expanded to include reconnaissance study of the geology of the eastern Harquahala district prospects (Table 4).

The Tiger Wash district consists of several occurrences of barite mineralization with some development and a minor fluorite prospect. The only published description of the Tiger Wash occurrences is by Stewart and Pfister (1960) who report production of 600 tons from the Princess Ann group. Currently, these prospects have a deep open cut adjacent to a bulldozer-scraped area. The White or Blue Bird claims, the other developed occurrence, contain four contiguous unpatented claims that were established in 1950. Developments include a 65 m long haulage adit, and numerous open cuts.

Geologic Setting

The Tiger Wash District occurs in a sequence of Miocene mafic volcanic flows that overlie and are interbedded with arkosic sandstone and conglomerate, which locally rests unconformably on Precambrian crystalline rocks. The Miocene volcanic-sedimentary sequence is in the upper plate of the Bullard detachment-fault which is buried beneath the recent gravels of Tiger Wash (Figure 11). The Miocene sequence dips west toward the detachment fault at moderate angles and is displaced along low-angle normal faults. The mafic volcanic-sedimentary sequence of the Tiger Wash district correlates with the Dead Horse basalt member of the Big Horn volcanics (Capps et al., 1985). The Dead Horse basalt occurs near the base of the Tertiary section. In the Tiger Wash district, a generalized stratigraphic sequence from bottom to top is: (1) 35 m of arkosic conglomerate with mostly Precambrian crystalline clasts; (2) 90 m of aphyric basalt flows intercalated with fine- to medium-grained arkose beds that are as thick as 25 m; (3) 3 m of partially welded biotite tuff; and (4) 105 m of basalt flows that cap the sequence.

An outcrop of Paleozoic limestone, quartzite, and dolomite hosts a small fluorite prospect one kilometer south of the Princess Ann group. The Paleozoic rocks dip gently to the northeast, and are cut by numerous minor faults. The exposed sequence, from top to bottom, includes the following: 16 m of quartzite; 2m of limestone; 1 m limonite bearing phyllite; 23 m of quartzite with interbedded siliceous limestone; and 23 m of brown dolomite that grades into blue-grey limestone.

Structural Setting

The Tiger Wash barite-fluorite district is in the upper plate of the

Table 4. Tiger Wash District.

PROSPECT	LOCATION	PRODUCTION/ DEVELOPMENT	HOST	STRUCTURE/ GEOMETRY	MINERALOGY/ GEOCHEMISTRY
Paleozoic Block	SW 1/4, Sec 4 T4N R10W Lone Mtn. Mtn 15'.	No production or development.	Limestone.	Mineralization is in pods along a NW-trending, SW-dipping low angle fault.	Fluorite is in massive veins up to 12cm thick. Fluorite is mostly green with some purple. There are minor inclusions of chalcpy. in fluor. Chrysocolla and poss. turq. are present. Limestone host has silicic, sericiti and dolomitic alteration.
Princess Ann claims	NW 1/4, NE 1/4 Sec 4 T4N R10W Lone Mtn. 15'.	100 tons production in 1930. Present development includes a single open cut and a 30m X 60m scrapped area.	Basalt.	Deposit is veins that extend over 600m. Largest vein is 6m wide. Vein along major cut is on N55W 35NE fault.	About 5% of vein material is green and purple fluorite. USBM (Stewart and Pfister, 1960) assey: 53% barite; 15.6% fluorite; 1.7% calcite.

Unnamed prospect	Center NW 1/4 Sec 35 T5N R10W Lone Mtn. 15'.	No recorded production or development.	Basalt and arkose.	Veinlets and breccia clasts extend for 0.4 km along N65W to N55W 30NE fault. Most barite is in footwall arkose, althought some is in hanging wall basaltic andiste.	No fluorite.
White Rock claims	SW 1/4, NW 1/4 Sec 35 T5N R10W Lone Mtn. 15'.	No recorded production development consists of a 60m long haulage adit and open cuts.	Arkosic conglomerate and basalt.	Anastomozing veins ranging from 3cm to 1m are subparallel blades. Fluorite ave. 0.3 cm Barite extends over 15 to 20m wide by 60m long area. Veins are localized along E-W-trending, low-angle, normal faults.	Veins ave. 6cm and are mostly massive with lesser rosettes and single cubes which are mostly clear to straw yellow, rarely, purple. USBM assey: 86.5 % barite: 7.7% fluorite: 3.4% calcite.

Table 5. Eastern Harquahala District.

PROSPECT	LOCATION	PRODUCTION/ DEVELOPMENT	HOST	STRUCTURE/ GEOMETRY	MINERALOGY/ GEOCHEMISTRY
Alaska Mine	SE 1/4 Sec 33, T5N R10W, Lone Mtn. 15′	No recorded production but 30m X 10m X 3m tailing pile indicates some production. Numerous dozer cuts extend over 1 acre. App. 12 new drill holes on road.	Chloritic breccia.	Disseminated mineraliz..	Vein material is milky qtz. and white calc. Hematite staining of chlor. brecc. is common. Dump mater. has chryso-colla coat-ings.
Rainbow Mine	NW 1/4 Sec 7, T4N R10W, Lone Mtn. 15′.	No recorded production. Dozer cuts extend over 30m X 20m area. 25m X 11m X 6m stockpile rests beside south edge of cuts.	Chlorit. granite.	Quartz veins and pods, ave 2cm thick of irregular direction.	90% of dump material has hematite stain. Spec-ularite is common. Some purple fluor. and massive white barite. Trace chrysocolla.

Rainbow Mine Extension	Cent. Sec 6, T4N R10W, Lone Mtn. 15′.	No recorded production. Development is on 60m diameter hill that is completely scraped.	Chloritic, mylonitic schist and highly iron oxide stained, mylon. granite.	Disseminated mineraliz.	Specularite common. Pervasive py. ave. 0.1 mm. Limo. aft. py up to 2mm common. Native gold.
Snowball Mine	SE 1/4 Sec 29 T5N R10W, Lone Mtn. 15′.	No recorded production. Prospected area is extensive, consisting of many open cuts and scraped areas. Evidence of recent explor. activity.	Chloritized schist.	Fluorite miner. is in N60 to N75W 30 to 78N fault Up to 8m thick and app. 660m long.	Fluorite is abundant. Mostly grn. Black Calc. abun. but less comm. Limonite, hematite, and barite minor.
Weldon Mine	NW 1/4 Sec 7, T4N R10W, Lone Mtn.	No recorded production. Two inclines that are roughly 20m deep.	Qtzite. Qtzose. metaseds.	15 cm to 1m thick vein coincident with crystalloblastic foliation. Exposed for 30m along strike.	Quartz and fluorite, in places euhedral Limo. aft. py. common. Specularite abundant. Crysocolla rare. Paragen: cpy,fl,qtz, spec,bar, calc.

Figure 11. Location map for the Tiger Wash and eastern Harquahala districts showing the Bullard-detachment-fault (from unpublished mapping by S. Richard, 1984).

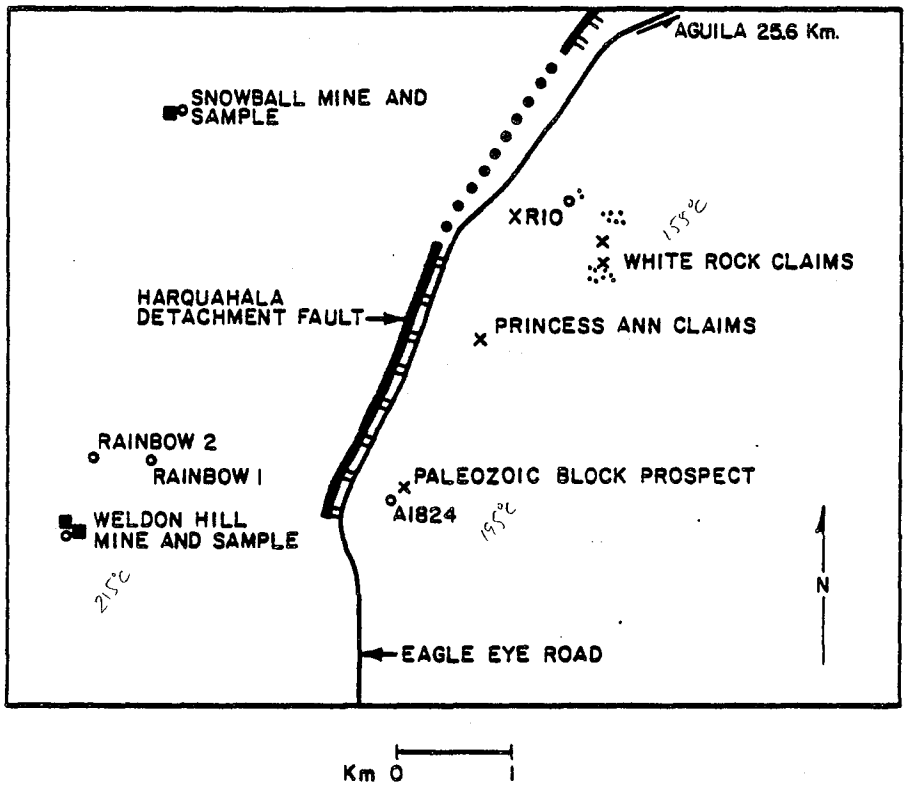

LOCATION MAP OF THE TIGER WASH BARITE-FLUORITE DISTRICT AND EASTERN HARQUAHALA DISTRICT

Harquahala detachment fault, dotted where concealed, hatchures on upper plate (from Richard, 1985)

■ mine

× prospect

○ sample location

undeveloped barite mineralization

Figure 12. Geologic map of the northern portion of the Tiger Wash district.

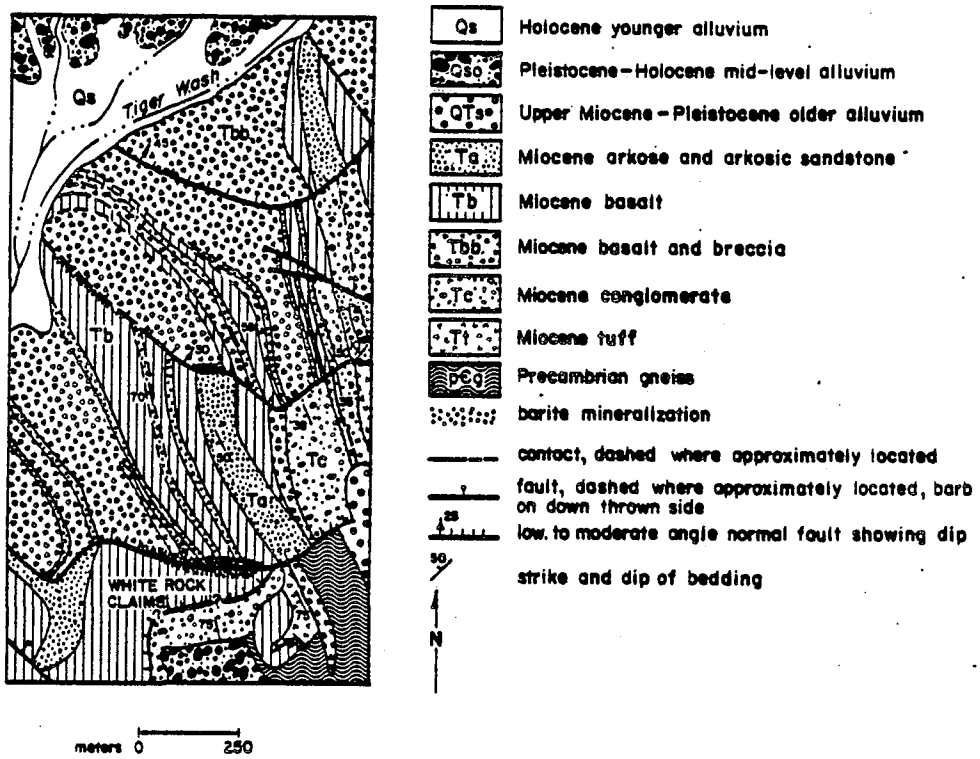

GEOLOGIC MAP OF THE NORTHERN
PORTION OF THE TIGER WASH BARITE-FLUORITE DISTRICT

Bullard detachment fault (Rehrig and Reynolds, 1980; Reynolds, 1982). The detachment fault is sporadically exposed through the gravels 0.1 to 1 kilometer west of the district (Figure 11). Upper-plate non-mylonitic volcanic and sedimentary rocks dip 45° to the west and discordantly abut into the detachment fault, which overlies highly deformed lower-plate Precambrian, Paleozoic, and Mesozoic rocks. To the north and northeast of the barite-fluorite mineralization, the Miocene section gradually bends toward the northwest strikes and dips become much more erratic. Listric faults, spaced 0.5 to 1 km apart, are probably responsible for the variation in attitude. The strike of these faults systematically varies from north-south at the southernmost barite prospect to N50°W at the northernmost occurrence (Figure 12). The dips remain moderate. The systematic change in the strike of the bedding and listric faults may be the result of large-scale drag folding along the detachment fault, such as describe elsewhere (Reynolds, 1982: Reynolds and Spencer, 1985). The Paleozoic section on average strikes N65°W and dips 35°NE. Minor faulting complicates the structure at the southern extreme of the Paleozoic block. Alteration and minor brecciation along bedding planes in the central part of the block suggest some bedding-plane displacement. In places the quartzite unit is brecciated along the margins of the block. Inferences from regional geology and attributes specific to this block strongly suggest a megabreccia origin and permit speculation that the block maybe triply allocthonous (Reynolds et al., this volume).

Structural Control Over Mineralization

The three barite-fluorite occurrences of the district are all localized on or near faults (Figure 12). The Princess Ann claims are

directly above and to the east of the Bullard detachment fault and are localized along a fault that strikes N55°W and dips 30°NE. This occurrence is more vein-like than the less productive White Rock claims and the adjacent, unnamed occurrences to the north. The White Rock and nearby unnamed occurrences are all localized along low-angle normal faults, with mineralization occurring both in the hanging wall and footwall. Where the exposure is most clear, the hanging wall is the preferred locus of barite mineralization and basaltic andesite is the preferred host. The occurrence to the north of the White Rock claims displays arkose host for barite breccia.

Mineralization in the Paleozoic Block is also localized along structures. The fluorite pods at the southern end of the block are localized along a N45°W-striking, southwest-dipping, low-angle fault. A zone of limonite after pyrite exists along a possible low-angle, bedding-plane fault in the northern one third of the Paleozoic block.

Paragenesis

Barite, fluorite, and calcite are the only phases noted by Stewart and Pfister (1960) in the Princess Ann and the White Rock claims. This author never observed calcite directly associated with barite mineralization in the district, but fluorite was consistently seen to exists both as a vug filling in barite and to be completely encased in barite at the Princess Ann and White Rock claims. These observations suggest that either barite preceded fluorite and a phase of barite mineralization followed, or the phases co-precipitated. The mineral occurrence immediately north of the White Rock claims has barite only. The Paleozoic block has fluorite with less than 10 percent calcite, minor chrysocolla, and some possible turquoise. There are also small

metallic blebs in fluorite that may be chalcopyrite. The relationship of the fluorite to the calcite is undetermined, but the chalcopyrite (?) presumably preceded the fluorite, and the copper silicate and phosphate evolved after fluorite. The absence of dissolution textures or observed crosscutting veins permits the inference that all of the phases precipitated in a narrow time frame.

Fluid Inclusion Studies

Fluid inclusion studies were undertaken on fluorite collected from five prospects in the Tiger Wash and eastern Harquahala districts (Figure 11). Cleavage slivers of fluorite were used for all of the inclusion studies. Homogenization temperatures, freezing point depressions, and preliminary crushing experiments were done to characterize the ore-forming solutions. A major pitfall in working with fluorite is the likelihood of stretching during heating or cooling (Bodnar, and Bethke, 1984). Two procedures were employed to guard against stretching. First, all of the homogenization determinations were made before any freezing was done because freezing is more likely to stretch an inclusion than heating (Bodnar and Bethke, 1984). Secondly, when freezing determinations were run, some of the freezing runs were immediately coupled with homogenization determinations to see if the homogenization temperature was anomalously higher than the previously characterized population. Also, homogenization and freezing point depressions were commonly done two or more times on each inclusion. Although the sum of these precautions does not eliminate the possibility of systematic error, the absence of any evidence of stretching from these cross checks is reassuring.

Fluid inclusions from all of the prospects are liquid-vapor

inclusions, commonly with a third gas phase present. All of the samples displayed two styles of inclusions. Fluid inclusions from the Princess Ann prospect consist of solitary inclusions that are primary and extended arrays that are pseudosecondary. The primary inclusions are generally spheroids and less commonly have rectilinear outlines. They range in size from 10 microns to 100 microns and are typically 30 microns. On average, they have 11 percent vapor, most of which is assumed to be water. Many of the the inclusions have faint double annuli, reflecting the likely presence of a third phase. The pseudosecondary inclusions are characterisitically smaller than the primary inclusions. These inclusions range from 5 microns to 30 microns. The pseudosecondary inclusions are generally spheroidal. Their arrays do not cut across the primary inclusions. The pseudosecondary inclusions average about 11 percent vapor. However, the trace of a second annulus is much less common in these secondary-appearing inclusions.

The fluid inclusions from the White Rock prospect are not markedly different from those at the Princess Ann. One distinction is that the pseudosecondary inclusions more commonly have rectilinear outlines than do the secondary inclusions from the Princess Ann. The White Rock pseudosecondary inclusions are also smaller, on average, than those from the Princess Ann. There are many arrays of 3 micron and smaller pseudosecondary inclusions in the White Rock samples. A second distinction is that the White Rock fluid inclusions average 9 percent vapor as opposed to the 11 percent total vapor for the Princess Ann inclusions. Although the second annulus is as ill-defined in the White Rock samples as in the Princess Ann, many of the primary inclusions, and

some of the pseudosecondary inclusions appear to have a third phase.

The fluid inclusions from the Paleozoic block fluorite are similar in character to the aforementioned populations, but they tend to be larger. Their size ranges up to 200 microns. The distinction between the primary and pseudosecondary inclusions is more marked than it is with the fluorite from the two barite prospects. The vapor fraction ranges from 9 to 12 percent, and a slight second annulus is generally evident.

Fluorite from the Snowball and Weldon mines of the eastern Harquahala district were selected for fluid inclusion study. Fluid inclusions from the Snowball Mine (Figure 11) are large (averaging 40 microns, varying from 20 to 120 microns), commonly necked, and very abundant. They have an average of 8 percent water vapor and nearly all show a slight second annulus of a third phase. The majority of these inclusions are presumed to be pseudosecondary. A small percentage of the inclusions are solitary and, for that reason are assumed to be primary. The Weldon Mine inclusions are descriptively similar to the Snowball fluid inclusions except that the average vapor volume of the assumed primary inclusions is 11 percent. The pseudosecondary inclusions from the Weldon Mine can also be distinguished from their correlaries at the Snowball on the basis of vapor percentage. The Weldon Mine pseudosecondary inclusions typically have 5 to 8 percent vapor.

A total of 137 homogenization temperatures and 26 freezing-point depressions were determined for the Tiger Wash district. The results (Figure 13) show distinct clustering of the homogenization temperatures. The plotted temperatures are not pressure corrected. Estimation of the overlying column of rock during the mid-Tertiary suggests 0.3 to 0.5 km burial. Since conditions of <3.8 mole percent CO_2 and 20 percent NaCl

require less than 20 temperature correction for pressures at 200° C. (Roedder, 1984), a temperature correction for pressure is not needed. The homogenization temperatures for the Princess Ann and White Rock claims range from 135° to 190° C with a few isolated determinations extending the range from 123° to 200° C. Fluid inclusions from the fluorite prospect on the Paleozoic block have homogenization temperatures that are distinct from the Princess Ann and White Rock barite-fluorite prospects homogenization temperatures. The fluorite temperatures narrowly cluster from 190o to 210° C (Figure 13).

Fifty homogenization temperature determinations on fluorite were made from the Snowball and Weldon mines of the eastern Harquahala district material. Between the two mines there is a distinct bimodal distribution (Figure 13). The Snowball Mine displays a range from 160° to 190° C with a few determinations in the 200° to 220° C range. In contrast, the bulk of the Weldon Mine homogenizations cluster from 200° to 230° C around a peak of 210° to 220° C.

The salinities (Figure 14) are total NaCl equivalent calculated from freezing-point depressions using the equation from Potter et al. (1978). The raw data is presented and not corrected for possible CO_2 content because the numerous uncertainties over the species and volume of possible CO_2 in these inclusions. Collins (1979) and Hedenquist and Henley (1985) discuss the important controls that non-water phases, and CO_2 in particular, have over freezing point depression. To determine the extent of CO_2 in the Tiger Wash fluid inclusions, a number of samples were cooled to minus 96° C. No clathrates formed and no double melting point was observed. The large size of the observed inclusions (greater than 100 microns) makes it seem unlikely that the clathrates

Figure 13. Histograms of homogenization temperatures from range wide fluid inclusion locations. Determinations are not pressure corrected. Fluid inclusion host minerals are as follows: Eastern Harquahala district, fluorite; Tiger Wash district, fluorite; Aguila district, calcite; Osborne district; the US mine, fluorite, the Contact mine, amythestine quartz, the Scott mine, calcite. Small, single blocks indicate a single determination. Large blocks indicate a number of determinations that fall within a 5° C range.

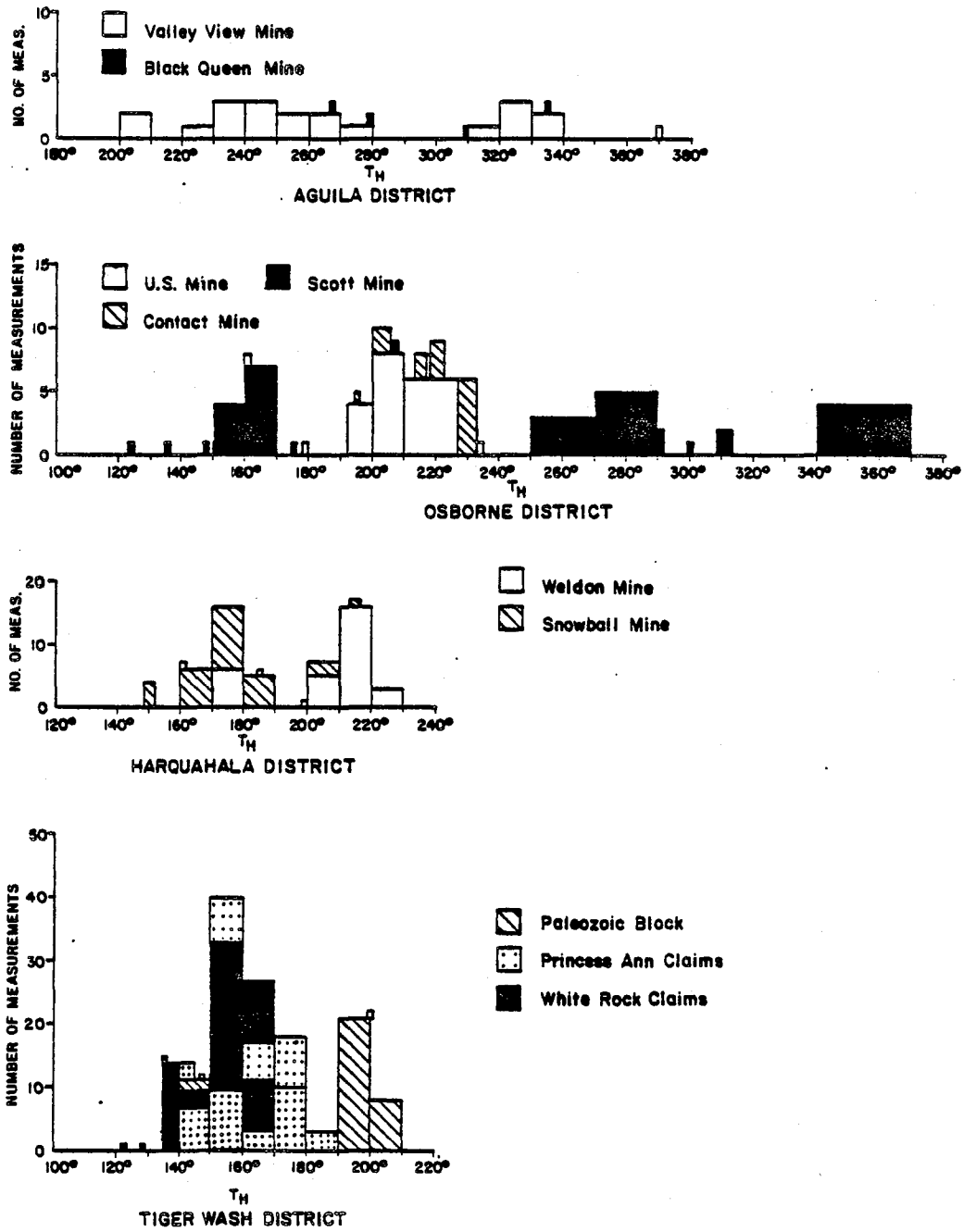

HISTOGRAMS OF HOMOGENIZATION TEMPERATURES FROM FLUID INCLUSIONS

Figure 14. Histograms of weight percent NaCl equivalence of fluid inclusions from the Big Horns. Salinities are not corrected for CO_2 content or probable high potassium proportion. Fluid inclusion host minerals are as follows: Eastern Harquahala district, fluorite; Tiger Wash district, fluorite; Aguila district, calcite; Osborne district, the US mine, fluorite; the Contact mine, amythestine quartz; the Scott mine, calcite. Small, single blocks indicate a single determination. Large blocks indicate a number of determinations that fall within a 5° C range.

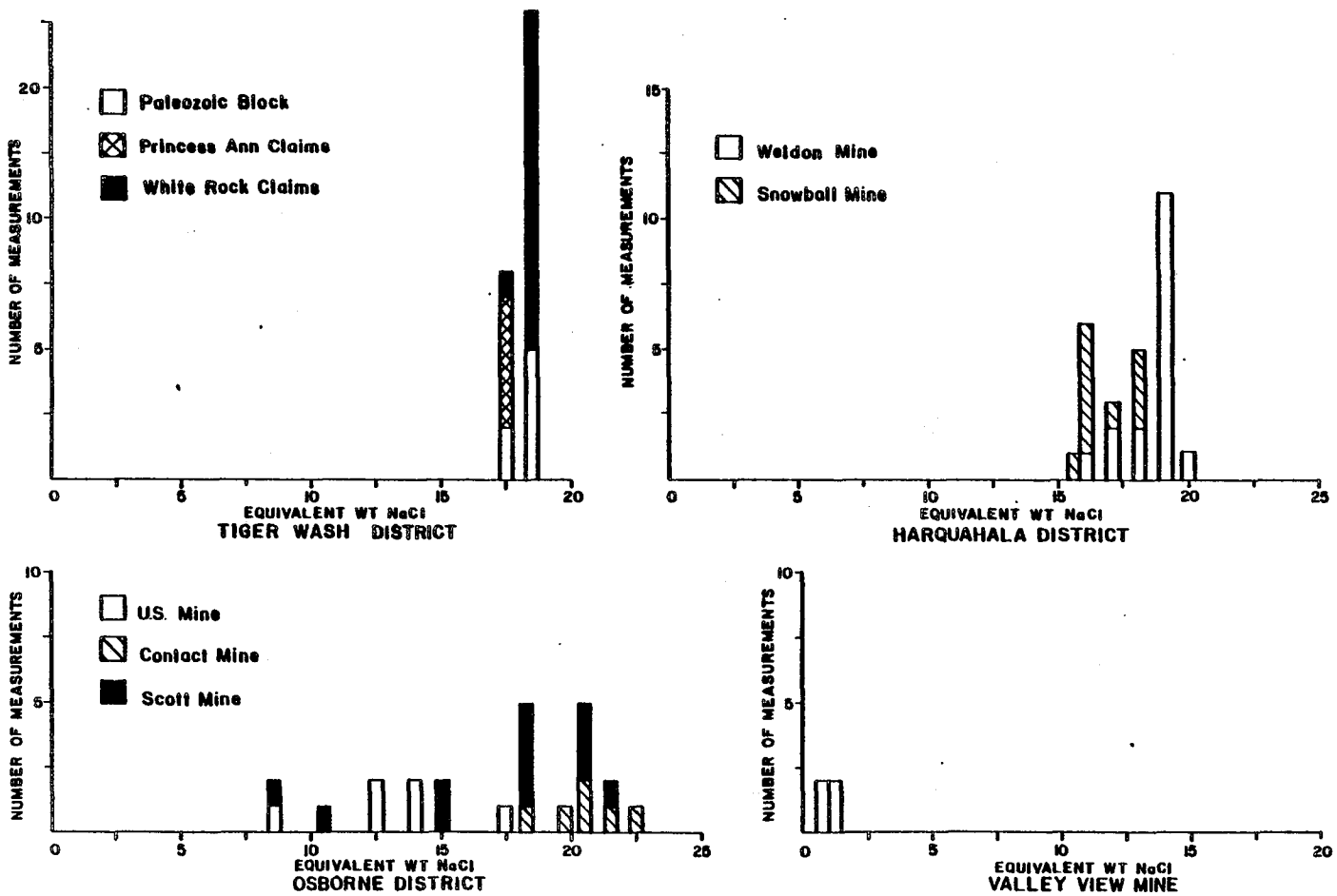

HISTOGRAMS OF WEIGHT PERCENT NaCl EQUIVALENT OF FLUID INCLUSIONS

were missed. Alternatively, it is assumed either that the CO_2 content is too low to allow clathrate formation, or that the annulus on the water vapor bubbles is from another phase. Preliminary crushing experiments with both glycerine and kerosene indicated the presence of both CO_2 and methane, or possibly, a more complex hydrocarbon.

A total of 41 freezing-point depression measurements were obtained from the Tiger Wash district fluorites (Figure 14). The salinities cluster tightly at 17 to 18 percent. Twenty seven freezing-point depression measurements were obtained from the eastern Harquahala district prospects. The NaCl equivalents of the Snowball Mine range from 16 to 18 percent. The NaCl equivalents for the Weldon Mine range from 16 to 20 percent.

The fluid characteristics from the Snowball Mine are not notably different from those of the barite-fluorite prospects in the Tiger Wash district. The uncertainties over compressible gas content render the absolute value of the NaCl equivalent of unknown significance. The fact, however, that the NaCl equivalents are high, 17 to 18 percent, and all cluster tightly together remains notable. The nearly identical salinities suggest all of these occurrences evolved from the same hydrothermal system. The high NaCl equivalents for an epithermal deposit, even when corrected for as much as 7 percent CO_2 which would require a 50 percent salinity correction of the average NaCl equivalent to 12 percent, places the Tiger Wash-forming hydrothermal solutions at the extreme end of salinities for epithermal systems (Roedder, 1984). The high salinities suggest either a magmatic, metamorphic, or basinal brine component to the fluids responsible for Tiger Wash district mineralization (Beane and Wilkins, 1985).

Hypothetical Mechanisms for Barite-Fluorite Mineralization

Holland and Malinin (1979) outlined likely mechanisms for barite and fluorite precipitation. Viable mechanisms for fluorite precipitation include an increase in salinity, decrease in temperature, increase in pH, and mixing of fluorine-bearing solutions with calcium-rich solutions. Viable mechanism to precipitate barite include decreased total NaCl, decreased temperature, and mixing of connate brines with hydrothermal solutions.

A comparison of the fluid characteristics and styles of mineralization of the detachment-hosted deposits in the Harquahala district to those of the Tiger Wash district permits testing the assumption that the heat source for upper-plate mineralization is the elevated geothermal gradients of the middle-crustal, lower-plate rocks. By assuming fluid flow from the detachment surface into the upper plate, the differences in fluid characteristics between the zones serves to model the efficacy of mineral-precipitation mechanisms.

In comparing the characteristics of the Weldon Mine fluorite fluid inclusions to those of the Tiger Wash district, a weak case can be made for a salinity gradient, but a fairly significant temperature gradient can be inferred from the homogenization temperature differences between the areas. The clustering of the Weldon homogenization temperatures around 215° C contrasts with the Paleozoic-block, fluorite homogenization temperatures that cluster around 195° C and even more markedly so with those of the White Rock claims that cluster at 155° C. The data suggest a 60° C temperature differential between the precious metal detachment hosted fluorite gangue and fluorite from 5 km to the northwest.

Efficacy calculations based on this 60° temperature difference,

thermochemical data from Richardson and Holland (1979), and the assumption that the White Rock prospects have a total of 100 tons of fluorite that was deposited from 2 molal NaCl solutions, yield a flow rate of 150,000 liters/year for 100,000 years as the necessary volume to deposit 100 tons. The 1 to 2 percent total salinity difference between the Weldon and the White Rock claims is too small to be significant in view of the extensive uncertainties of these calculations. In any case, a decrease in salinity causes dissolution of fluorite, not precipitation, thus rendering salinity change an unlikely cause of fluorite precipitation in the Tiger Wash district. None of the observations made for this study can constrain the possibility of a change in pH as control over fluorite precipitation. The fourth of the viable mechanisms for fluorite precipitation that Holland and Malinin (1979) discuss is the mixing of fluorite-rich waters with calcium-rich waters. Some geologic evidence can constrain the possible influence of this mechanism. The occurrence of the White Rock claims (Figure 12) at the fault contact between calcium-basalt on the hanging wall and arkosic conglomerate in a lower footwall allow for rising fluorine rich solutions mixing with fluids in equilibrium with the upper calcium-rich basalt.

The difference in fluid characteristics from the Weldon Mine to the White Rock prospects can also be used to test the viability of mechanisms for barite precipitation. Using the thermochemical data from Blount (1977) and the assumption of 2 molal NaCl solutions, a 900 ton barite deposit can be generated by means of the 60° C difference at a rate of 350,000 liters of hydrothermal fluid per year for 100,000 years. Using the 2 percent weight NaCl equivalent difference from the

Weldon Mine to the White Rock, and assuming the fluids were at 200° C and 500 bars, Blount's (1977) data shows a rate of 350,000 liters hydrothermal fluid/year for 100,000 years would also yield the 900 tons of barite. None of the research engaged here lends direct bearing on the mixing model for barite deposition. The suggestion that detachment-related, high-salinity fluids may have a basinal brine component, (Beane and Wilkins, 1985) coupled with the observation that the mineral deposition is roughly contemporaneous with volcanism, permits, but does not prove, mixing of hydrothermal fluids with basin brines.

A Model for Barite-Fluorite Mineralization

The precise chronology of mineralization with respect local faulting and detachment faulting remains elusive. The absence of bedded deposits, which one might expect if the mineralization completely preceded faulting, makes a completely pre-deformation origin unlikely. The presence of barite clasts in fault breccia at the northernmost of the occurrences places an upper age bracket on mineralization, and demonstrates that at least some of the mineralization was contemporaneous with faulting. The east-northeast to northeast offset of the Tiger Wash prospects from the Weldon mine is consistent with the sense of offset along the Bullard detachment. If the fluids flowed up into the upper plate and the Tiger Wash occurrences are the upper-level expressions of the Weldon mine mineralization, then the mineralization occurred before the final 4 to 8 kilometers of offset along the Bullard detachment.

The hydrothermal gradient implied in drawing a source line from the Weldon Mine in the Harquahala district through the Paleozoic-block fluorite prospect to the Princess Ann prospect and beyond to the White

Rock claims suggests an evolution of fluids. Schematically, the fluids start as fluorine and barium rich at 220° C, then flow northeast toward the Paleozoic block where a cooling of 15° C causes precipitation of fluorite and minor sulfides. Further flow to the Princess Ann prospect is attended by a 25° C temperature drop and a slight dilution of 1 to 2 weight percent NaCl, whereupon barite and fluorite are deposited. Temperature drops centered on the low-angle faults of the White Rock area cause further barite and fluorite deposition. The fluid is thereafter so depleted in fluorine that only barite precipitates upon further cooling in the northernmost prospects. If one allows for cooling as the only mechanism for fluorite precipitation and cooling coupled with dilution for barite precipitation, fluids take 150,000 and 175,000 years respectively to account for an estimated 1000 tons of 10 percent fluorite and 90 percent barite.

AGUILA DISTRICT

Introduction

The Aguila manganese district, located in the western and west-central Big Horn Mountain, ranks as the second greatest producer of manganese in Arizona. Production was 186,117 lb. (Welty et al. 1985). At the present-day price of 70 cents per pound of manganese, production from the Aguila district is valued at $32,000,000, which is thirty times the value of Bighorn gold district production and ten times the value of Osborne district production.

Previous Investigations

The individual mine geology, development status, and production history of the Aguila district are described in Jones and Ransome (1919), Wilson and Butler (1930), and Farnham and Stewart (1958). These authors focused on ore-body geometries, localizing structures, and major features of host lithologies and paragenesis. Their work is the basis for the individual prospect tabulation (Table 6). The early workers did not address the relationship of the mineralization to district-wide or regional structures. This present study was directed at understanding the influence of regional structures and host-rock types on mineralization.

Welty et al. (1985) characterized the district mineralization and state that the abundance of manganese prospects hosted in mid-Tertiary volcanics requires that mineralization be mid-Tertiary or younger. They did not discuss the possible relationship to detachment events.

Geologic Setting

The regional setting of the Aguila district is the same as the Big

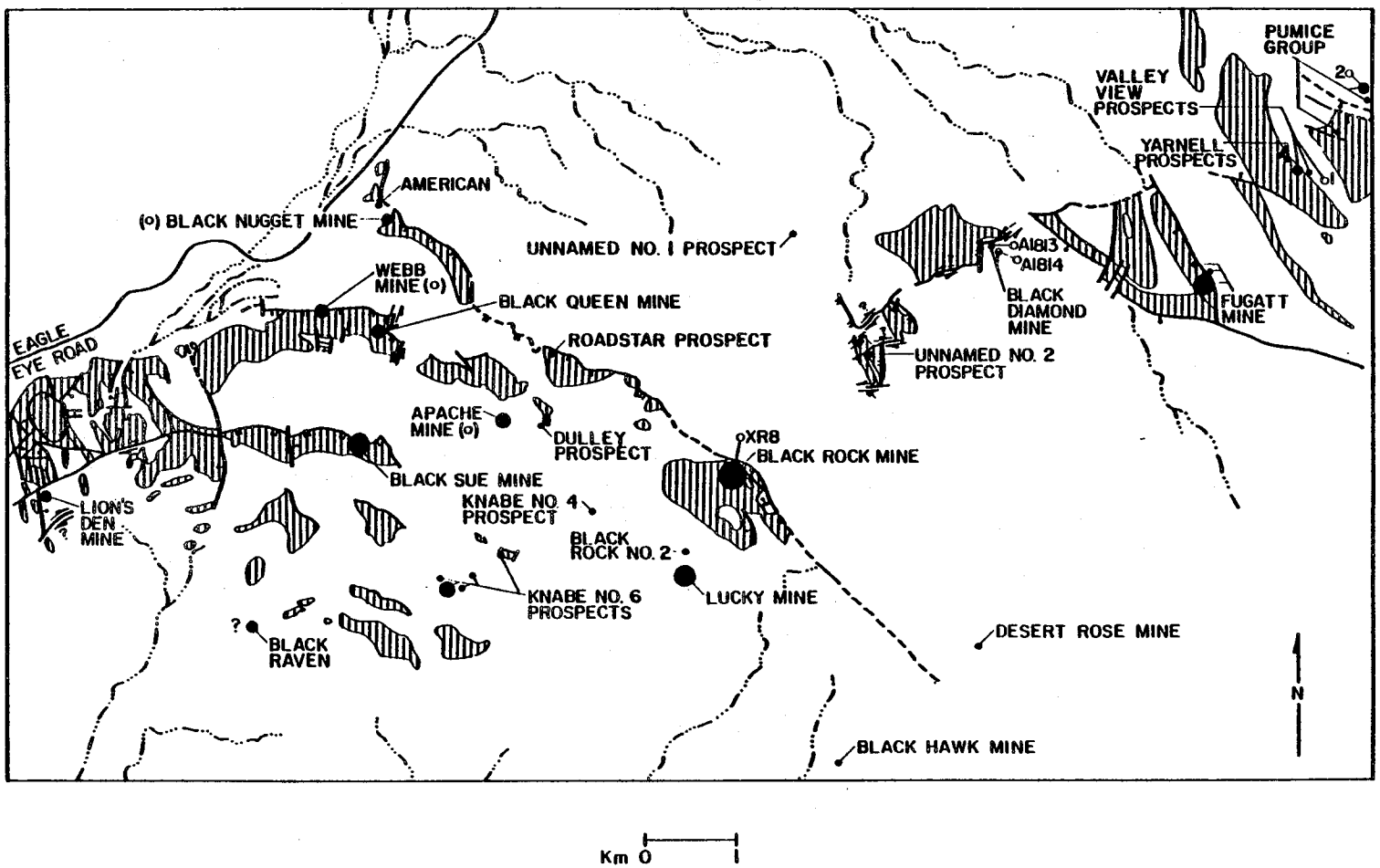

MAP OF THE AGUILA MANGANESE DISTRICT

Figure 15. Outcrop map of Dead Horse basalt, structures, and mine locations for the Aguila manganese district. Assays from individual prospects (Table 2) are from high grade dump samples. Individual prospects are described in Table 6.

Dead Horse basalt

contact

fault, dashed where approximately located

moderate to low angle normal fault, bars on down thrown side

high angle normal fault, barb on down thrown side

tear fault, arrows showing relative movement

sample location, keyed to Table

MANGANESE PRODUCTION

<100 tons

>100 <1,000 tons

>1,000 >10,000 tons

>10,000 <100,000 tons

>100,000 <200,000 tons

Table 6. Aguila Manganese District.

PROSPECT	LOCATION	PRODUCTION/ DEVELOPMENT	HOST	STRUCTURE/ GEOMETRY	MINERALOGY/ GEOCHEMISTRY
American F&S 1958 { Black Nugget U.S. Group	SE 1/4 Sec 19, T5N R9W, Aguila 15'. pit in Sec 20 Am.	Small. Pits and open cuts.	Basalt.	3 vein fracture zones ranging from 1 to 5m wide and seperated by intervals of 60 to 150m. West vein is 50m long, central vein is 60m, east vein is 150m long. Veins strike north and dip steeply westward.	Commoon Mn oxides.
Apache adjoins Dulcy (Dulcey) Dulcy Gallagher Flynn	SE 1/4 Sec 10, T5N Big Horn 15'. F&S 1958 Se 29 T 5N R 9W	Total of 320 tons ave. 22.8 % Mn. 8m long incline of unk. depth, 22m sq. open pit.	Precambrian granite. E vein is in granite-andesite contact (Dulcey vein) W-vein Apache in granite	Two veins. One 24m long, 1 to 1.5 m wide, the other 120m X 1 to 1.5m. Both strike north with steep dips The east vein dips to the east (?), the west vein dips to the west.	Pyrolusite and and some psilomelane. Calcite is major gangue.

Black Bart (Lucky)	SW 1/4 Sec 32, T5N R 9W, Big Horn 15'. f&s pot in sec35	Small production. Shallow pits and cuts along 60m X 1.5m vein.	Precambrian granite.	Many veins with 30 to 210m of seperation between them. The most extensive vein is 60 X 1 to 1.5m. Each strikes due north and dips steeply westward.	Mn oxides with calcite and quartz.
Black Crow f&s 1958: (ATKINS or incadees)	SE 1/4 Sec 10, T5N R8W, Aguila 15'.	Small. Three shafts: 3m, 16m and 22m deep.	Precambrian granite and gneiss.	2 veins of unknown orientation. 3 parallel veins in w-trending, steep-sdip Shearzone, other prospects to west	Mn oxides (?)

75

F&S 1958	Black Diamond (Kat Head)	SW 1/4 Sec 24, T5N R9W, Aguila 15′.	Small production. Shallow open cuts and pits. Most extensive is 16m long, about 1m wide, and 2 to 3m deep.	Basalt.	2 veins approx. 60m apart. East vein is 90m long X 0.6 to 1.5 m wide. West vein outcrops only for 15m and is 0.6 to 1.2m wide. Both strike NE and dip to the NW.	Pyrolusite and and some psilomelane.
	Black Hawk	NW 1/4 Sec 10, T4N R9W, Big Horn 15′.	Production assumed to be minor. Development consists of scattered open pits.	Late Cretaceous monzonite.	Veins of short extent and presumed NW strike.	Mn oxides.
	Black Queen (Armour Group)	NW 1/4 Sec 29, T5N R9W, Aguila 15′. F&S potin Sec 30	8600 tons ave. 21.53% Mn. 1.5 to 15m X 246m X 30m deep cut.	Precambrian granite and schist. F&S say andesite & Tsf	Zone about 240m long and 1.5 to 15m wide. Veins in zone strike north to NNE and dip steeply to the west and east. A series of east- to WNW-trending faults offset the zone. Veins are in the hanging wall of an extensive low angle fault.	Pyrolusite and psilomelane. Abundant calcite.

Black Raven Crow, pittsburgh Wisconsin		NW 1/4 Sec 1, T4N R10W, Big Horn 15'.	500 tons ave. 23% Mn. Development status unknown.	Late Cretaceous monzonite. Schistose & granitic rock	10 or more veins. Some extend for 60 to 90m. Thicknesses range from 0.3m to 2.5m. Attitudes vary greatly. Most are either north tending and steeply westward dipping or east striking and moderately south dipping. Very widely in attitude	Pyrolusite, manganite psilomelane. Abundant calcite.
Black Rock	F&S 1958	NE 1/4 Sec 34, T5 R9W, Big Horn 15'. Sec 26 5N 9W	158,566 tons ave. 19.82% Mn from 1956 through 1959. Open 270m in diameter and 110m deep. And many adits. F&S were there in 1954	Basalt and tuff.	Manganese is localized betw. NW striking moderately NE dipping normal faults. Mine is at the top of the Dead Horse section in the hanging wall of the regional Little Horn Peak fault. Several Northerly trending fracture zones 1.2m wide	Psilomelane pyrolusite manganite, calcite, a qtz. Anthony and others (1977) report Ramsdellite.

Black Rock #3 FS 1958 Black Rock	SW 1/4 Sec 34, T5 R9W, Big Horn 15′.	Several hundred tons. Shallow pits and open cuts. Largest cut is 33m X 1m X 2m.	Basalt and tuff.	Vein at least 30m long X 0.7 to 1.5m wide. Unknown orientation. vein dips 45° E	Mn oxides (?).
Black Sue	SE 1/4 Sec 30, T5N R9W, Big Horn 15′. FS 1958	9100 tons. 100 X 70m and 27 X 12 X 6m workings.	Basalt and tuff.	Fracture zone 105m X 6 to 12m wide. NW striking and south dipping. Localized at the top of the Dead Horse section in the hanging wall of an east striking, moderate- to low- angle south dipping normal fault.	Pyrolusite calcite, and quartz.

Desert Rose	SW 1/4 Sec 2, T4N R9W, Big Horn 15′.	No production. 16 X 9 X 9m pit.	Basalt.	Fault or fracture zone trending N10E 55SE. East side appears to be down.	Mn oxides.
Dulcey	SW 1/4 Sec 28, T5N R9W, Big Horn 15′.	Production not differentiated from the Apache. 24 X 10 X 1.5m open cut.	At the fault between Precambrian granite and basalt.	Vein 23m X 0.8 to 1.2 m. North strike with presumed east dip.	Pyrolusite some psilomelane and calcite.
Fugatt purple pansy	NW 1/4 Sec 19, T5N R8W, Aguila 15′.	7,500 plus tons. 100 X 65m open pit.	Basalt. andesite	Veinlets and irregular masses in sheared and brecciated Mn. Extent is 330 X 60 to 90m wide. Zone is NW striking and steeply SW dipping. Zone is at the top of the Dead Horse section in the hanging wall of an extensive NNW striking SW-dipping moderate- to low- angle normal fault.	Pyrolusite psilomelane, magnetite, limonite, and abundant calcite.

✓	Knabe #4	SE 1/4 Sec 33, T5N R9W, Big Horn 15'. F&S put in sec34	12,000 tons low grades screened to yield 1000 to 2000 tons of screened material ave. 17%. Mn. Overall 370m square open pits.	Precambrian (?) Granite.	Two fracture zones. East zone is 18 X 32m. West is 50 X 6 to 9m. Both strike to the north and dip steeply to the west.	Pyrolusite, calcite, and quartz.
✓	Knabe #6	Sec 6 T4N R9W S 1/2 Sec 32, T5N R8W, Big Horn 15'.	1000 tons 9% Mn. 25 X 16m open pit.	Precambrian granite.	Shear or breccia zone 30 X 10 to 16m wide. North trending.	Pyrolusite, calcite, and quartz.
	Lion's Den	NE 1/4 Sec 25, T5N R10W, Lone Mtn. 15'. Sec 35	600 tons. 12 X 3 X 3m open cut and incline. 3m deep open cut.	Basalt. and tuff.	Breccia zones 30m X 3 to 7m. Zone strikes to the north. Zone is in hanging wall of a north-trending steeply easterly dipping normal fault.	Mn oxide calcite, and iron oxide.

Pumice	SW 1/4 Sec 16, T5N R8W, Aguila 15′.	Several hundred tons of low grade. Open cuts and shallow incline shaft.	Basalt. and Sugarloaf rhyolite.	Veins and breccia zones. Major features are four veins ranging from 0.8 to 1.8m in thickness. One occurrence had irregular seams outcropping over 600m. in N-trending zone	Pyrolusite, manganite, calcite, and quartz.
Roadside	NW 1/4 Sec 28, T5N R9W, Big Horn 15′. F&S pot in Sec 21	Small. 10 X 3 X 2m cut.	Basalt.	Two fracture zones. West zone is 30 X 1 to 2m. East zone is 90 X 6 to 9m. Both trend north.	Pyrolusite and calcite.
Sambo Aguila	SW 1/4 Sec 36, T5N R8W, Aguila	4300 tons plus at 39% Mn ave. grade. 30 X and 3 shafts 3 to 7m deep.	Basalt. and tuff.	Over 10 fracture zones. The most extensive zone is 30 X 15m. The zones trend north.	Pyrolusite, manganite, psilomelane, and calcite.
Unnamed #1	SW 1/4 Sec 23, T5N R9W, Aguila 15′.	No production. Minor pits.	Precambrian granite.	Unknown geometry and orientation.	Mn oxides.
Unnamed #2	NE 1/4 Sec 25, T5N R9W, Big Horn 15′.	No production. Minor pits.	Tuff.	Unknown geometry and orientation.	Mn oxides (?).

(andesite ?)

f&S 58 notes	Yarnell & Valley View?	NE 1/4 Sec 20, T5N R8W, Aguila 15'.	Production not differentiated from the Valley View. Open cuts.	Basalt.	Veins are the western extension of the Valley View veins. Orientations are the same as Valley View. West-trending veins dip steep S.	Assumed to be same as the Valley View.

Valley View	NW 1/4 Sec 20, T5N R8W, Aguila 15′.	1300 tons estimated. Open cuts.	Basalt.	Four veins 30 to 60m apart. The major vein is the Valley View which extends for over 330 m and ranges from 0.3 to 3m in thickness. All of the veins strike east-west and dip steeply to the south.	Manganite, pyrolusite psilomelane, and abundant calcite. Hewitt (1964) reports fluorite and barite and an assay yielding 2.9 oz. Ag/ton and 15% Pb.
Webb	SE 1/4 Sec 19, T5N R9W, Aguila 15′.	Several 1000 tons of low grade. 30 X 6 X 6m incline.	Basalt	Two fractured zones 24m apart. Northern zone is 45m X 6m. Southern zone is 20 X 5 to 6.5m. Both are east-west trending and south dipping. Zones are in the hanging wall of an extensive moderate to low angle normal fault with the same attitude as the zones.	Pyrolusite, some psilomelane and calcite.

Horn district.

Geology of the Manganese Deposits

A generalized description of the manganese occurrences is as follows (Farnham and Stewart, 1958):

> The individual deposits range from narrow veins, with small but enriched ore shoots, to wide shear and breccia zones of lower grade material. The chief manganese minerals are the common oxides, usually occurring as a mixture of pyrolusite, psilomelane, wad, and manganite. The gangue is composed largely of calcite, quartz; and unreplaced fragments of wall rock.

The individual occurrence descriptions are summarized in Table 6.

Host Rocks

Manganese mineralization occurs in the Proterozoic granite, Late Cretaceous monzodiorite, and Miocene Dead Horse basalt and tuff. Seven occurrences are in the Proterozoic granite, two are in the Late Cretaceous monzodiorite, eleven occurrences are in the basalt, and two are in mid-Miocene tuff. Many of the basalt-hosted occurrences include minor amounts of biotite tuff. Ninety-three percent of the total production was from deposits hosted in basalt. The remaining fraction of production came from occurrences hosted in Proterozoic (MRDS,1983).

Structural Relations to Mineralization

The Aguila district is coincident with a regional antiform described by Rehrig et al. (1980). All of the manganese occurrences are localized along tectonic structures, and none are strataform. Nearly all of the production tonnage was localized at the top of the Miocene section proximal to regional north-northwest-striking, northeast and southwest-dipping, low- to moderate- angle, normal faults (Figure 15). The easternmost occurrences, in the Pumice group, are localized along

roughly east-west striking, south-dipping structures. Individual manganese pods are localized along minor high-angle normal faults. The cross section of the south- facing wall of the Black Rock mine, the major producer of the district, illustrates the localization of manganese pods along small scale structures (Figure 16). The two largest mines, the Black Rock and the Fugatt, are localized at minor inflections in the fault traces. The Proterozoic-hosted occurrences are almost exclusively localized along north-trending, steeply west-dipping, fractures or, possibly, faults. The Desert Rose mine, hosted in Late Cretaceous monzodiorite, is along a structure that strikes N10°E and dips 55°SE structure.

Timing of Mineralization

Well-exposed geologic relations in the Black Rock pit constrain the timing of mineralization with respect to regional detachment events. The pit floor of the Black Rock mine (Figure 16) is Proterozoic schist and gneisses, whereas the pit walls are Miocene basalt. The contact between the two units is the Little Horn Peak normal fault which strikes N30°W, and dips 20°SW (Reynolds et al., this volume). Mineralization does not extend into the footwall, so mineralization probably started after the onset of faulting. The presence of manganese minerals smeared along minor faults suggests that the mineralization was, in part, pre-faulting. The overall fissure filling and vein character of the mineralization, however, makes it unlikely that mineralization was entirely pre-faulting because one would expect some strataform manganese occurrences if pre-faulting manganese precipitation had occurred. Since translation along low-to moderate-angle faults in the upper plates of detachment regimes is contemporaneous with detachment faulting, and the

Figure 16. Geologic cross-section of the south-facing wall of the Black Rock mine.

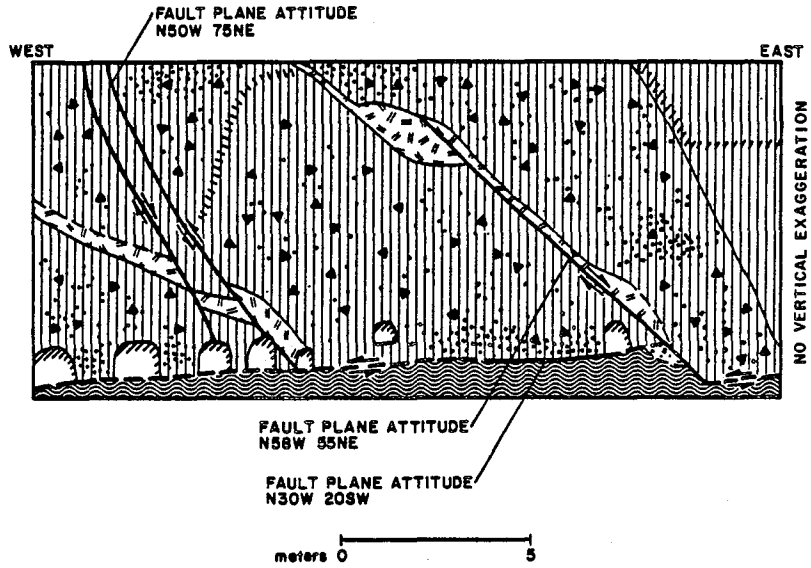

GEOLOGIC CROSS SECTION OF THE SOUTH FACING WALL OF THE BLACK ROCK MINE

- Takd — Miocene (?) arkose dike – sill
- Tsd — Miocene (?) silicic dike
- Tbab — Miocene (?) basaltic andesite
- pEc — Precambrian crystalline rocks
- contact
- fault, dashed where approximately located, arrows showing relative displacement
- adit
- breccia
- manganese oxide mineralization

mineralization appears to be contemporaneous with faulting, the mineralization is contemporaneous with middle Tertiary detachment faulting.

Paragenesis

All of the Aguila district occurrences, except for the Valley View prospects at the eastern end of the district, consist of manganese oxides in a gangue of calcite, and, less commonly, quartz. Psilomelane and pyrolusite are the most abundant manganese minerals, but manganite is locally present. Ramsdellite, a rare manganese oxide, is found only at the Black Rock Mine (Anthony et al., 1977). Hewett (1972) implies that most of the manganese oxides are hypogene and contemporaneous with calcite. No relationship was established between quartz and the rest of the suite. The Valley View Mine displays layers of barite and fluorite crystals that alternate with black calcite (Hewett, 1964). The sequence of deposition in a well-exposed vein was: manganese oxides followed by fluorite, barite, and calcite (Hewett, 1964). Hewett (1964) notes that manganese mineralization hosted in mafic volcanics is ubiquitously associated with three-quarters to wholesale replacement of plagioclase by adularia.

Fluid-Inclusion Studies

To characterize ore-forming fluids, fluid-inclusion homogenization temperatures and freezing point depressions were determined from calcite that is associated with manganese oxides in the the Black Queen and Valley View prospects were selected. Fluid inclusions from both prospects are jagged or elongate in outline and contain liquid plus vapor. The Black Queen inclusions average 20 microns in their largest

diameter and ranged from 9 to 12 percent in vapor content. The Valley View inclusions average 7 microns in their largest diameter and have a considerable range in vapor volumes, from 3 to 18 percent. No double menisci are found in either set of fluid inclusions. Therefore, there is probably little to no CO_2.

The difficulty of finding suitable inclusions permitted homogenization determinations only on four inclusions from the Black Queen and nineteen from the Valley View mine. The determinations are spread from 200° to 340° C with a gap from 280° to 310° C and a solitary determination at 370° C (Figure 13). No inclusions from the Black Queen mine were found suitable for freezing-point depression determinations. Four inclusions from the Valley View Mine yielded freezing point depressions that all clustered around 1 to 2 percent NaCl equivalent (Figure 14). The wide range of homogenization temperatures combined with the anomalously low salinities suggest the solutions were boiling at the time of deposition of calcite. The paucity of the data and the necked appearance of the inclusions place these conclusions in question.

Genesis of the Aguila District

A few generalities about the Aguila district emerge from field relations and observations of paragenesis, mineralogical, and alteration (Hewett, 1964, 1972). The Aguila occurrences are calcite-dominated, hypogene, manganese-oxide, vein deposits, which are hosted at the top of a mafic volcanic flow sequence along steep local structures that are ancillary to extensive regional low- to moderate-angle normal faults. A hot springs origin is indicated by the following: (1) modern analogs to Aguila-like, manganese vein systems (Hewett, 1964): (2) the location of

most of the occurrences at the top of the Miocene section: (3) and the fluid-inclusion characteristics.

Boiling of the fluids in the western and west-central portion of the Big Horn Mountains was probably facilitated by the highly fractured character of the basalts. The high fracture density might be a result of fracturing during the formation of the Big Horn Mountains' antiform. In the Midway Mountains of southeastern California, manganese vein occurrences are found in fensters above antiforms in the underlying detachment-fault (Berg et al., 1982). If the antiform described by Rehrig et al. (1980) is a reflection of an arch in the detachment surface, a relationship may exist between rugousities in underlying detachment surfaces, fracture density in upper plate rocks, and consequent permeability.

The source of the manganese and of the hydrothermal fluids in the hot springs is more problematic. Most studies of hotsprings deposits reveal a dominantly meteoric origin for the fluids (White, 1980), but place few constraints on the origin of metals. Hewett's (1964) observation of potassium metasomatism ubiquitously associated with mafic-volcanic-hosted manganese occurrences and the presence of intense K-metasomatism in the Big Horn Mountains (Reynolds et al., this volume) suggest a genetic model solely dependent on K-rich, CO_2-bearing solutions reacting with mafic volcanics.

Mass-balance calculations indicate that alteration of 20 percent of the total plagioclase in the basalt of the western Big Horn Mountains to adularia can account for all of the calcite observed and some of the manganese. The generation of calcite is a consequence of cation exchange of potassium for calcium, consequent supersaturation of fluids with calcium, and concurrent immiscibile separation of CO_2 during

boiling. The manganese is presumed to evolve during K-metasomatism of plagioclase because adularia contains between 2 and 10 times less manganese than intermediate plagioclase (Wedepohl, 1969-1978). Calcite, amounting to twelve percent of the total volume of basalt in the western Big Horn Mountains and one seventh the total manganese produced (12,500,000) are evolved if one assumes the following: an average content of 10 ppm Mn in adularia, 60 ppm Mn in plagioclase, 29 percent plagioclase in basalt (Turner et al., 1979), sufficient CO_2 in the fluids to generate $CaCO_3$, and that 20 percent of the plagioclase in 2.8 Km cubed (estimated total volume of basalt in the western Big Horn Mountains) is altered to adularia.

These calculations, all their uncertainties notwithstanding, demonstrate that the observed alteration of plagioclase to adularia can account for commonplace calcite gangue and some of the manganese. Although none of this study constrains the alteration of amphibole and pyroxene, the reaction of these minerals with alkali-rich solutions presumably could account for much of the manganese without having to resort to initially manganese-bearing solutions. If this model is correct, and the solutions were K-rich, then these solutions may have had a brine character prior to boiling, and therefore would be affine to the Tiger Wash hydrothermal fluids.

OSBORNE DISTRICT

Introduction

The Osborne district is a group of approximately twenty Pb-Zn-Ag-Au-Cu occurrences that cluster in a north-northeast trend in the east-central and eastern Big Horn Mountains (Figure 17). The Osborne district is one of twenty-five middle Tertiary base-metal districts in Arizona (Keith et al., 1983). Of these districts twenty two are Pb-Zn-Ag dominant and three are silver-dominant with lesser Pb and Zn. The Ag-dominant districts are the source of the vast majority of the dollar value from the middle Tertiary base-metal districts. The Osborne district ranks eighth in terms of present day value of production from these middle Tertiary districts (Welty et al., 1985). The district produced 1,369,000 lbs. Cu,7,710,000 lbs. Pb, 500 lbs. Zn, 13,000 oz. Au, and 195,000 oz. Ag (Keith et al., 1983).

Mid-Tertiary base-metal districts can be subdivided into those districts that are hosted in tilted volcanics and those that are not. The distinction is noteworthy in two regards. First, two of the three silver-dominated districts are in nontilted volcanics, and the third, Mineral Hill, is hosted in Pinal Schist. Therefore, the silver-rich mid-Tertiary base-metal deposits are not located in detachment terranes. Secondly, of the districts hosted in tilted volcanic rocks, the Osborne ranks third in present day value of historic production.

Geologic Setting

The oldest rocks in the district are Proterozoic rocks that consist of phyllite and schist in the eastern half of the district and are dominantly amphibolite with some gneisse and meta-granitoid in the western portion of the district (Capps et al. 1985). There is also a

single occurrence of gabbro that is assumed to be Proterozoic. The northwest portion of the district has extensive outcrops of Late Cretaceous granitoids that are typically sphene-bearing granodiorite. Unconformably overlying these units are the lower and middle Miocene Big Horn volcanics, which are 1000 to 3500 m thick and are the predominant outcropping rocks of the central Osborne district. The basal unit of the Miocene sequence ranges from a coarse sandstone and conglomerate to laharic sedimentary rocks. These basal clastic rocks are overlain by basalt and basaltic andesite flows and pyroclastic rocks of the Dead Horse basalt member. Overlying and interlayered with the Dead Horse basalts are a series of rhyolite to rhyodacite flows of the Old Camp and Hummingbird Springs rhyolites. These flows, along with the overlying Mine Wash andesite, Sugarloaf rhyolite, Moon Anchor andesites, and Beer Bottle rhyolite outcrop in the central portion of the district. The eastern portion of the district has Morning Star rhyolite as the basal silicic flow instead of the Old Camp rhyolite. Rocks younger than the Big Horn volcanics include middle to upper Miocene landslide-type megabreccias, sedimentary breccias and fanglomerates, Middle Miocene Hot Rock basalt, and various generations of alluvium.

The middle Tertiary structures in the Osborne district are complex (Reynolds et al, this volume). The major structures are regionally extensive N25°W-to N45°W-striking, dominantly southwest-dipping, moderate-to low-angle normal faults. A set of N20°E- to N80°E-striking faults of apparent strike-slip displacement, offset or otherwise terminate the low-to moderate-angle normal faults. Three to four kilometers of strike-slip offset is suggested by the outcrop pattern along the N45°E-trending fault that dissects the north-central portion

Figure 17. Osborne district prospect location map. Individual prospect desciptions are found in Table 7.

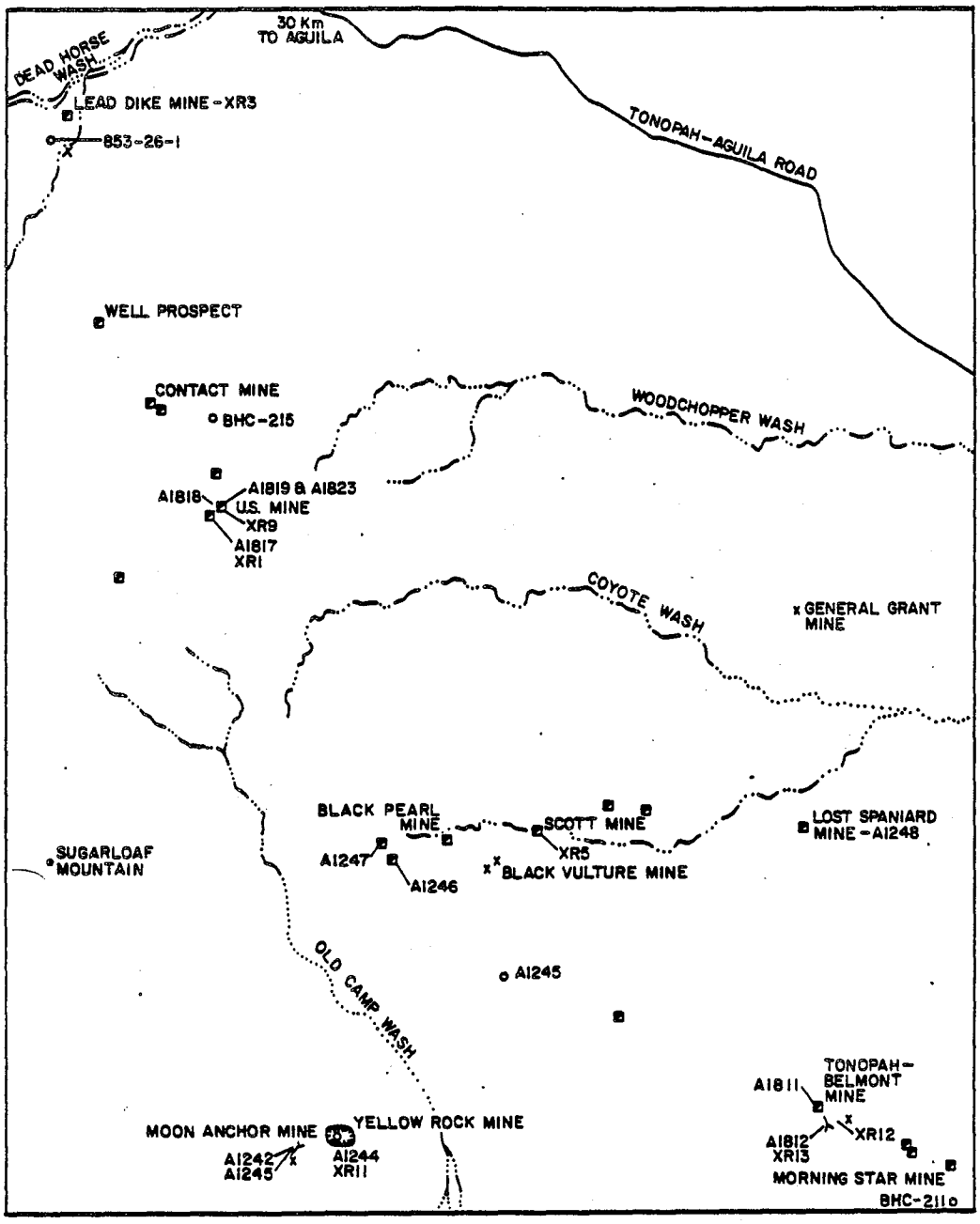

OSBORNE DISTRICT LOCATION MAP

ROAD

WASH

ADIT

x PIT

SHAFT OR INCLINE

DOZER SCRAPPED

o A555 SAMPLE LOCATION

Table 7. Osborne District.

PROSPECT	LOCATION	PRODUCTION/ DEVELOPMENT	HOST	STRUCTURE/ GEOMETRY	MINERALOGY/ GEOCHEMISTRY
Black Pearl Mine	NW 1/4 Sec 20 T4N R7W, Belmont Mts. 15'.	No prod., one shaft and some pits.	Basalt. Also limo. aft. py-bearing, iron-oxide-stained, 10 X 6m plug.	Vein. 2 to 3m wide. Exposed for 4m at incline. Extends sporatically for 120m. Trends N35W 70NE.	Main incline has specularite, calcite veining and quartz veining with black calcite in the core.
Black Vulture Mine	NW 1/4 Sec 21 T4N R7W, Belmont Mts. 15'.	No prod., minor workings.	Basalt.	Unknown.	Mn oxides, calcite, hematite, and manganite.
Contact Mine	NW 1/4 Sec 31 T5N R7W, Big Horn Mts. 15'.	No recorded produc. Two shafts, an adit, and scattered open cuts over 0.4 km vn strike length.	Gneiss. Pods of garnet-bearing peg. Fine-grained mafic dikes spatially associated w/ mineralization.	Vein traceable for 2 km. ranges up to 2m wide. Attitude ranges from N30 N50W, varied dips, typically moderate angles.	Vein of amythest up to 1.5 m. wide. Chrysocolla is common.

General Grant Mine	NE 1/4 Sec 11 T4N R7W Belmont 15'.	No prod. One adit, infilled pits, and trench	Hummingbird Springs rhyolite and andesite.	210 to 240m long X 45 to 60m wide zone of breccia- appears to to NW. Dip is unclear.	Limonite aft. py in calcite veinlets. 1 to 2 cm irregular veinlets. Basalt is propylitically altered.
Lead Dike Mine	NE 1/4 Sec 21, T4N R7W Aguila 15'.	No prod. One 8m, one 24m shaft. Cuts and pits.	Late K sphene-bearing grano-diorite.	6 m-long breccia-dike zone trending N8W 74NE at main shaft. Sporatic out-crops show vein system extends for at least 90m in the immediate area.	Galena and cerrusite on main dump. Some amythest. At pit 65m SE of main shaft is minor crys-ocolla and possible barite.
Lost Spaniard Mine	NW 1/4 Sec 24, T4N R7W, Belmont Mts. 15'.	No prod. One 30m shaft. One adit.	Hummingbird rhyolite and basaltic andesite. Precambrian or Belmont granite as country rock.	Vein in fault zone w basaltic andesite on HW and Old Camp rhyolite on FW. Vein-fault trend N65E 30NW.	Unusual mineral suite (Anthony et al., 1977,). Ajoite, cerrusite creaseyite,croicite, hemihedrite, hydro-cerrusite, laumontite, masicot, minium, duftite phoenicochroite, shattuckite, vaulque-linite, wickenburgite, galena, chalcopyrite, bornite, cerrusite, malachite, azurite, qtz. fluor.

Moon Anchor Mine	SW 1/4 Sec 31 T4N R7W Big Horn Mts. 15'.	Small prod. 16 X 7m room driven. 30 X 8 X 2 m pit.	Morning Star rhyolite and basalt.	N35E 30 striking vein along fault. Estimated size of pod is 15 X 9 m.	Unusual mineral suite (Anthony et al., 1977). Beudatite, fornacite, mimetite, ajoite, alamosite, phoenicochroite, wickenburgite, quartz, and possible fluorite. Probable new species now at the Smithsonian (Bill Hunt, personal communication).
Morning Star Mine	NW 1/4 Sec 6 T3N R7W Belmont Mts. 15'.	31 tons. One shaft 120m deep another 28m. 30m open cut betw. inclines.	Basalt and Old Camp rhyolite.	Vein is 1.3 m X 30 m. Trending N80E 30 NW at west end and N70E 60NW at east end.	Quartz, chalcopy., copper carbonates. Ore reportedly had 31% carbonates (AZBGMTF).
Morning Star Extension	SW 1/4 Sec 36 T4N R7W Belmont Mts. 15'.	No prod. 30m shaft.	Basalt.	Dike is 10 X 30m. Trend is N20W 65NE along apparent fault.	No visible mineralization.
Scott Mine	NW 1/4 T4N R7W Belmont Mts.	17 tons oz/ton. 30m shaft.	Basalt.	Vein 1 X 33m. Trends N70W 65NE at shaft. Iron oxide stained 20m west of shaft trends N60W 90.	Black calcite ~~is~~ has probable minium. Pyrite, chrysocolla, and probable rhodocrosite.

Tonopah-Belmont Mine	SW 1/4 Sec 36 T4N R7W Belmont Mts. 15'.	50,000+ tons. 100,000+ oz Ag. 8000+ oz Au. 1 mill.+ lbs. Cu. 3 inclines to 120m depth. Many surf.	Basaltic andesite, laharic sedimentary rocks, and Morning Star rhyolite.	North vein 1 to 12m wide 120m long, trends N70E 60SW. South vein 2 to 10m wide, 150m long, trends N75E 80NW.	Unusual mineral suite (Anthony et al., 1977). See text. High graded dump sample shows significant enrichment in Cu, Pb, Zn, Au. Ag, As, Cd, and Sb. Co and U are somewhat enriched. Extensive argillic alt.
US Mine	NW 1/4 Sec 1 T4N R7W Big Horn Mts. 15'.	4200 plus tons prod. at 0.141 oz Au/ton and 0.755 Cu. Two shafts, one 20m adit, many pits. 565,000 tons at 0.09 oz Au/ ton now blocked out.	Beer Bottle rhyolite, laharic sedimentary rocks, and basaltic andesite.	North breccia-vein zone is 5 to 25m wide and traceable for 200m. It trends due north, and is vertical. The south vein zone varies 5 to 25m and extends for 300m. Trends due north to N40E. 90 to NW	Quartz and fluorite are major gangue. Amythest is rare. Specularite and malachite are common. Azurite rare. Galena, sphalerite, and chalcopy. reported at depth. High-graded dump sample indicates anamalous Cu and Au. Slight enrichment in Ag, W. and Pb. Gold is reported as native.
Well Prospect	NW 1/4 Sec T5N R7W Big Horn Mts. 15'.	No prod. Two major pits along vein. One is 2m deep.	Late K monzonite and aplitic monzonite.	Veins and indistinct pods At 15' map shaft vein trends N20W 50 to 75SW. 50m north of main shaft is 2.5 X 11m vein.	Milky qtz and fluor. Abundant iron-oxide staining.

Yellow Rock Mine	SW 1/4 Sec 31 T4N R7W Big Horn Mts. 15'.	No prod. currently under devel. App. 30m X 60m scraped area.	Basaltic andesite.	Veinlets and two larger veins. Vein at adit is 0.5m wide, trending N20 to 30E 28SE. Hosting flow trends N48W 50NE.	Black calcite is major gangue. Chrysocolla is widespread but not abundant. Rare green fluorite.

of the district through the US mine. The presence of an extensive fenster in the southern portion of the district, with high-angle normal faults cutting the upper plate, suggests at least two distinct episodes of middle Tertiary-faulting.

Characterization of Mineralization

Beyond the fact that the occurrences are base-metal dominant, fracture or fault localized, and epithermal in character, the Osborne district prospects have few unifying attributes (Table 7). The occurrences can be grouped by several classifications based on differences in host rock types (silicic vs. mafic rocks), trends of localizing structures (north to northwest vs. east-west), or gangue suites (calcite vs. quartz plus or minus fluorite). Generally, the calcite-dominated, mafic-rock-hosted occurrences have a Pb-Ag metal suite, whereas, the quartz-dominated, silicic-rock-hosted occurrences have a Cu-Au-Pb-Zn-Ag metal suite. The mafic-rock-hosted occurrences cluster from unnamed locale A1247 in the west through the Lost Spaniard mine seven kilometers to the east (Figure 17). These occurrences include calcite- and quartz-dominated gangue systems. The cluster of occurrences from the US mine northwest to the Lead Dike mine includes most of the prospects localized along north-northwest-trending structures. These prospects are mostly quartz-dominated and include both mafic and silicic hosts. To illustrates the variety of mineral occurrences in the Osborne district, the geology of major mines is described below. Individual occurrence descriptions are summarized in Table 7.

The US Mine

The US mine is located near the head of Woodchopper Wash. The

Figure 18. Geologic cross section and map of the US mine.

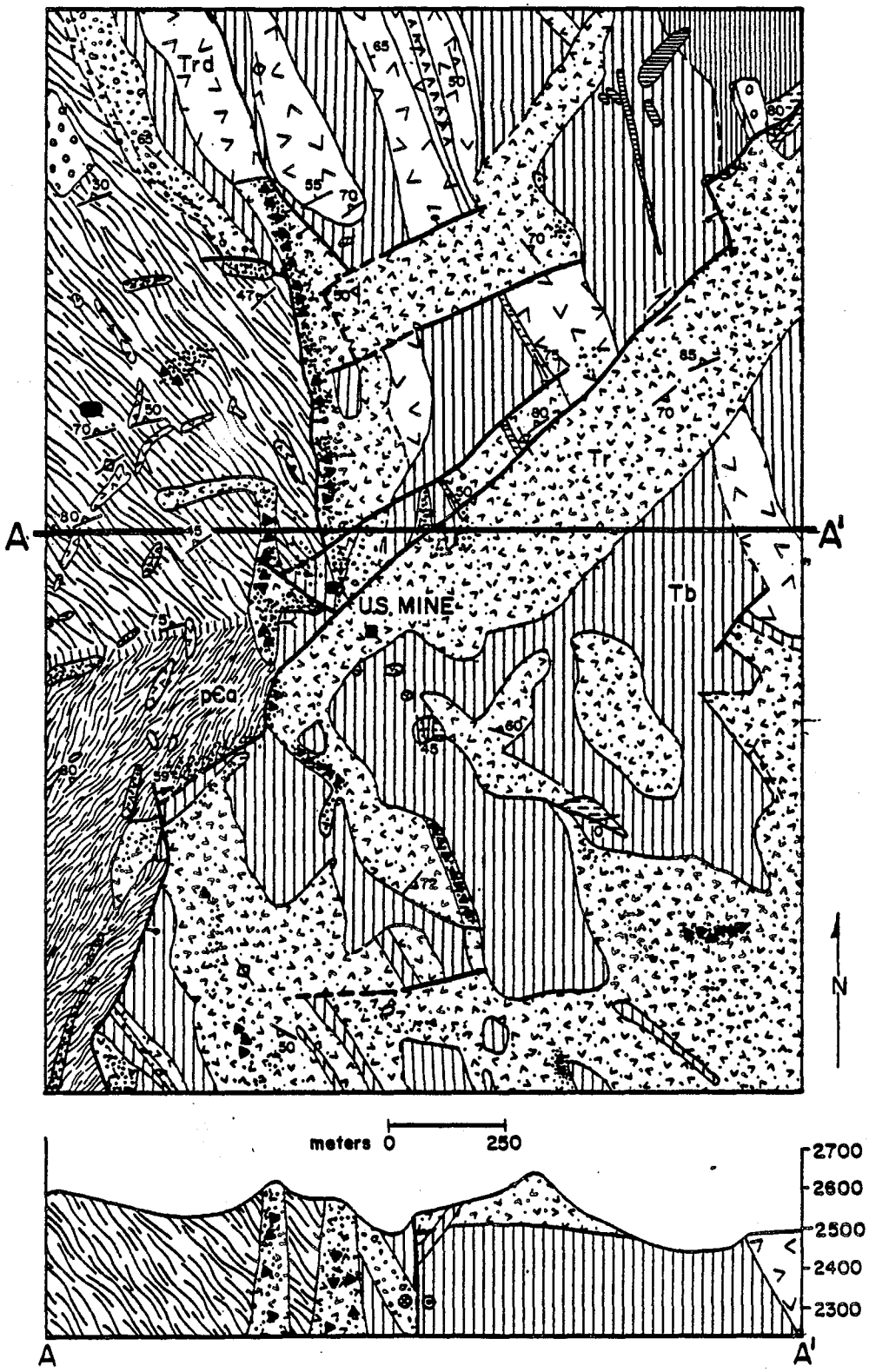

GEOLOGIC MAP AND CROSS SECTION OF THE U.S. MINE

prospects cover a north-trending ridge top that contains the most conspicuously iron-oxide-stained rocks in the Big Horn Mountains. Roddy Resources Inc. of Vancouver, B.C. currently controls the property, which consists of ten patented and twelve unpatented claims (Balik, 1985). The property contains two 150 m-deep shafts with crosscuts at the 30 m and 60 m levels. There is also a 30 m adit at the north end of the property. 4,500 tons of dump ore with grades of 0.128 oz Au/ton and 0.5 to 0.75 percent Cu were milled in 1943 (Belik, 1985). In 1961, 133 tons of ore averaging 0.091 oz Au/ton and 2.01 percent Cu were shipped (Belik, 1985). Roddy Resources reports blocking out 565,000 tons of ore at 0.09 oz Au/ton. The geologic setting of the mine is complex. Two, or possibly three, Proterozoic units occur in the western third of the mine area (Figure 18). A medium-grained amphibolite crops out in the southwestern portion of the area. In gradational contact with the amphibolite is a medium-grained to porphyritic gneissic granite. The gneissic granite is commonly mylonitized and inter-tongued with lenses of amphibolite. A small outcrop of tourmalinite (70 percent tourmaline in a milky quartz matrix) exists in the gneissic-granite, but does not have a metamorphic fabric. Consequently, its age is unclear.

Unconformably overlying the basement is 3 to 30 m of greenish, to purplish, laharic sedimentary breccia. Interlayered throughout the Miocene sequence are the mafic flows of Dead Horse basalt. They have highly varied thicknesses and are of discontinuous lateral extent. The flows are purplish-grey or reddish, and generally aphyric, but locally contain clinopyroxene or biotite. The oldest silicic flow unit in the Miocene sequence are grey rhyodacite flows and related dikes and tuffs of the Old Camp member. The unit consists of multiple flows that

typically have 8 to 12 percent plagioclase phenocrysts, 2 to 3 percent biotite, and zero to 3 percent quartz. Overlying the Old Camp member, in the northeast corner of the mapped area, is a locally mappable varient of the Dead Horse basalt. The unit consists of red clinopyroxene-bearing dikes and derivative, immature, sedimentary rocks. Lying in angular unconformity over the remainder of the Miocene package are the intensely flow-foliated flows of the Beer Bottle rhyolite. In the US mine area the flows have 5 to 12 percent potassium feldspar phenocrysts, 3 to 5 percent quartz phenocrysts, and, commonly, 1 to 3 percent limonite after pyrite crystals that are usually less than 1 mm in diameter.

The structural setting of the US mine, with a few important distinctions, ascribes to the outline established in the overall geologic setting. In contrast to the regional setting where north-northwest-trending normal faults predominate and northeast-trending structures are of subordinate significance, northeast-trending structures are the loci of major displacement, and north-trending, instead of north-northwest-trending structures, are the secondary loci of displacement (Figure 18). The north- to north-northwest-trending faults appear to be moderate- to high-angle normal faults. These faults dip to the west in the northern quarter of the mapped area, and to the east in the southern three quarters of the mapped area. The northeast-trending faults consistently crosscut the north-trending faults and appear to be right-lateral, strike-slip faults in the southern half of the mapped area, where they have large offsets, and left-lateral faults in the northern part of the area. The northeast-trending faults that offset a block of Beer Bottle rhyolite north of the center of the map are likely to be normal faults with some strike-slip displacement. The

major northeast-trending, strike-slip fault that transverses the center of the area demonstrates at least 0.5 km of offset when the immature laharic unit is projected back from the US mine shaft to its companion outcrop in the southwest corner of the map.

Mineralization at the US mine centers on two vertical quartz-veined breccia zones that are offset along a northeast-trending fault. The northern zone varies in thickness from 5 to 25 m and can be traced for 200 m along strike. The southern zone varies similarly in thickness and can be discontinuously traced for 300 m (Kerr et al., 1984). Aerial photographs demonstrate that the US mine is in the northern third of a zone of iron oxide-staining that extends in a north-south trend for over 10 km.

Mineralization occurs as veins and stockworks of quartz at the Proterozoic-middle Tertiary unconformity. In dump material, replacement textures are more prevalent than open-space fillings, but both occur. The ore-grade material is hosted in Beer Bottle rhyolite intrusive dikes, and to a much lesser extent, in the basal laharic sedimentary rocks (Figure 18). The northern ore body is in the hanging wall of a high-angle normal fault of unknown displacement. The fact that the laharic sedimentary rocks are in depositional contact with gneissic granite directly to the north of the mineralized zone suggests that the displacement along the high-angle fault is minimal. The outcropping slickenside planes bounding the ore zone may be a consequence of dike intrusion and rather than true tectonic displacement. Ore-grade material blocked out in the southern zone is more discontinuous, but is also hosted in dikes of Beer Bottle rhyolite, and, to a lesser extent, in basalt.

Iron-oxide staining and argillic alteration extend for up to 0.25 km to the east of the ore zones into the adjacent Beer Bottle Rhyolite. The alteration is much more subdued in the Proterozoic rocks to the west of the main ore zones and in the basalt to the south of the US mine shaft. The Beer Bottle rhyolite has sporatic argillic alteration and limonite-staining throughout the US Mine area. A single multi-element assay of dump material shows the ore to be markedly enriched in Cu and Au and slightly enriched in Ag, W, and Pb (Table 3, XR1 and XR2). Dump material from the US Mine shaft area consists of completely replaced Beer Bottle rhyolite that is now earthy hematite, jarosite, octahedral fluorite,and specularite. Fluorite constitutes a considerable percentage of the gangue and fluorite veins locally occur to 10 cm thicknesses. The most intensely miner-alized rocks have copper carbonates, oxides, and silicates that locally range up to 5 to 10 percent by volume (Belik, 1985). The gold occurs as native gold (Belik, 1985). Inaccessibility of the workings prevented establishing if a sulfide suite still exists, and, therefore, what its paragenesis might be. Observation of the cross-cutting and mutually enclosing relationships of fluorite, specularite, and quartz reveal that they mutually cross-cut each other.

On the assumption that fluorite fluid inclusions are representative of ore-forming conditions at the US mine, homogenization temperatures and freezing point depression temperatures were determined. Fluid inclusions are water liquid-vapor type, and are very abundant in the US Mine specimens. About half of them are sigmoidal and half have angular profiles. Rare inclusions have negative tetrahedral shapes. The inclusions range in their largest diameter from 8 to 50 microns. Vapor bubble volume does not greatly vary and averaged around 10 percent. All

of the bubbles had traces of double menisci which are assumed to be a third phase. Preliminary crushing experiments in glycerine revealed some evolution of gas which is presumed to be CO_2. No clathrates were observed upon freezing. Twenty-nine homogenization temperatures were determined (Figure 13). They cluster in a range from 190° to 225° C. One determination was at 235° C. Seven freezing point depressions were determined (Figure 14). These are recorded in NaCl weight equivalents as calculated from Potter (1977), and are not corrected for potential CO_2. The freezing point depressions occur in three groups that range from 8 to 14 percent NaCl equivalent. If a CO_2 correction for 7 percent CO_2 were imposed on the NaCl equivalents, the NaCl equivalents would range from approximately 5.5 to 9.5 percent NaCl weight equivalent (Collins, 1979).

Fluid inclusions in amethyst from the nearby Contact mine were similarly studied to test the assumption that the fluorite from the US mine is representative of fluids at the time of mineralization. Contact mine inclusions are very similar in their morphology to inclusions from US mine fluorite. Seventeen homogenization temperatures were determined. They are coincident in their temperature range with the US mine fluorite homogenizations (Figure 13). Six freezing-point depressions were determined (Figure 14). These were plotted identically to the procedure for other inclusion suites. The NaCl weight equivalents range from 17 to 25 percent. Correction for 7 percent CO_2 (a maximum for non-clathrating CO_2) yields 11.5 to 14.5 percent NaCl equivalent.

Data presented above establish important constraints over the chronology of mineralization in relation to structural history and over

the character of mineralizing fluids. The presence of mineralization in the Beer Bottle rhyolite limits the ore forming event to post-emplacement of the Beer Bottle rhyolite, latest Miocene silicic flow, dated at 16.4 Ma (Reynolds et al., this volume). The fact that the Beer Bottle rhyolite lies in angular unconformity over earlier tilted flows argues that mineralization occurred after most of the deformation. The prevalence of vertical to sub-vertical veins throughout the district also argues for a post-tilting chronology. The offsetting of the ore body by splinter faults off of the major northeast-trending strike-slip fault further constrains the timing to prior to the last movement along faults synchronous with the eruption of the Big Horn volcanic. Regional mapping (Capps et al., 1985) suggests that the displacement along the northeast-trending fault is on the order of three to four kilometers. The fact that mineralization is only offset 0.25 km supports the inference that mineralization occurred prior to the end of tectonism.

The fluid inclusion data from both the US mine and the Contact mine display consistent homogenization temperatures, and, even when corrected for possible CO_2, consistently elevated salinities. The consistency of homogenization temperatures from two different gangues that were 1.5 km apart suggest temperature and pressure homogeneity over extended distances. The elevated salinities necessitate a non-meteoric fluid component. The relatively diluted salinities of the US mine in contrast to those of the Contact mine may be interpreted as a function of gradual influx of meteoric fluids over time at the potentially longer lived, US mine system. Alternatively, the salinitiy differences may reflect variation in CO_2 content which exaggerates freezing point depressions (Collins, 1979).

The Tonopah-Belmont Mine

The Tonopah-Belmont mine is located in the eastern part of the Big Horn Mountains and at the west end of the Belmont Mountains (Figure 17). Recorded production from the mine spans from 1926 to 1957, and consists of approximately 1 million lbs. of Cu, 150,000 oz Ag, and 8500 oz Au (AZBGMTfiles). The only current source of activity at the mine is from mineral collectors exploiting the unusual supergene suite found at the mine (Anthony et al., 1977). Mine workings consist of two steep inclines on the north side of Belmont Mountain, a 20 m adit on the south side of Belmont Mountain, a glory hole opening from stopes to the adit, and numerous open cuts circumscribing Belmont Mountain. The workings are reported to have extended to the 125 m level where the ore is faulted off (AZBGMTfiles).

The geologic setting is moderately complex (Figure 19). The mine is hosted in a structurally isolated block of Miocene rocks that are surrounded by Proterozoic phyllite on all sides except to the southeast where the Miocene block is in fault contact with mid-Tertiary (?) Belmont Granite (Capps et al., 1985). The oldest rocks in the mine area are Proterozoic phyllites, which are laminated, steel-grey when fresh, and brown to tan where weathered. Typically the phyllite is fine-grained and consists of 10 percent quartz and 90 percent muscovite. The phyllite generally strikes northeast with highly varied dips that are typically steep. Unconformably overlying the phyllite is a basalt flow that is 10 to 13 m thick. Overlying the earliest basalt flow is a 12 to 18 m of laharic sedimentary rock that is dark grey in outcrop and green-tinted in fresh specimens. The unit has 30 percent subangular phyllite clasts that range from 1 mm to 1.5 cm in diameter.

Rounded quartz pebbles constitute 3 percent of the clasts. Overlying the laharic unit is a flow of basalt that also overlies the Morning Star rhyolite (Capps et al., 1985a). In the mine area the earliest Morning Star rocks are the flow-foliated flows or intrusions that form Belmont Mountain. Phenocryst content is less than 1 percent feldspars that are argillically altered. These rhyolites are commonly brecciated, silicified and slightly to moderately iron-oxide stained. Limonite after pyrite cubes that average 0.1 mm in diameter typically make up 0.1 to 1 percent of the rock. On the northeast end of Belmont Mountain, in uncertain stratigraphic relation to the Belmont Mountain flow-foliated rhyolite, is a sequence of Morning Star tuffs and flow-foliated rhyolite flows. From bottom to top, the sequence is as follows: (1) 6 m of flow foliated, fragmented aphyric rhyolite with 0.3 percent limonite after pyrite and iron oxide stain; (2) 3 m of punky, nonlithic, very fine-grained aphyric tuff of moderate induration, and bearing 0.5 percent, 0.5-mm-on-a-side, cubes of limonite after pyrite cubes; (4) 2.5 m of white and pink moderately-indurated lithic tuff with 40 percent aphyric silicic flow volcanic fragments whose average size is 1 cm; the tuff beds are 3 to 5 cm thick with a trace of limonite after pyrite; (5) 10 m of lithic tuff-bearing 40 to 55 percent aphyric silicic lithic fragments and 5 percent basalt fragments: (6) 11 m of blocky flow-foliated rhyolite with 0.5 percent quartz phenocrysts that average 1mm in diameter, and limonite after pyrite that constitutes 0.8 percent, and averages 0.5 mm in diameter. Rhyodacite dikes that have up to 7 percent plagioclase phenocrysts and sparse quartz phenocrysts intrude the entire sequence, including the youngest basalt flow. The precise extent of the rhyodacite intrusive period is unclear.

Figure 19. Geologic cross section and map of the Tonopah-Belmont mine.

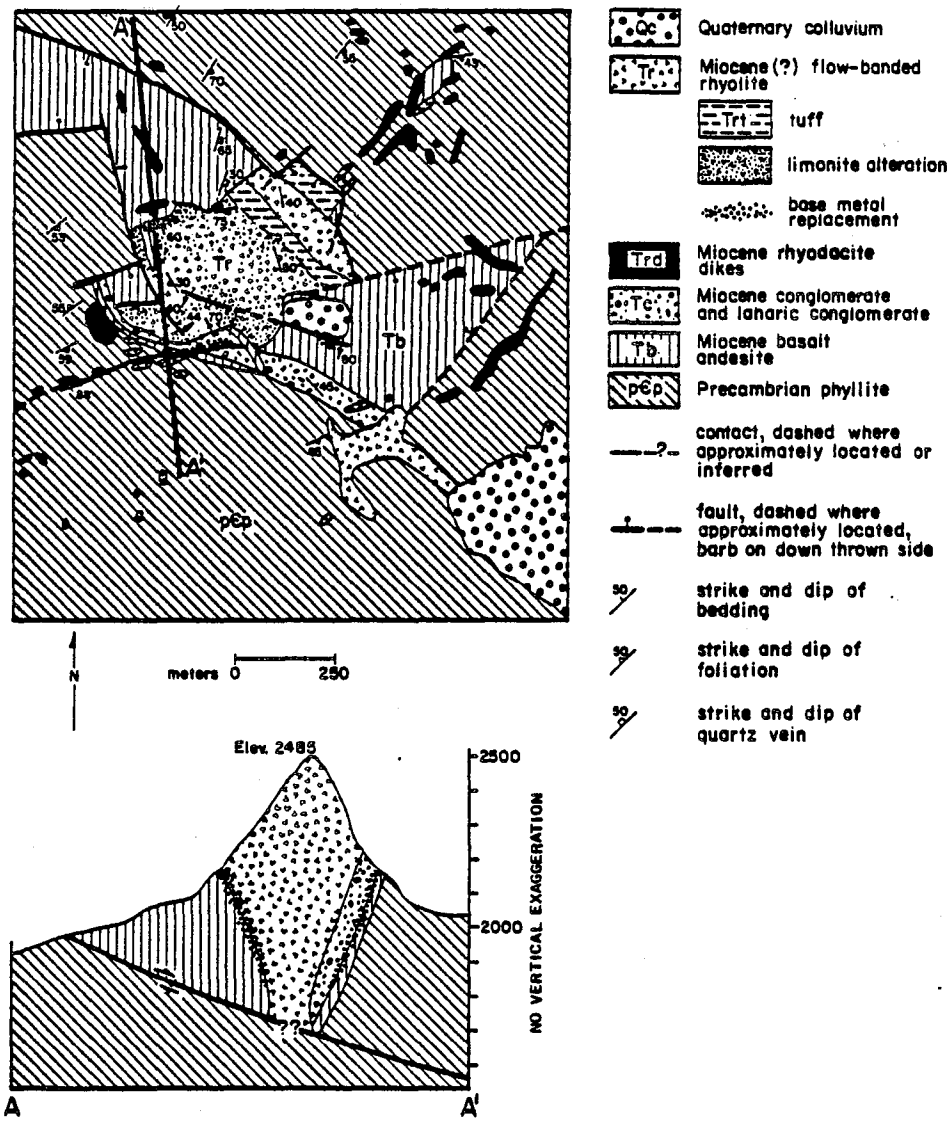

GEOLOGIC MAP AND CROSS SECTION OF THE TONOPAH BELMONT MINE

The major structure of the area is a N40°W-striking, southwest-dipping, low-angle fault that outcrops from 0.5 km northwest of Belmont Mountain for 2 km to the southeast where the fault changes to a north strike and a west dip (Capps et al. 1985). The low- angle fault juxtaposes moderately northeast-dipping rocks in the hanging wall against the Proterozoic phyllite. This major fault is offset by east-northeast-striking cross faults that are loci of mineralization (Figure 19). The N75°E- to N65°E-striking, southeast-dipping normal faults are the localizing structures of the south and north Tonopah-Belmont veins. A N20°W-striking, northeast-dipping normal fault cuts off both veins on the west end of Belmont Mountain. On the east end of Belmont Mountain the northern vein appears to die out whereas the southern vein is offset by a N70W-striking, southwest-dipping normal fault. The structural relationships suggest that mineralization occurred during low-angle-faulting, but did not continue after tectonism. The fact that the veins were cut off by a fault at the 130 m level (AZBGMTfiles) supports a syn-tectonism age of mineralization.

The north vein trends N70°E 60°SW, is exposed along strike for 120 m of strike length, and ranges in thickness from 1 to 12 m. The vein is mostly banded milky quartz with lesser copper carbonates as fracture fillings in a fault zone. The encompassing fault zone is at the contact between the basal Morning Star rhyolite flow or intrusion and a basalt flow. Whether the Morning Star unit is an intrusion or a flow determines the exact nature of the localizing contact. The character of this contact is obscured by the highly varied vertical flow foliations in the rhyolite, the absence of demonstrable offset on the north and south sides of the outcrop, and the unclear nature of the contact

between the Belmont Mountain massif and the Morning Star tuff to the northeast. The south vein trends N75°E, dips 80°NW, extends for 150 m, and varies from 2 to 10 m in thickness. The south vein is localized at the contact of the basal laharic unit with the lowermost basalt, both of which are in the hanging wall of a steeply-dipping normal fault of small displacement. This vein has mostly milky quartz breccia and replacement textures in contrast to the banded, fracture filling appearance of the northern vein.

Two assays (Table 3, XR12 and XR13), one from slightly iron-oxide-stained Morning Star rhyolite, and the other from high-grade vein material reveal significant enrichment in Cu, Pb, Zn, Au, Ag, As, Cd, and Sb. Cobalt and U are also somewhat anomalous. W. Hunt (personal communication, 1985) reports the presence of 33 phases in the ore: aurichalcite, barite, brochantite, caledonite, cerussite, chalcophanite, chrysocolla, coronadite, covellite, creaseyite, cryptomelane, descloizite, epidote, fornacite, galena, goethite, garnet, hemimorphite, jarosite, lepidochrosite, linarite, malachite, massicot, minium, murdochite, plumbojarosite, pyromorphite, rosasite, tenorite, vanadinite, vauquelenite, willemite, and wulfenite. This author also found sphalerite and calcite. A preliminary paragenesis, of major phases, from early to late is: sphalerite-pyrite-chalcopyrite-galena as primary sulfides, quartz as primary gangue, and aurichalcite, smithsonite, azurite, malachite-calcite, and jarosite as supergene minerals. A single whole-rock analyses of the Morning Star rhyolite (Table 8, XR12, K_2O is 9.99 percent) suggests that the host rocks are potassium metasomatized. A single slide of quartz with sphalerite and copper carbonates was examined for fluid inclusions. The quartz has myriad small inclusions. A couple of two phase, liquid and vapor water

inclusions, of workable size were found. They averaged around 5 microns in size. None of the inclusions homogenized at temperatures up to 350° C. It is presumed that the small size of the inclusions metastabily prevented homogenization.

The Scott Mine

The Scott Mine is located eastern Big Horn Mountains. Reported production is from the years 1942 through 1949 when approximately 12,000 lbs. Pb, 500 lbs. Zn, and 100 oz Ag were produced (AZBGMT files). There is a single 30-m-deep shaft. There are also two recently drilled exploration holes of unknown depth.

The Scott Mine is in a topographic basin that has poor exposures. The surrounding terrane is mostly calcite-veined Dead Horse basalt, and lesser Morning Star rhyolite (Capps et al., 1985). The basin is bounded by circuit normal faults on its west, north and east sides. The southern basin margin may also be fault bounded. The Scott Mine is hosted in Dead Horse basalt. Mineralization occurs as a 32 m long vein that ranges from 1 to 2.5 m wide, and varies from a N55°W strike, and 80° NE dip at its southeast end to a N70°W strike and 65°NE dip at its northwest end. The vein is cored by 10 to 40 cm of black calcite and contains outer vein selvages of banded quartz that is 0.5 m thick. Typical dump material is 30 percent black calcite and 70 percent highly altered basalt. The black calcite has a orange mineral found in calcite cleavages that is presumed to be minium. There are small crystals of pyrite in quartz veinlets from dump material of basaltic andesite breccia. Minor chrysocolla and probable rhodocrosite also occur. Two assays of high-grade dump samples assays, one for Pb, Zn and Ag, the other for Ag and Au, suggest the prospect is significantly enriched in

Pb and Ag, but not anomalously enriched in Au or Zn.

Vying on the assumption that the Pb- and Ag-bearing anomalous black calcite is paragenetically contemporaneous with the metal phases, fluid inclusion homogenization temperatures and freezing point depression determinations were obtained from calcite. The inclusions are two-phase, liquid-vapor type, that display no evidence of a third phase. The inclusions are commonly dendritic in profile, appear to be necked, and are found in rhombohedral cleavages. One quarter of the inclusions deemed suitable for thermometry are angular in profile and three quarters are spheroidal. The inclusions range in their largest diameter from 10 to 20 microns. Thermometry procedures outlined in earlier sections were followed for these determinations. Thirty-eight homogenization temperatures were obtained. They range from 125° to 370° C and cluster in three groups: from 150° to 170° C, from 250° to 290° C, and from 340° to 370° C (Figure 13). Twelve freezing-point depression determinations ranged from 8 to 22 NaCl weight percent equivalent (Figure 14). The small size of the sample population prevents distinct clusterings from being identified. The wide distribution of both the homogenization temperatures and the freezing point depressions, however, are permissive of a boiling interpretation for the genesis of the calcite. Thermodynamic constraints (Drummand and Ohmoto, 1985) also suggest boiling as a likely genesis for hydrothermal calcite.

Volcanic Enrichment Factors

Assays for fifty-three elements were obtained for four of the major silicic Big Horn volcanic units in order to see if any of the rhyolites are anomalously enriched in base or precious metals, and, therefore, could be a preferred ore host or source. Ratios of elements analyzed

Figure 20. Volcanic enrichment factors plotted as earliest silicic mid-Tertiary eruptive (Morning Star rhyolite) over the latest mid-Tertiary silicic eruptive (Beer Bottle rhyolite). Elements without bars mean both assays were below detection limits. Bars with arrows mean the depleated rock's assay was below detection limits. Where bars are of equal length for each assay, the assays are of equal value.

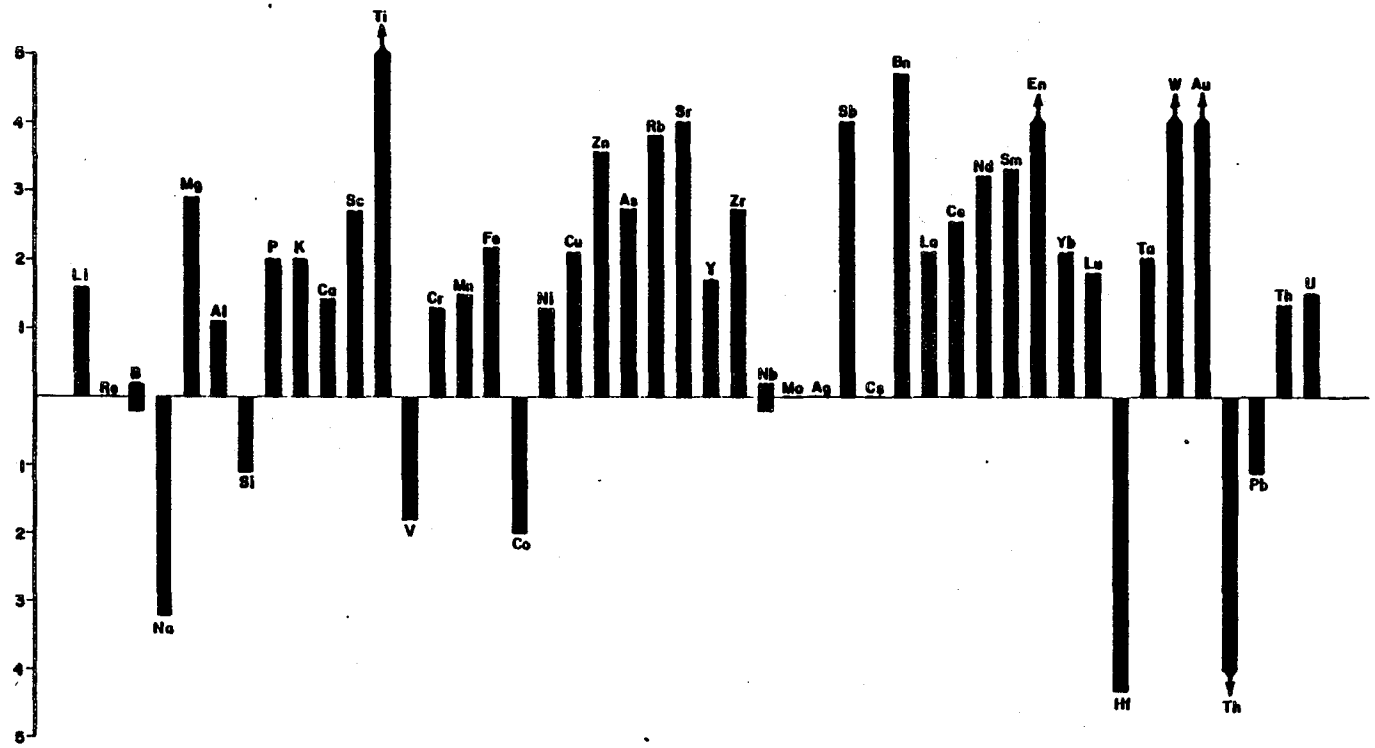

VOLCANIC ENRICHMENT FACTORS

from a pristine sample of Morning Star rhyolite, the earliest silicic eruptive, divided by analyses of pristine Beer Bottle Rhyolite, the latest silicic eruptive were plotted as volcanic enrichment factors to constrain whether concentration of metals early or late in the eruptive history of the volcanics has any relationship to host-rock systematics or chronology-chronology of mineralization (Figure 20). The plot shows enrichment of Cu-Zn-As-Au and W in the earliest eruptive. Pb is enriched in the latest, and Ag assays were below detection limits for both.

Osborne District Summary

Osborne district mineral occurrences display a variety of gangue suites, vein orientations, metal suites, and especially, host rock types. Mineralizations occurs in Proterozoic amphibolite, Late Cretaceous granodiorite, Miocene laharic conglomerate, Miocene Dead Horse basalt Miocene Morning Star Rhyolite, Miocene Old Camp volcanics, and Miocene Beer Bottle rhyolite. Limited geochemical data suggest there are two metal suites that correlate to the two major gangue suites. The gangue suite of quartz plus or minus fluorite correlates to the Cu-Au-Pb-Zn-Ag metal suite, and the gangue suite of black calcite plus or minus quartz correlates to the Pb-Ag metal suite. Vein orientations vary widely, but there is a weak correlation between east-west strikes and the calcite-dominated occurrences at the Valley View group and the Scott lead mine. The Black Pearl mine, the only other calcite-dominated occurrence has a different orientation.

The most obvious overall correlation between these criteria is that the Cu-Au-Pb-Zn-Ag suite is dominantly in the quartz-fluorite occurrences,which are mostly hosted in rhyolites or at the lower

contact between rhyolite and the basal laharic sedimentary rocks or basalt. An exception is the Contact mine, which is proximal to the basal Tertiary contact, but is hosted in gneiss, muscovite granite, and a mafic dike. The Well mine is also an exception because it is hosted in Late Cretaceous Granodiorite. The Pb-Ag occurrences also elude systematic correlation of descriptive criteria. However, three of the five Pb-Ag occurrences (The Scott Lead, the Black Pearl, and the Yellow Rock) all occur in basalt and have predominantly black calcite gangue. The Valley View mine, discussed previouly in the Aguila distruct, is exceptional because it is a Pb-Ag-rich manganese occurrence hosted in Sugarloaf rhyolite.

Osborne District Discussion

The fact that most of the Osborne district occurrences are hosted in mid-Tertiary volcanics, along mid-Tertiary structures, and in a discrete north-northwest trending belt, argue for a mid-Tertiary metallogenesis for the entire district. The absence of mineralization that is extensively offset by faults, and the good exposures of slightly offset mineralization in Beer Bottle Rhyolite at the US mine suggest mineralization occurred up until the latest moderate-angle normal fault displacements, approximately 16 Ma (Reynolds et al., this volume). The absence of mineralization in the latest high-angle normal faults makes it unlikely that mineralization continued beyond 16-15 Ma. The presence of mineral occurrences along low-angle structures in the Morning Star Rhyolite at the Moon Anchor mine places a lower time bracket of 21 Ma (radiometric date of Morning Star, Reynolds et al., this volume) on mineralization. The fact that the mineralization is along low-angle faults lends support to this maximum age of

mineralization because the low-angle normal faults are likely to be originally formed moderate- to high-angle normal faults that have been rotated to more gentle dips by continued extension. (Reynolds et al., this volume). The constraining of Osborne mineralization to the middle Miocene indicates that the hydrothermal events were contemporaneous with extensive translation of the Big Horn Mountains during middle Tertiary detachment-faulting as documented by Reynolds and Spencer (1985).

The probable contemporaniety of diversely hosted occurrences and the clustering of the district in a north-northwest trend suggests a regionally extensive hydrothermal system was active. The local variation in gangue and metal suites, therefore, may be a function of various of degrees equilibration between the hydrothermal fluids and host rocks. The volcanic enrichment factors lend support to the inference that mineralization is not directly related to the emplacement of specific volcanic flows. The predominant concentration of metals in the earliest flows would lead one to expect that if mineralization were solely related to the emplacement of flows, then mineralization would be restricted to the earliest flows and structures. The fact that the only known ore body in the district occurs in the latest eruptive argues against important influence of local flow's trace element content over mineralization. The high salinities of fluid inclusions selectively studied from the district also support the notion that fluids are regional in character and not local meteoric fluids.

Different mechanisms of mineral precipitation also appear to control metal suites. The relatively high sulfide character (in

contrast to the calcite-dominated occurrences) of the US mine and Tonopah-Belmont mine suggest that bisulfide complexing of gold (Barnes, 1979) may have been significant for the gold-rich occurrences. The wide range of salinity values in the US mine fluorites suggests dilution as the mechanism of gold precipitation for these systems. In contrast, the base-metal rich systems, like the Scott Lead mine, seem to be relatively low-sulfide systems. Theoretical studies suggest that base-metals travel as chloride complexes (Barnes, 1979). The preponderance of calcite and permissive evidence of boiling at these occurrences argue that the chloride-complexed, base-metals precipitated as base-metal minerals when the CO_2 buffer was destroyed during boiling (Drummand and Ohmoto, 1985).

Interrelationship of Middle Tertiary Districts

Diverse sets of data suggest that the Harquahala precious metal, the Tiger Wash barite-fluorite, the Aguila manganese, and the Osborne base and precious metal districts have an interrelated genesis. The most provocative evidence is the tight spatial overlap of the four districts. The Harquahala district precious-metal and fluorite occurrences end within two kilometers of the westernmost Tiger Wash occurrence (Figure 11). The westernmost manganese-calcite is 0.3 km west of the easternmost barite occurrence, the White Rock claims. The Aguila district is devoid of base-metal values until its easternmost extent, at the Valley View claims (Figure 13), where assays run as high as 2.9 oz Ag/ton and 15 percent lead (Hewett, 1964). The precise chronological relationships between these districts is not obvious. The localization of each of these districts in middle Tertiary structures, in conjunction with K-Ar chronology, brackets them all between Early and Middle Miocene. Host-rock relationships permit mineralization to have begun after the emplacement of the earliest volcanic flows in each respective section. The presence of manganese in the Sugarloaf rhyolite at the Pumice claims (Figure 13) suggests some manganese mineralization occurred after 19.6 Ma (Reynolds et al., this volume). The presence of Osborne district mineralization in the highest silicic flows requires that some Osborne district mineralization postdates the 16.4 Ma Beer Bottle rhyolite (Reynolds et al. this volume). These brackets imply that mineralization is progressively younger to the east.

Limited fluid-inclusion data from each district present provocative similarities. The apparent absence of secondary inclusions from each district argues against important multiple phases of mineralization. The

coincidence of homogenization temperatures and freezing-point depressions from occurrences lacking evidence of boiling furthers this inference. The pervasively high salinities found in all inclusions that lack evidence of boiling is suggestive evidence for a similar provenance of fluids for each district. Roedder (1984) reports that the NaCl weight equivalents (salinities) of epithermal occurrences are generally low, ranging from 0 to 5 percent; 12 percent is considered to be the extreme of typical epithermal occurrences. The salinities throughout the Big Horn Mountains and in the Harquahala district are mostly above 12 percent, even if one accounts for the maximum possible exaggeration by CO_2 clathrating. These salinities suggest that either some unknown process is concentrating alkalis throughout the range or that all of the fluids have a non-meteoric character, and therefore, may have a similar origin.

The observation of widespread K-metasomatism presents another attribute, which, along with the fluid-inclusion data, suggest affinity of range-wide hydrothermal fluids. Rehrig et al. (1980) established the presence of high-K rocks in the adjacent Vulture Mountains, and Capps et al. (this volume) present similar evidence for widespread, albeit, sporatic, K-metasomatism of the Big Horn volcanics (Table 8). The potassium enrichment of Late Cretaceous granodiorite near the Blue Hope mine (Table 8) qualitatively illustrates the extent of K-metasomatism. If the model presented for generation of manganese occurrences by K-metasomatism model is accepted, then the observation of calcite veining in Dead Horse basalts from the easternmost barite occurrence all the way through the easternmost Osborne occurrence further illustrates the extent of metasomatism and its important spatial association in each

Figure 21. Schematic cross section through the mid-Tertiary mineral districts of the Big Horns. Big arrow represent high salinity, CO_2^- bearing fluids. Small arrows represent meteoric waters. The meteoric fluids flowing down the detachment are shown driving connate waters toward the east.

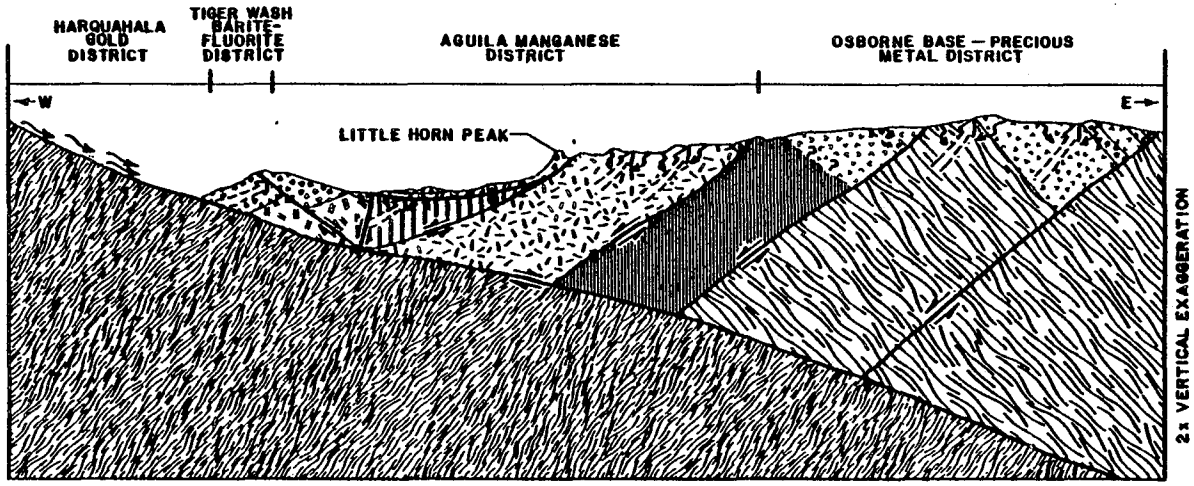

SCHEMATIC CROSS SECTION OF THE BIG HORN MOUNTAINS

Km 0 1 5

- Miocene rhyolite
- Miocene basalt
- Late Cretaceous monzodiorite to quartz diorite
- Precambrian granite
- Precambrian phyllite – amphibolite
- Precambrian phyllite
- Precambrian gneiss – schist – granite – amphibolite
- Lower-plate gneiss – schist – granite – mylonites
- fault
- connate waters
- meteoric waters
- ?_ contact, dashed where inferred

Table 8. Whole rock analyses are from widely seperated sample location of the same unit. They are displayed to qualitatively demonstrate the widespread occurrence of potassium metasomatism in the region. The upper assay of the pairs is a relatively pristine sample. The lower assay or assays are potassium metasomatised. The lower assay from the basalts is probably not K-metasomatised. The sample locations and rock types are as follows: 853-26-1, S 1/2 Sec 13, T5N R8W, Aguila 15', Blue Hope, N 1/2 Sec 31, T5N R8W, Big Horn 15', both are Late Cretaceous Granodiorite; BH-56, S 1/2 Sec 22, T5N R8W, Aguila 15', 72-60, N1/2 Sec 24 (Rehrig et al., 1980), T7N R6W, Vulture Mountains 15', both are mid-Miocene basaltic andesite; BHC-211 S 1/2 Sec 6, T3N R7W, Belmont Mts. 15', Beer Bottle rhyolite, BHC-215 S 1/2 Sec 30, T5N R7W, Big Horn 15', Old Camp rhyolite, and XR12, W 1/2 Sec 36, T4N R7W, Belmont Mts. 15', Morning Star rhyolite.

Table 8. Potassium-Metasomatized Rocks

Sample	SIO2	AL2O3	CAO	MGO	NA2O	K2O	FE2O3	MNO
Unaltered-								
*Altered								
853-26-1	66.7	15.5	3.51	1.56	3.73	3.87	3.66	0.06
*Blue Hope	65.5	15.8	2.96	1.77	3.20	5.03	4.18	3.20
BH-56	49.0	15.4	11.2	9.08	2.66	0.77	8.88	0.14
72-60	59.8	14.3	6.40	4.54	2.92	1.84	2.38	0.10
BHC-211	77.3	12.2	0.33	0.08	4.36	4.45	0.81	210ppm
*BHC-215	71.2	13.9	0.28	0.29	1.61	9.58	1.70	620ppm
*XR12	74.0	12.6	0.26	0.17	0.30	9.99	1..7	40ppm

Sample	TIO2	P2O5	CR2O3	LOI	SUM	RB	SR	Y	ZR	NB	BA
853-26-1	0.42	0.13	0.01	0.62	100.0	150	590	10	160	10	1010
*Blue Hope	0.41	0.14	0.03	3.39	100.4	200	830	10	160	10	2290
BH-56	1.00	0.42	0.03	1.47	100.2	30	760	20	110	20	440
72-60	0.80	---	---	---	---	--	---	--	---	--	---
BHC-211	----	0.03	130ppm	0.54	100.0	120	10	30	60	40	110
*BHC-215	0.32	0.06	62ppm	0.93	100.1	290	80	40	300	30	1420
*XR12	0.22	0.04	0.02	0.70	99.7	250	70	50	210	30	1380

district.

Although the major differences in the character of the middle Tertiary districts suggests different ore-forming conditions, a few occurrences suggests nearly identical ore-forming conditions existed in distinct districts. The character of the important US mine deposit and the gold occurrences on the Bullard detachment fault both suggest that CO_2-bearing, Au, Ag, Cu, Si, Fe, and F enriched fluids precipitated minerals at temperatures between 160° to 230° C, under low f_S and high f_{O2}. The solutions probably differed in their alkali and base metal content. The Bullard fluids were probably Ca-rich, K-poor, and depleted in Pb and Zn, whereas the US mine fluids were probably K-rich, Ca-poor, and enriched in Pb and Zn. The silver-lead-rich, calcite-gangue-dominated character of the Valley View prospects in the Aguila district and the Scott Lead and Black Vulture prospects of the Osborne district suggest that CO_2-bearing fluids enriched in Ag, Pb, and possibly Zn, precipitated metals under low f_s, very high f_{O2}, boiling conditions.

A Model for Middle Tertiary Districts of the Big Horn Mountains

Mineralization in the Harquahala district, the Tiger Wash district, the Aguila district, and the Osborne district is a result of intense local thermochemical changes precipitating metals that were probably locally derived from host rocks proximal to the site of the mineral occurrences. The fluids originally were high-K, CO_2-bearing solutions of basinal brine (?) origin which were mobilized throughout the upper-plate of a detachment fault. Fluid-flow associated with the formation of specific mineral occurrences may be driven by one or more of the following: regional and local geothermal gradients, topographically

controlled fluid regimes, and tilting of upper-plate structural block (Figure 21).

Controls over thermal and hydrologic gradients for the eastern Harquahala and Tiger Wash districts are: (1) the initially elevated temperatures of brines compared to meteoric water (Beane and Wilkins, 1985); (2) tilting of upper-plate blocks and consequent gravity-driven fluid-flow; and (3) regionally elevated geothermal gradients as a result of middle- to lower-crustal rocks rising to upper-crustal levels (Spencer and Welty, 1985). Beane and Wilkins (personal communication, 1985) invoke basinal brine solutions as the detachment-fault-related, ore-forming fluids to account for the high salinities, commonplace CO_2, local methane, and high fluid-inclusion homogenization temperatures of lower-plate fluid inclusions. They believe that the fluids had to be thermally elevated before interacting with the hot lower-plate rocks because they believe lower-plate rocks are not hot enough to account for the 200° to 300° homogenization temperatures. The mineral occurrences of the eastern Harquahala district are probably the result of local thermal gradients directly above the Bullard detachment fault. The overlying column of rock, and probable depth of mineralization was probably the Tiger Wash Miocene section, which is approximately 1 km thick. Presumably, the gold-copper-rich (plus or minus fluorite) character of the Harquahala occurrences is a reflection of metal scavenging from lower-plate amphibolite and granite. The barite-fluorite occurrences of the Tiger Wash district are presumed to be a consequence of cooling and dilution of fluids that flowed up from the hot lower plate. The barite-fluorite occurrences probably formed 0.3 to 0.5 km below the paleo-surface. The source of the ionic species is unconstrained, but preliminary speculation is warranted. The presence

of sulfides in the eastern Harquahala district, and the likelyhood that these fluids flowed into the overlying Miocene volcanics points to the lower-plate as a source of SO_4. The common presence of fluorite in the Bullard detachment-hosted occurrences similarly suggests F originated from the lower-plate rocks. Isotopic studies on similar occurrences suggest Ca is derived from the fluorite-hosting basalts (Ruiz et al., 1985). Presumably, the Ba was derived from the arkoses and arkosic conglomerates which are proximal to the occurrences.

The hydrologic regime of the Aguila district may have been a consequence of: (1) meteoric waters recharging off of the southeastern flank of the Harquahala Mountains antiform, and, subsequently, driving K-rich, CO_2-bearing, connate waters to the east, down into the Big Horn Mountains upper-plate; and (2) gravity driven, downward, fluid-flow as a consequence of tilting of upper-plate blocks and subsequent heating of the water at the hot, lower-plate rocks. Leach et al. (1983) postulate a meteoric recharge system for the Mississippi Valley ore-forming fluids. They envisioned the foreland of the Ouachita Mountains as a recharge area driving basinal brines to the north. The presence of a relatively thick sequence of fluvial sedimentary rocks at the west end of the Big Horn Mountains suggests surface waters may have been recharged there. The rapid mid-Tertiary extension rates, and consequent tilting of upper-plate rocks, may account for some gravity driven fluid-flow. When the fluids reach the high heat-flow from the lower-plate a hydrothermal cell would be set up. Upon encountering the Miocene basalts, high in the upper- plate (approximately 0.3 km from the surface), the K-rich fluids reacted with Ca-bearing phases in the basalt, thereby, evolving Ca and Mn. Concurrent boiling, as a result of

released pressure in fracture and fault zones, caused co-precipitation of calcite and manganese oxides.

Thermal and hydrological regimes for the Osborne district are much more difficult to constrain than those for the eastern Harquahala, Tiger Wash, and Aguila districts. Significant flushing of connate waters by meteoric waters is unlikely because of the large distance from the proposed Bullard recharge zone, and the fact that Osborne occurrences are generally not localized along major structures. Instead, elevated thermal gradients attendant to the emplacement of high-level-rhyolite-feeder dikes, and gravity driven fluid-flow (outlined above) are presumed to be the causes of fluid-flow in the Osborne district.

Local emplacement of high-level, rhyolite, feeder stocks is assumed to be the major control over the genesis of gold-rich occurrences (US mine, and Tonopah-Belmont mine) in the Osborne district. Presumably, high-K, CO_2-bearing fluids were mobilized as a consequence of stock emplacement. The longest-lived systems extensively equilibrated with country rocks, and, during the thermal decline of the systems, precipitated base- and precious-metals in response to cooling and dilution. The dilution of the ore-bearing fluids is a result of the influx of meteoric fluids. The widespread occurrence of breccia at the US mine suggests boiling may also have contributed to metal precipitation.

Because precipitation of metals in the Pb-Ag-rich occurrences of the Osborne district occurred predominantly in a major north-northwest-trending fracture zone that extends for over 12 km, and not along the regional normal faults which are assumed to be through-going to a underlying detachment fault or faults, it is unlikely that major faults influenced mineralization. Consequently, the model for gravity-induced

fluid-flow is preferred in explaining the majority of the Osborne district occurrences. Flow up into the upper-plate structural blocks presumably allowed cation exchange of the K-rich fluids with the Ca-rich host rocks thereby causing the fluids to be saturated with Ca. The highly fractured character of the hosting basalts caused boiling and consequent precipitation of calcite. The sudden drop in f_{CO2} caused destabilization of base-metal chloride complexes and consequent base-metal precipitation. The base-metal character of the fluids is assumed to be a result of leaching of metals from the metavolcanic-Proterozoic basement. The fact that manganese oxides are sparingly present suggests the f_{O2} of the fluids was significantly lower than the f_{O2} of the Aguila district fluids.

APPENDIX: INDUSTRIAL MINERAL RESOURCES

Magnetitic Alluvium

Approximately 6,000 acres of alluvial plain have been located by Fred R. Brown of Picacho as a large magnetite placer deposit in the Big Horn Mountains... The alluvial area comprises parts of secs 9, 10, 14, 15, 16, 17, 19, 20, 21, 22, 23, 27, 28, 29, 30, and 32, T4N, R9W... The magnetite placer area starts about 17 miles south of the town of Aguila, just east of the Aguila Tonopah road.

Titaniferous magnetite occurs in alluvium and stream gravels reportedly ranging from a few feet to more than 100 feet. The magnetite with minor amounts of ilmenite makes up 3 to 7 percent of the alluvium; parts of the deposit contain as much as 10 percent magnetite.

Benefication tests made by lessees in 1961, including screening and megnetic seperation, yielded concentrates containing 65 to 69 pecent iron and 0.3 to 0.8 percent titania. The area has been prospected by scattered pits 10 and 15 feet deep. (Harrier, 1964).

Perlite

Outcrops of the Sugarloaf rhyolite in Sec 10, 11, 14, and 15, T4N R8W, Big Horn Mts. 15' have an unassessed amount of perlite (MRDS).

REFERENCES

Anthony, J.W., Williams, S.A., and Bideaux, R.A., 1977, Mineralogy of Arizona: Tucson, University of Arizona Press, 255 p.

AZBGMT files (Arizona Bureau of Geology and Mineral Technology Files).

Barnes, H.L., 1979, Solubility of ore minerals, in Barnes, H.L. ed., Geochemistry of Hydrothermal Ore Deposits (2d ed.): New York, John Wiley & Sons, p. 404-454.

Beane, R.E., and Wilkins, J. Jr., 1985, Thermal Regimes in the Detachment Fault Environment as Deduced From Fluid Inclusions [abs.]: Sedona, AZ., Lunar and Planetary Science Conference.

Belik, G.D., 1985, Preliminary economic evaluation of the Big Horn Gold

Prospect, private report prepared for Roddy Resources Inc.: Vancouvar, B.C., 15 p.

Berg, L., Leveille, G., and Geis, P., 1982, Mid-Tertiary detachment faulting and manganese mineralization in the Midway Mountains, Imperial County, California, in Frost, E.G., and Martin, D.L. eds., Mesozoic-Cenozoic tectonic evolution of the Colorado River Region, California, Arizona, Nevada: San Diego, Cordilleran Publishers, p. 299-311.

Blount, C.W., 1977, Barite solubilities and thermodynamic quantities up to 300 degree C and 1400 bars: Ame. Mineral., v. 62, p. 942-957.

Bodnar, R.J., and Bethke, P.M., 1984, Systematics of stretching of fluid inclusions I: Fluorite and sphalerite at 1 atmosphere confining pressure: Econ. Geol., v. 79, p.141-162.

Boyle, 1979, The Geochemistry of Gold and its deposits: Geologic Survey of Canada, Bulletin 280, 584 p.

Capps, R.C., Reynolds, S.J., Stimac, J.A., Kortemeier, C.P., Allen, G.B., and Scott, E.A., 1985, Preliminary geologic map of the Belmont and eastern Big Horn Mountains, West-Central Arizona: Arizona Bureau of Geology and Mineral Technology Open File 85-15, 25 p.

Carmichael, I.S.E., Turner, F.J., and Verhoogan, J., 1974, Igeneous Petrology: New York, McGraw-Hill, p.33.

Collins, P.L.F., 1979, Gas Hydrates in CO2-bearing fluid inclusions and the use of freezing data for the estimation of salinity: Econ. Geol., v. 74, p. 1455-1444.

Colvinel, A.C., Andrews, A.J., Cherryl, M.E., Durocher, M.E., Fyon, A.J., Lavigne, Jr., M.J., MacDonald, A.J., Soussan Marmontl, Poulson, K.H., Springer, J.S., and Troop, D.G., 1984, An integrated model for the origin of Archean lode gold deposits: Ontario Geological Survey, 100 p.

Coney, P.J., Reynolds, S.J., 1980, Cordilleran metamorphic core complexes and their uranium favorability: U.S. Dept. of Energy, 627 p.

Davis, G.H., 1981, Regional strain analysis of the superposed deformations in southeast Arizona and the eastern Great Basin: Arizona Geological Society Digest, v. 14, p. 155-172.

Denton, T.C., and Kumke, C. A., 1949, Investigation of the Snowball Fluorite Deposit, Maricopa Count, Arizona: U.S. Bureau of Mines Report of Investigation 4540, 15 p.

Dreier, J., 1985, Regional tectonic control of epithermal veins in the western United States and Mexico: Arizona Geological Society Digest, v 15, p. 28-53.

Drummand, S.E., and Ohmoto, H., 1985, Chemical evolution and mineral deposition in boiling hydrothermal systems: Econ. Geol., v. 80, p. 126-147.

Farnham, L.L., and Stewart, L.A., 1958, Manganese deposits of western Arizona: U.S. Bureau of Mines Information Circular 7843, 87 p.

Hardy, J.J.,Jr., 1984, The structural geology, tectonics, and metamorphic geology of the Arrastre Gulch Window, south-central Harquahala Mountains, Maricopa County, Arizona (M.S. thesis): Flagstaff, Northern Arizona University, 99 p.

Hedenquist, J.W., and Henley, R.W., 1985, The importance of CO_2 on freezing point measurements of fluid inclusions: evidence from active geothermal systems and implications for epithermal ore deposit: Econ. Geol., v. 80, p. 1376-1406.

Hewett, D.F., 1964, Veins of hypogene manganese oxide minerals in the southwestern United States. Econ. Geol., v.59., p. 1429-1472.

Hewett, D.F., 1972, Manganite, hausmannite, braunite: features, modes of origin. Econ. Geol., v. 67, p. 83-102.

Hewett, D.F., and Fleischer, M., 1960, Deposits of the manganese oxides, Econ. Geol., v. 55., p 1-55.

Holland, H.D., and Malinin, S.D., 1979, The solubility and occurrence of non-ore minerals, in Barnes, H.L. ed.: New York, Geochemistry of Hydrothermal Ore Deposits, John Wiley & Sons, p. 461-508.

Jones, E.L., and Ransome, F.L., 1920, Deposits of manganese ore in Arizona: in Ransome, F.L. and Burchard, E.F., eds. Contributions to Economic Geology, U.S.G.S. Bulletin 710, p. 135-143.

Keith, S.B., Gest, D.E., DeWitt, E., Woode-Toll, N., and Everson, B.A., 1983, Metallic mineral districts and production in Arizona: Arizona Bureau of Geology and Mineral Technology Bulletin 194, 58 p., scale 1:1,000,000.

Kerr, Dawson, and Associates, 1984, Report on the Big Horn property, Maricopa County, Arizona, U.S.A.: Roddy Resources, Vancouvar, B.C., 33 p.

Leach, D.L., Viets, J.G., Rowan, L., Appalachian-Ouachita orogeny and Mississippi Valley-type lead-zinc deposits [abs]: GSA Abstracts and Programs, v. 16, p. 572.

Masuda, A., Nakamura, N., and tanaka, T., 1973, Fine structures of mutually normalized rare-earth patterns of chon drites: Geochim. et Cosmochim. Acta, v.37, p. 239-248.

Metzger, O.H., 1938, Gold mining and milling in the Wickenburg Area, Maricopa and Yavapai Counties, Arizona: U.S. Bureau of Mines Information Circular, no. 6991, 78 p.

MRDS (Mineral Resource Data System), 1983: U.S. Geological Survey.

Potter, R.W., Clynne, M.A., and Brown, D.L., 1978, Freezing point depressions of aqueous sodium chloride solutions: Econ. Geol., v. 73, p., 284-285.

Roedder, E., 1984, Fluid inclusions: Reviews in mineralogy, Amer. Miner., v. 12, 644 p.

Rehrig, W.A., Shafiqullah, M., and Damon, P.E., 1980, Geochronology, geology, and listric normal faulting of the Vulture Mountains, Maricopa County, Arizona: Arizona Geological Society Digest, v. 12, p.89-110.

Rehrig, W.A., and Reynolds, S.J., 1980, Geologic and geo- chronologic reconnaissance of a northwest-trending zone of metamorphic core complexes in southern and western Arizona, in Crittenden, M.D., Jr., et al., eds., Cordilleran Metamorphic Core Complexes: Geologic Society of America Memoirs 153, p. 131-157.

Rehrig, W.A., and Heidrick, T.L., 1972, Regional fracturing in Laramide stocks of Arizona and its relationship to porphyry copper mineralization: Econ. Geol., v. 67, p. 198-213.

Reynolds, S.J., 1980, Geologic framework of West-Central Arizona: Arizona Geological Society Digest, v. 12, p.1-14.

Reynolds, S.J., 1982, Multiple deformation in the Harcuvar and Harquahala Mountains, west-central Arizona, in Frost, E.G., and Martin, D.L. (eds.), Mesozoic-Cenozoic tectonic evolution of the Colorado River Region: San Diego, Cordilleran Publishers, p. 137-142.

Reynolds, S.J., 1985, Geology and geochronology of the South

Mountains, central Arizona: Arizona Bureau of Geology and Mineral Technology Bulletin 195, 61 p., scale 1:24,000.

Reynolds, S.J., Spencer, J.E., and Richard, S.M., 1983, A field guide to the northwestern Granite Wash Mountains west-central Arizona: Arizona Bureau of Geology and Mineral Technology Open-File Report 83-24, 9 p.

Reynolds, S.J., and Spencer, J.E., 1984, Geologic map of the Aguila Ridge-Bullard Peak area, eastern Harcuvar Mountains, west-central Arizona: Arizona Bureau of Geology and Mineral Technology Open-File Report 84-4, scale 1:24,000.

Reynolds, S.J., and Spencer, J.E., 1985, Evidence for large - scale transport of the Bullard Detachment fault, West-Central Arizona, Geology, v. 13, no.5, p. 353-357.

Reynolds, S.J., Scott, E.A., and O'Haire, R.T., 1985, A Fluorite Bearing Granite, Fieldnotes: Ariz. Bureau of Geol. and Min. Tech., v.15, no.2, p.3-5.

Reynolds, S.J., Capps, R.C., Allen, G.B., Stimac, J.A., Kortemeier, K. P., Spencer, J.E., and Scott, E. ., in preperation, Geology and mineral resources of the Big Horn and Belmont Mountains: Arizona Bureau of Geology and Mineral Technology.

Richardson, C.K., and Holland, H.D., 1979a, The solubility of fluorite in hydrothermal solutions, an experimental study: Geochim. et Cosmochim. Acta., v. 43, p. 1313-1325.

_____, 1979b, Fluorite deposition in hydrothermal systems: Geochim. et Cosmochim. Acta, v. 43, p. 1327-1335.

Ruiz, J., Kesler, S.E., Jones, L.M., 1985, Strontium isotope geochemistry of fluorite mineralization associated with fluorite-rich igneous rocks from the Sierra Madre Occidental, Mexico: possible exploration significance: Econ. Geol., v. 80, pp. 33-42.

Spencer, J.E., and Welty, J.W., 1985, Possible controls of base and precious metal mineralization associated with Tertiary detachment faults in the Lower Colorado River Trough, Arizona and California, Geology, in press.

Stewart, L.A., and Pfister, A.J., 1960, Barite deposits of Arizona: U.S. Bureau of Mines Report of Investigation 5651, 89 p.

Van Nordt, S.D., and Harris,M., 1985, Geology and mineralization of the Picacho Gold Prospect, Imperial County, California: Arizona Geological Society Digest, v. 15, p. 175-187.

Welty, J.W., Spencer, J.E., Allen, G.B., Reynolds, S.J., and Trapp., R.A., 1985, Geology and production of middle Tertiary Mineral districts in Arizona, Arizona Bureau of Geology and Mineral Technology Open File report 85-1.

Wedepohl, K.H., executive director, 1969-1978, Handbook of Geochemistry 2 vols: New York, Springer, 25-D-12 and 13.

Wernicke, B., 1981, Low-angle normal faults in the Basin and Range Province: nappe tectonics in an extended orogen: Nature, v. 291, p. 645-648.

White, D.E., 1980, Active geothermal systems and hydrothermal ore deposits: Econ. Geol., 75th annaversary volume, p. 392-423.

Wilkins, J. Jr., and Heidrick, T.L., 1982, Base and precious metal mineralization related to low-angle tectonic features in the Whipple Mountains, California and Buckskin Mountains, Arizona, in Frost, E.G., and Martin, D.L., eds., Mesozoic-Cenozoic tectonic evolution of the Colorado River Region, California, Arizona, and Nevada: San Diego, Calif., Cordilleran Publishers, p. 182-204.

Wilson, E.D., Moore, R.T., and Pierce, H.W., 1957, Geologic map of Maricopa County, Arizona: Arizona Bureau of Mines, scale 1:375,000.

Wilson, E.D., and Butler, G.M., 1930, Manganese ore deposits in Arizona: Arizona Bureau of Mines Bulletin 127, 107 p.

Wilson, E.D., Moore, R.T., and Cooper, J.R., compilers, 1969, Geologic map of Arizona Arizona Bureau of Mines and U.S. Geological Survey, Scale 1:500,000.